



# PSP High Altitude

## Spaceshot Project System Requirements Review and Conceptual Design Review

December 2022

---

## Contents

<b>1</b>	<b>Introduction</b>	<b>6</b>
1.1	Purdue Space Program High Altitude . . . . .	6
1.2	Budget . . . . .	6
<b>2</b>	<b>Spaceshot Requirements</b>	<b>8</b>
2.1	Internal Stakeholder Requirements . . . . .	8
2.2	External Stakeholder Requirements . . . . .	9
2.2.1	Federal Aviation Administration . . . . .	10
2.2.2	Purdue Zucrow Laboratories . . . . .	10
2.2.3	Launch Sites . . . . .	11
2.3	Functional Requirements . . . . .	11
2.3.1	Flight-Critical Requirements . . . . .	11
2.3.2	Recovery Requirements . . . . .	12
2.3.3	Non-Flight Critical Requirements . . . . .	13
2.4	System Requirements . . . . .	13
2.4.1	Propulsion . . . . .	13
2.4.2	Avionics . . . . .	13
2.4.3	Mechanisms . . . . .	14
2.4.4	Structures . . . . .	15
<b>3</b>	<b>Vehicle Sizing</b>	<b>16</b>
3.1	Introduction . . . . .	16
3.2	Figure of Merit and Pareto Analysis . . . . .	16
3.3	One Degree of Freedom Analysis . . . . .	19
3.4	Mass Estimation and Sizing System . . . . .	21
3.4.1	General Operation and Information . . . . .	21
3.4.2	Analysis . . . . .	23
3.4.3	Results . . . . .	23
3.5	Trajectory Analysis Model and Statistical Methods (6DOF) . . . . .	25
3.5.1	Strengths and Shortcomings . . . . .	25
3.5.2	Stability . . . . .	27
3.5.3	Statistical Methods . . . . .	27
3.5.4	Results . . . . .	27

---

---

3.5.5 Validation . . . . .	28
<b>4 Propulsion</b>	<b>30</b>
4.1 Introduction . . . . .	30
4.2 Performance . . . . .	30
4.3 Ignition . . . . .	30
4.4 Manufacturing . . . . .	32
4.5 Testing . . . . .	33
4.6 Analysis and Simulation . . . . .	36
4.7 Combustion Modeling . . . . .	38
<b>5 Avionics</b>	<b>45</b>
5.1 State Estimation and Apogee Determination . . . . .	45
5.1.1 System Architecture . . . . .	45
5.1.2 Data Fusion Algorithm . . . . .	46
5.1.3 Testing . . . . .	47
5.2 In-Flight Events . . . . .	47
5.2.1 Safety . . . . .	48
5.3 Downlink . . . . .	49
5.4 Payload . . . . .	50
5.5 Durability . . . . .	50
<b>6 Mechanisms</b>	<b>52</b>
6.1 Recovery System . . . . .	52
6.1.1 First Stage Recovery . . . . .	52
6.1.2 Second Stage Recovery . . . . .	53
6.2 Separation Mechanism . . . . .	54
6.3 Inter-Stage Mechanism . . . . .	56
6.4 De-Spin Mechanism . . . . .	56
<b>7 Structures</b>	<b>60</b>
7.1 First Stage . . . . .	60
7.1.1 First Stage Airframe . . . . .	60
7.1.2 First Stage Fins . . . . .	61
7.1.3 Interstage . . . . .	63
7.2 Second Stage . . . . .	64

---

---

7.2.1	Second Stage Airframe . . . . .	64
7.2.2	Avionics Bay . . . . .	65
7.2.3	Second Stage Fins . . . . .	65
7.2.4	Nosecone . . . . .	66
7.3	Thermal Analysis . . . . .	68
7.3.1	Nosecone . . . . .	68
7.3.2	Airframe . . . . .	68
<b>8</b>	<b>Next Steps</b>	<b>70</b>
8.1	Highest Risks . . . . .	70
8.2	Testing Capabilities . . . . .	71
8.3	Timeline . . . . .	73
<b>Appendix A</b>	<b>Acronyms and Glossary</b>	<b>74</b>
<b>Appendix B</b>	<b>System Requirement Tables</b>	<b>76</b>
B.1	Internal Stakeholder Requirements . . . . .	76
B.2	External Stakeholder Requirements . . . . .	76
B.2.1	Federal Aviation Administration . . . . .	76
B.2.2	Purdue Zucrow Laboratories . . . . .	77
B.2.3	Launch Sites . . . . .	77
B.3	Functional Requirements . . . . .	77
B.3.1	Flight-Critical Requirements . . . . .	77
B.3.2	Recovery Requirements . . . . .	78
B.3.3	Non-Flight Critical Requirements . . . . .	79
B.4	Systems Requirements . . . . .	79
B.4.1	Propulsion . . . . .	79
B.4.2	Avionics . . . . .	81
B.4.3	Mechanisms . . . . .	82
B.4.4	Structures . . . . .	82
<b>Appendix C</b>	<b>Recovery System Line Diagrams</b>	<b>85</b>
<b>Appendix D</b>	<b>Avionics In-Flight Event Overview</b>	<b>87</b>
<b>Appendix E</b>	<b>Propulsion System Safety Procedures</b>	<b>91</b>
E.1	Example Procedure for Crawford Bomb Testing . . . . .	91

---

---

E.2 Example Procedure for Hot Fire Test . . . . .	92
<b>Appendix F PSP High Altitude Team Members</b>	<b>98</b>
<b>Bibliography</b>	<b>99</b>

## 1 Introduction

This report corresponds to the System Requirements Review and Conceptual Design Review for the Spaceshot project of Purdue Space Program's High Altitude team. The purpose of this review is twofold: first, we seek feedback on our system requirements; we have a set of stakeholder requirements, which we have flowed down to the level of each vehicle subsystem, and we believe these requirements are complete and sufficient to define our project. Second, we present our conceptual design of the vehicle, and show that it is capable of meeting the requirements we have specified.

We believe the report is structured logically to achieve those objectives. In this section we offer a short introduction to the team and its finances. Next, Section 2 covers the stakeholder and functional requirements, and flows them down to the level of each subsystem. Section 3 begins discussion of the vehicle design with the initial sizing process, and our goals for future simulation. The propulsion system is next, in Section 4, followed by avionics in Section 5, mechanisms in Section 6, and structures in Section 7. Each of these component sections discusses the motivating requirements and the planned implementation that will satisfy them. Finally, Section 8 discusses our next steps with the project after this review, including aspects of the project we consider highest risk.

### 1.1 Purdue Space Program High Altitude

High Altitude (HA) is a project team within Purdue Space Program (PSP) that was formed in May 2021. High Altitude's objective is to design, build and fly a two stage rocket to the Kármán Line: 100 kilometers above mean sea level. The team was formed with the experience and leadership from the now-defunct PSP Solids team, which competed annually in the Spaceport America Cup from 2018 to 2020. Over the course of the past year, High Altitude has continued to develop skills across the team through several design iterations and test flights as the team continues to move into more detailed work on the spaceshot rocket.

Since its formation, High Altitude has been involved in rapid iteration and prototyping of many smaller-scale rockets. Last year, the team conducted three test flights to familiarize ourselves with both launch operations and systems engineering across a design's entire life cycle. This started with an initial L2 kit rocket, the Wildman Darkstar Extreme, and its launch in September 2021. The team's next launch was in December; it was fully designed and constructed by our team and made primarily out of carbon fiber. The third and most recent launch was a reflight of the Darkstar. After these launches, the team began work on the spaceshot project; this Design Review will conclude the first phase of that work.

### 1.2 Budget

The High Altitude team receives funding each semester from Purdue organizations including Purdue Engineering Student Council (PESC) and the Purdue Engineering President's Council (PEPC). These merit funds total up to \$6,000 per semester. The team launched a successful crowdfunding campaign in the Spring of 2022 to raise over \$3,000 and also participates in fundraising events through Purdue Athletics. In addition, we have applied for scientific research grants through organizations such as NASA to support the project's development. These research grants are

---

*Introduction*

limited by the type of research being completed by HA as there is not an experimental payload included onboard the rockets.

These funds are reallocated each semester to each technical team based on the current projects of each team. Currently, HA has about \$8,000 with an expected addition of \$3,000 from the PESC Merit Fund before the end of the year. For the Spring 2023 semester, the Avionics team will receive \$2,000 for the research and development of a flight computer as well as the purchase of a commercial avionics board to be tested on an L1 kit rocket. The Mechanisms team will receive \$500 to construct and test the de-spin mechanism as well as the recovery system. The Propulsion team will be designing and building a test stand at Zucrow Laboratories to characterize solid rocket motors; the cost of this project is dependent upon the involvement of other research groups. Structures will continue to finalize the design for spaceshot; prototyping, manufacturing, and testing the airframe is estimated to cost between \$4,000 - \$10,000 which will be allocated incrementally during the next few semesters. Future budgeting will involve attempting to obtain funding from companies, institutions, and foundations.

## 2 Spaceshot Requirements

This section includes our highest-level requirements for the spaceshot project. Throughout the rest of the report other sections will reference the specific requirement a particular design is satisfying, in order to motivate it. Each requirement ID in the rest of this report is a clickable hyperlink to the appropriate part of Appendix B, where all of our requirements are tabulated, with their derivations when appropriate.

Some of these requirements are dependent on whether or not we expend the first stage of the vehicle. Our team has decided to not include first stage recovery as an internal stakeholder requirement. However, there may or may not be external factors that require us to recover the stage. Currently, we have worked on designs for subsystems like avionics and recovery that will be included in the first stage, if and only if it is to be recovered. **For the rest of this report, requirements that only exist if the first stage is to be recovered are marked with a \*, and requirements that only exist if the first stage is able to be expended are marked with a †.**

### 2.1 Internal Stakeholder Requirements

Our stakeholder requirements are derived from entities involved in the development, launch, or regulation of an amateur rocket. In this case, the customer of this rocket is the PSP High Altitude team. These were decided in a team-wide planning meeting early in the vehicle design process.

Req. ID	Requirement
SR.1	The rocket shall reach 100 km mean sea level.
Our mission statement is to reach space, for which we use 100 km above sea level as the target height as that is widely regarded as the boundary between Earth and space.	

Req. ID	Requirement
SR.2	The rocket shall have two powered stages.
We want to learn from the complexity of the separation mechanism, develop valuable learning experiences, and become the first successful two stage spaceshot rocket built by a student team. Although 100 km is achievable with a single motor, mixing and casting a motor of this size introduces challenges as these processes are overseen by Zucrow Labs <sup>1</sup> . Additionally, the multistage design meets the team's vision and creates design challenges that the team wants to take on.	

<sup>1</sup>For a motor that big, we would need to use more than 100 lb of propellant, which the Hobart mixer in ZL6 cannot even cast a single grain of at one time. With two stages, we will still have to cast multiple batches, however, we can still cast a single grain at once — avoiding the problem of two mixes per grain.

Req. ID	Requirement
SR.3	The rocket shall have one or more motors created by students at Purdue Zucrow Labs.
Part of our vision is to involve as much student design as possible within the rocket. We have access to a propulsion lab and the equipment needed to mix our own solid rocket motor, which will allow us to fine tune our thrust profiles and not limit our designs to commercially available solid motors.	

Req. ID	Requirement
SR.4	The upper rocket stage shall be recoverable <sup>2</sup> .
To be able to physically analyze the effects of high speed flight and verify any data recorded onboard.	

Req. ID	Requirement
SR.5	The rocket shall carry a payload non-essential to rocket performance.
We want to put an object inside the rocket that is meaningful to the team and launch it to space. It should not be a critical part of the vehicle.	

Req. ID	Requirement
SR.6	The rocket development shall follow systems documentation.
This is a requirement meant to address some of the documentation shortcomings of our previous PSP rocket teams. Documentation tends to be lacking, and whenever a core member leaves the team, limited knowledge gets transferred, resulting in having to start certain research from the beginning. This will also standardize the explanation of the function of a system across the teams and pass on our knowledge to future teams and groups.	

## 2.2 External Stakeholder Requirements

These are the primary requirements set by non-PSP organizations that may constrain our design.

---

<sup>2</sup>If we are not able to expend the first stage, this requirement would extend to both.

### 2.2.1 Federal Aviation Administration

Req. ID	Requirement
EX.1.1	There shall not be a 90 person per square mile population area within a quarter range of vehicle targeted height.
The FAA is mainly concerned about the possible areas that the parts of our rocket can land. The given parameters are the known general ballpark numbers they use for high power rockets, though additional restrictions may apply. They want to make sure that none of our rockets will land on personal property or a person.	

Req. ID	Requirement
EX.1.2	Certificate of Authorization shall be approved by the FAA.
This is to obtain airspace clearance from the FAA. They will be looking to see that it is not a high air traffic area. Looking at our launch locations, the main group that will have priority over us for airspace is the US Air Force.	

Req. ID	Requirement
EX.1.3	The rocket shall not reach above 150 km.
Above 150km, the vehicle would no longer be classified as an amateur rocket and would be subject to a different set of FAA requirements.	

Req. ID	Requirement
EX.1.4	Form 7711-2 shall be approved by the FAA.
This form contains information about our rocket and operation of our rocket. Completing this will allow the FAA to verify that the operation of our rocket will pose minimal harm to the area and people within our operational area.	

### 2.2.2 Purdue Zucrow Laboratories

Purdue Zucrow Laboratories (Zucrow) is a propulsion lab on campus that currently mixes and tests propellants and other energetics for a variety of purposes. PSP will have access to mixing equipment after a rigorous design review process.

Req. ID	Requirement
EX.2.1	Purdue Zucrow Laboratories shall set high level requirements based on our mission profile.
	Zucrow makes mixing requirements after looking at our target parameters to better provide assistance to the team. This is intended to make motor mixing less restricted to a common formula.

### 2.2.3 Launch Sites

Certain launch sites have additional requirements due to company policy or local regulations. These are blanket requirements that we have extrapolated from reading different launch sites and are reasonable enough to impose as a team wide requirement.

Req. ID	Requirement
EX.3.1	The team shall design its own launch rail.
	Many of the launch site operators request us to use our own launch rails due to the student developed motor possibly damaging the blast plate. This is dependent on the site, but creating our own design will prevent issues down the line. Providing our own launch rail will also allow us to customize our rail mounting points and take off characteristics.

## 2.3 Functional Requirements

### 2.3.1 Flight-Critical Requirements

After considering all of our stakeholder requirements, we derived the high level requirements for our vehicle to achieve its mission. Functional requirements are more focused on what the overall rocket has to do and not how. It will also have the physical components stated for a rocket to be a rocket. Again, requirements that only exist if the first stage is recovered are marked with a \*, and requirements that only exist if the first stage is expended are marked with a †.

Req. ID	Requirement	Rationale	Traced From
DEF1.1	Rocket stages shall have fundamental flight articles.	These are the minimum components for a stage of our rocket to be considered a stage.	SR.1
DEF1.1.1	The stage shall have an airframe.	Core structural part of a rocket that houses subsystems.	SR.1
DEF1.1.2	The stage shall have a motor.	Being a two stage powered rocket, all stages will have a motor.	SR.2
DEF1.1.3†	The stage shall have a recovery system.	To safely recover the stage.	SR.4

DEF1.3.1†	To be able to study the effects of high speed flight on all parts of the rocket on the ground.	The recovery system will be actively controlled for safety.	SR.4
DEF1.2	The lower stage shall have the required flight articles to be the first stage.	Lower stage may contain components that are not required on other stages.	SR.1
DEF1.2.1	The lower stage shall have fins.	Passively-stabilized rockets like ours usually require fins to remain stable throughout the flight.	SR.1
DEF1.3	The upper stage shall have the required flight articles to be the first stage.	Upper stage may contain components that are not required on other stages.	SR.1
DEF1.3.1	The upper stage shall have fins.	Passively-stabilized rockets like ours usually require fins to remain stable throughout the flight.	SR.1
DEF1.3.2	The upper stage shall have a nosecone.	Rockets usually require a nose cone to remain stable throughout the flight.	SR.1
DEF1.3.3*	The upper stage shall have a recovery system.	This stage travels to apogee and would be able to physically confirm height and performance.	SR.4
DEF1.3.3.1*	Stages with a non-autonomous recovery system shall have an avionics system.	The recovery system will be actively controlled for safety.	SR.4
DEF1.4	The vehicle shall have a staging mechanism between stages.	This allows the stages to separate.	SR.2
DEF1.5	The vehicle shall ignite the upper stage motor.	The second stage motor is ignited by the rocket itself as there will be no external mechanism for rocket ignition.	SR.1, SR.2

### 2.3.2 Recovery Requirements

Requirements for a successful recovery.

Req. ID	Requirement	Rationale	Traced From
DEF2.1	The upper <sup>3</sup> stage shall be recoverable.	The upper stage travels through the entire stage of the flight and records it.	SR.4
DEF2.1.1	The upper stage touchdown velocity shall be less than 20 ft per second.	The stage must touch down slow enough to prevent significant damage.	SR.4
DEF2.1.2*	The lower stage touchdown velocity shall be less than 20 feet per second.	The stage must touch down slow enough to prevent significant damage.	SR.4

<sup>3</sup>Both stages if they must both be recovered

### 2.3.3 Non-Flight Critical Requirements

Requirements not necessarily required for the vehicle but that fulfill a stakeholder requirement.

Req. ID	Requirement	Rationale	Traced From
DEF.3.1	The vehicle shall have a payload.	Satisfies the payload requirement, and gained data is directly useful as visual proof of rocket location.	SR.5
DEF.3.2	The vehicle shall determine its apogee.	To confirm that the rocket has reached the target apogee.	SR.1
DEF.3.3	The vehicle shall identify its location.	For easier post launch recovery.	SR.4
DEF.3.4	The vehicle shall check its state before igniting second stage.	Implied required safety feature for any two stage rocket.	EX.1.1, EX.1.2, EX.1.4

## 2.4 System Requirements

For the system requirements and for the remainder of this report, the rocket is conceptually divided into four sub-systems: propulsion, avionics, mechanisms, and structures. We believe these represent natural subdivisions of the requirements for the rocket. Based on this organization, the following requirements are categorized by PRO (propulsion), AVI (avionics), MEC (mechanisms), and STR (structures).

### 2.4.1 Propulsion

Functional requirement DEF1.1.2 dictates that both stages are powered, which leads to PRO.1, the upper stage motor, and PRO.2, the lower stage motor. Additionally, DEF1.5 requires that the rocket ignite the upper-stage motor; ignition-related requirements also fall under the scope of the propulsion system.

Req. ID	Requirement	Description	Traced From
PRO.1	Upper Stage	The rocket shall have an upper stage propulsion system	DEF1.1.2
PRO.2	Lower Stage	The rocket shall have a lower stage propulsion system	DEF1.1.2
PRO.1.2.1.2	Upper Stage Ignition	The charge will accept signal from avionics to activate	DEF1.5

### 2.4.2 Avionics

The first requirement on the avionics system, that of apogee verification, is derived from DEF3.2. The avionics system must also deploy the recovery system, and at the right time, derived from requirement DEF1.1.3.1. The other requirement corresponding to in-flight events is AVI.3,

concerned with stage separation and second stage ignition, and which is derived from DEF.1.5 and DEF.3.4, corresponding to those functions respectively. Another very important requirement is that the avionics system must allow the rocket to be located. This derives from DEF.3.3. Naturally, the avionics system must also survive the flight, and this is derived from the other avionics-related functional requirements; if the avionics system is not durable enough to survive, it will not be able to meet those requirements. Finally, the avionics system must contain a payload, as specified by DEF.3.1.

Req. ID	Requirement	Description	Traced From
AVI.1	Apogee Verification	The avionics shall verify the rocket's apogee.	DEF.3.2
AVI.2	Recovery System Deployment	The avionics shall activate the recovery system at the proper time.	DEF.1.1.3.1
AVI.3	Stage Separation and Second Stage Ignition	The avionics shall activate the stage separation and second stage ignition at the proper time.	DEF.1.5, DEF.3.4
AVI.4	Locating Rocket	The avionics shall locate the rocket after the flight.	DEF.3.3
AVI.5	Durability	The avionics systems shall be durable enough to safely fly on the vehicle.	DEF.1.1.3.1, DEF.1.5, DEF.3.1, DEF.3.2, DEF.3.3, DEF.3.4
AVI.6	Payload	The avionics shall have a payload.	DEF.3.1

### 2.4.3 Mechanisms

The Mechanisms system includes three separate subsystems, each deriving from functional requirements. Requirement DEF.2.1 dictates that the stage(s) be recoverable. Accomplishing this requires the rocket to despin (MEC.1), separate the two stages (MEC.3), and separate the airframe to deploy the parachute (MEC.2.2.2). MEC.3 also derives from DEF.1.4, which requires that the vehicle include a mechanism to separate the two stages.

Req. ID	Requirement	Description	Traced From
MEC.1	De-Spin	The rocket shall despin to no more than 60 revolutions per minute.	DEF.2.1
MEC.2	Recovery	Both stages <sup>4</sup> of the rocket shall be recoverable	DEF.1.4, DEF.2.1
MEC.3	Inter-Stage Separation	The two stages of the rocket shall separate at a predicted or commanded time.	DEF.1.4, DEF.2.1

<sup>4</sup>Only the second stage if the first may be expended.

#### 2.4.4 Structures

Each of the six components under structures derives from a required flight article. DEF.1.2.1 dictates that the rocket has lower fins, leading to STR.1. Likewise, DEF.1.3.1 requires upper fins, leading to STR.4. DEF.1.1.1 requires that the rocket have an airframe, from which derive STR.2 (lower airframe) and STR.5 (upper airframe). The staging mechanism required by DEF.1.4 is housed within an interstage, STR.3. Finally, DEF.1.3.2 requires that the upper stage of the rocket have a nose cone, leading to STR.6.

Req. ID	Requirement	Description	Traced From
STR.1	Lower Fins	The rocket shall have fins on the lower stage	DEF.1.2.1
STR.2	Lower Airframe	The rocket shall have a lower airframe	DEF.1.1.1
STR.3	Interstage	The rocket shall have an interstage	DEF.1.4
STR.4	Upper Fins	The rocket shall have fins on the upper stage	DEF.1.3.1
STR.5	Upper Airframe	The rocket shall have an upper airframe	DEF.1.1.1
STR.6	Nosecone	The rocket shall have a nosecone	DEF.1.3.2

## 3 Vehicle Sizing

### 3.1 Introduction

In order to verify that our vehicle is able to satisfy the mission requirements it is vital to have an understanding of what a proposed vehicle would look like in terms of its design aspects. Factors that include propulsive, structural, aerodynamic, thermal, and many others must be considered in order to properly assess if a contending vehicle design is viable in terms of matching requirements for the mission's success.

A large trade study was conducted in order to find a vehicle design that meets the individual requirements of each subteam. Since it was determined that the propulsion system of the launch vehicle has the most direct influence in a given design's ability to achieve the desired mission objectives, the figure of merit analysis started with the propulsion design.

The sizing process began at the highest level possible, evaluating the entire vehicle system. Our scope was then increasingly refined and candidate designs were filtered until only handful of viable point designs remained, all of which satisfactorily met our mission requirements.

This process first used a Pareto analysis to generate a large dataset of possible candidate designs. Then a 1-degree of freedom (1DOF) mathematical model was used to determine the propulsion requirements for each point design as well as forecast a projected time history of resulting flight to space. The propulsion analysis calculated metrics like propellant mass required and motor burn times, and the time history tracked flight parameters such as dynamic pressure experienced and delta-V split between the two stages. This data was then sifted through by the aerostructures team that looked at factors such as chamber pressure and temperature history, motor dimensions, inert mass, among others, to determine if designs were realistic candidates for further analysis. A point design was thrown out if the inert mass required to match the specified safety factors for structural stability was deemed to not be achievable. In the final step of this process, a comprehensive 6-degree of freedom (6DOF) mathematical model study was conducted that served two purposes: give a refined trajectory of the vehicle's mission, and verify that the outputs from the 1-dimensional model were reasonable, which gave a sanity check to the entire process. Ultimately the 6DOF gave a finishing polish on the process, giving the team confidence that the selected point designs had a high probability of completing the mission requirements successfully.

The validity of this process — the down-selecting of viable vehicle designs that satisfy all the mission requirements — is yet to be shown experimentally. However, we believe our outlined methodology to be sound on a conceptual level go on to document our assumptions, procedures and decisions in the following sections of this report.

### 3.2 Figure of Merit and Pareto Analysis

The Pareto analysis, a formal technique which may be useful where many possible courses of action are competing for attention, was paired with a figure of merit analysis that allowed both methods to complement each other with the desired goal of finding how the multitude of input

Parameter	Initial Run	Final Run
First Stage Diameter (in)	3.75, 4.0, 4.25, 4.5, 5.0	5.0, 5.25, 5.5
Second Stage Diameter (in)	3.0, 3.5, 4.0, 4.5	4.0, 4.25, 4.5, 4.75
Payload Mass (kg)	1, 3, 4, 5, 10	0.5
Desired Apogee Altitude (km)	100, 125, 150, 200, 250, 300, 400	100, 125, 150
First Stage $\Delta V$ Split	35%, 40%, 45%, 50%, 55%, 65%	35%, 42.5%
Propellant Mass Fraction ( $\lambda_p$ )	$\lambda_{p,1} = 0.85$ $\lambda_{p,2} = 0.785$	$\lambda_{p,1} = 0.7$ $\lambda_{p,2} = 0.6$
$I_{sp}$ Efficiency ( $\eta_{isp}$ )	0.925	0.9
Total Point Designs Tested	4200	72

Table 8: Summary of Pareto analysis vehicle parameters

$W_1$	$W_2$	$W_3$	$W_4$	$W_5$	$W_6$
-0.4	0.05	0.35	-0.4	-0.2	0.6
$t_{ref}$	$m_{pl,ref}$	$h_{ref}$	$m_{p,ref}$	$Q_{max}$	$L/D_{ref}$
10 sec	5 kg	103.57 km	119.522 kg	200 kPa	19.5

Table 9: Characteristic evaluation function weights and reference values

parameters affected the performance of a point design, and then show how the many point designs compared against each other. The figure of merit analysis generated a set of point designs for a possible launch vehicle with the parameters that were simulated summarized in Table 8, with every combination of parameters being a point design tested.

Each point design was evaluated using both the 1DOF model and the genetic algorithm, with the 1DOF model being the main computational engine in the sizing process. The genetic algorithm iterated on chamber pressure profiles for the first and second stage motors in order to maximize the following characteristic evaluation function.

$$CEF = W_1 \left( 1 - \frac{t_{ref}}{t_{b1} + t_{b2}} \right) + W_2 \left( \frac{m_{pl}}{m_{pl,ref}} \right) + W_3 \left( \frac{h}{h_{ref}} - 1 \right) \\ + W_4 \left( 1 - \frac{m_{p,ref} - m_p}{m_{p,ref}} \right) + W_5 \left( 1 - \frac{Q_{max,ref}}{Q_{max}} \right) + W_6 \left( 1 - \left[ \frac{L/D_{ref} - L/D}{L/D_{ref}} \right]^2 \right)$$

This characteristic evaluation function was the backbone to the Pareto analysis, which included six metrics that were chosen to best represent the performance of a potential design. The metrics chosen were: burnout times for the first and second stage ( $t_b$ ), payload mass ( $m_{pl}$ ), altitude at apogee ( $h$ ), mass of propellant for first and second stage ( $m_p$ ), maximum dynamic pressure experienced ( $Q_{max}$ ), and aspect ratio for the entire vehicle ( $L/D$ ). Reference values were utilized in the characteristic evaluation function in order to normalize the data as best as possible, with the

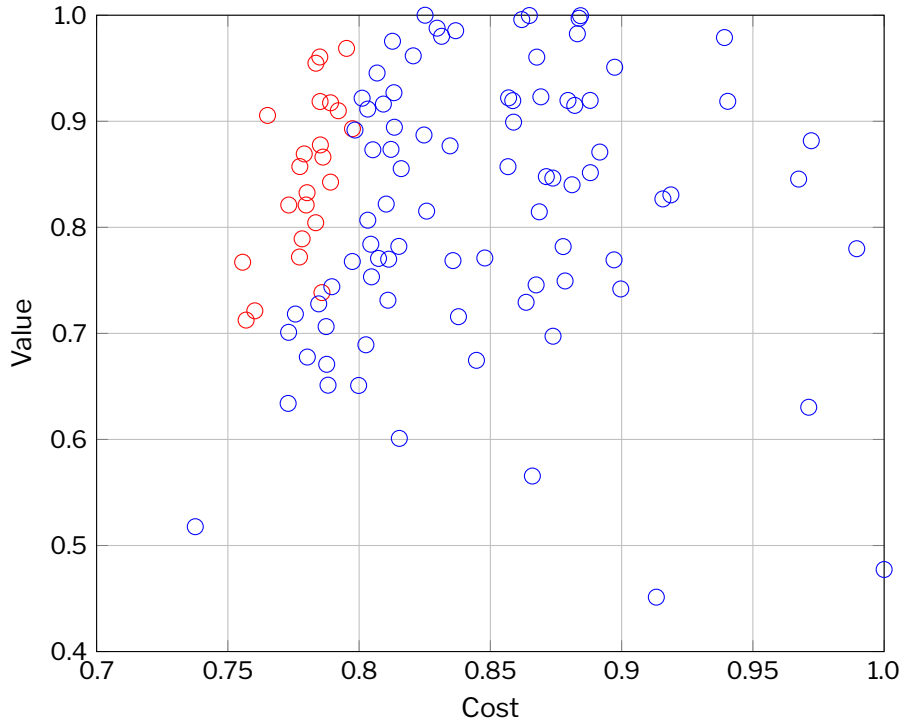


Figure 1: Pareto analysis results scatter plot

values used being summarized in Table 9. The weights chosen by our team as the values of  $W$  are designed to put emphasis on parameters deemed more impactful to the mission, and factors that have an unfavorable impact on the design have negative sign. In all, the characteristic evaluation function (CEF) is bound between -1 and 1, with a design performing the best with a score of 1. The overall distribution for point designs score of the CEF was modeled to be approximately normal. The reference values are modeled after Traveler IV, with the exception of  $t_{ref}$ ,  $m_{pl,ref}$ , and  $Q_{max}$ , which were all chosen using a point estimation for the population mean of the point designs tested in the set. Parameters such as desired altitude, payload mass, and to an extent aspect ratio are all direct input parameters to the system, whereas the rest of the values are outputs from the 1DOF model.

A plot for an example batch of point designs that have been normalized within the set are shown in Figure 1, where the “value” is defined as the factors in the CEF that are positive, and the “cost” are the factors that are negative. The point designs that are colored in red are chosen as favorable designs since they have the best balance between the costs and value, whereas the blue labeled points have corresponding designs that may perform at the same value but with minimal cost. This method of screening was used for the initial selection process for viable point designs. This region of red dots is known as the Pareto Frontier, and the slope of the frontier shows a direct visual trade off of certain parameters of a point design to the overall performance.

The genetic algorithm used converged on a point design when the characteristic evaluation function was maximized for a given chamber pressure profile. In order to best prevent the program from settling on a local maximum, a few measures were implemented to find the solution which converged with the highest value which was the best approximation of a global maximum. The first

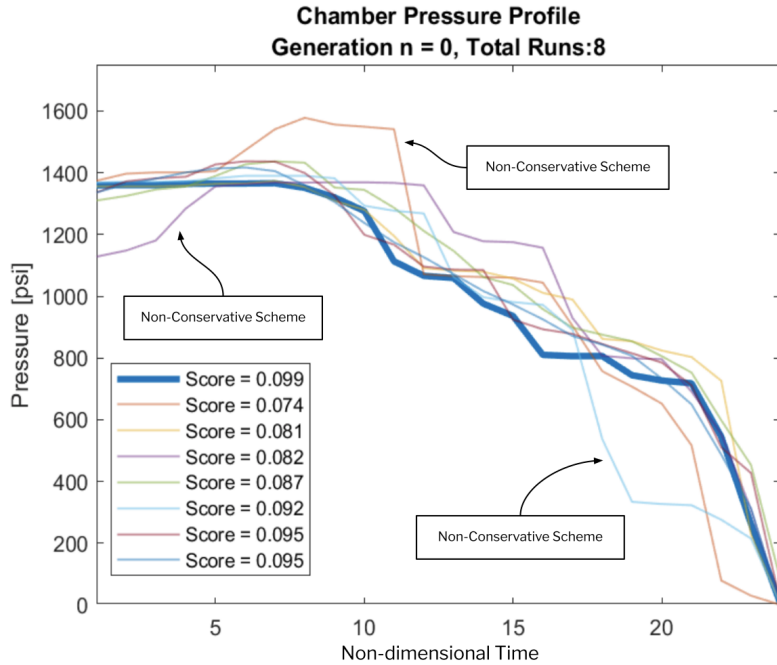


Figure 2: Example genetic algorithm run

generation that was run through the 1DOF model used a seed profile with a total of 7 “offspring” profiles, which were altered versions of the seed profile. Of the offspring, 4 were more conservative variations that were intended to refine the parent generation with minor adjustments, whose purpose was to converge on a local maximum of the characteristic evaluation function. The 3 other offspring profiles had much larger changes from the parent generation which are designed to bump the convergence from one local maximum to another. After the 8 profiles converged, the overall best score from the characteristic function was found, which then was chosen as the next parent seed for the following generation. This process was repeated for the designated amount of generations by the user. A visual example of this process is shown below in Figure 2, where an example is shown after all schemes have been tested, and the darkened profile is selected as the parent profile for the next generation since it has the highest characteristic evaluation function score. The entire selection process is simplified in the flowchart in Figure 3.

### 3.3 One Degree of Freedom Analysis

The 1DOF utilized in this process started by initializing a few key parameters that were held constant in each subsequent point design, which included: propellant characteristics and composition, nozzle characteristics with expansion ratio, empirical estimations for propellant mass fractions, and empirical estimation for  $I_{sp}$  efficiency.

These aspects were held to be constant with one notable exception, the propellant mass fraction estimate. Using historical data provided in Figure 3.4 of “Rocket Propulsion” [11] a rough approximation was made for the propellant mass fraction, which relates the total mass of the motor to the mass of propellant. It was found later from the structures sub team, that these empirical

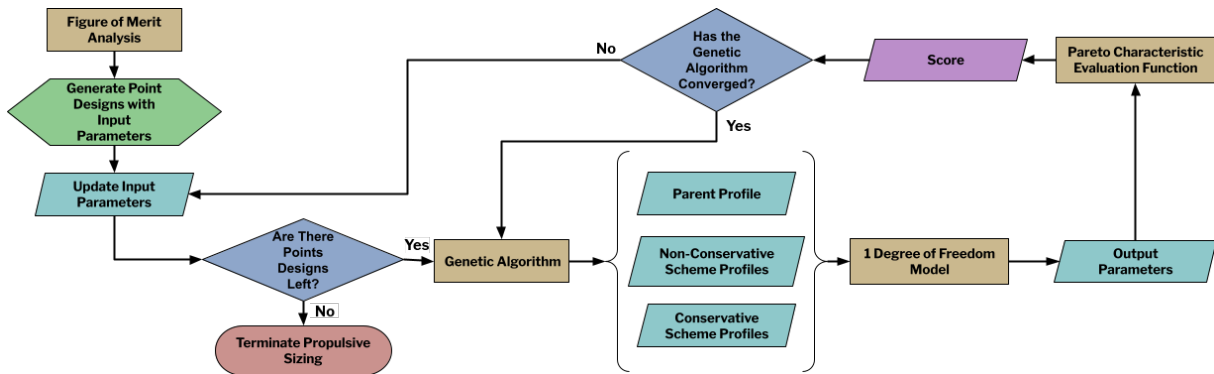


Figure 3: Genetic algorithm selection process flowchart

estimations were giving values for acceptable inert masses to be less than what could be reasonably done, therefore these values had to be adjusted in order to give more inert mass to each stage so an appropriate aerostructure could be designed while fitting the designated inert mass budget. The propellant mass fraction was different for both the first and second stage, with the second stage having more inert mass accounted for, and likewise a lower inert mass fraction, due to an interstage and other factors due to the two stage nature of the vehicle.

The propellant characteristics were not adjusted due to the limitation from faculty advisors to not develop our own proprietary propellant, which would allow for individual tailoring of different traits. This limited our total selection of propellants severely, and ultimately a propellant (TS - 78) derived from published literature from NATO was selected due to its high performance and relatively safe manufacturability. In further testing for the mission this input parameter of propellant performance will have the most direct impact on this model's results. Currently, the propellant is modeled using NASA CEA to give motor characteristics such as: exhaust velocity, chamber temperature, motor characteristic velocity, motor ISP, and exhaust static pressure. Further tests will give improved representations of these factors.

The nozzle was held constant since it added a few extra variables to the selection process, namely throat area, exit area, and therefore expansion ratio. It was decided that these factors could be adjusted after the selection process was done if need be.

In order to properly have a solution from the 1DOF, iteration was relied on heavily to fully define the variables in the system. The main variable that was iterated upon was the mission's total change in velocity ( $\Delta V$ ), which trickled down to a few other variables. If a value for total  $\Delta V$  was estimated, then using the ideal rocket equation with the propellant mass fractions and the stage specific impulse, a value for the vehicle's mass could be found broken up between first and second stage for its inert and propellant mass. Then, once propellant mass is found for each stage, burn time per motor can be iterated upon using the mass flow rate history of each stage (derived from the chamber pressure profile, throat area, and characteristic velocity) until the total mass accumulated is equivalent to the propellant mass found with the ideal rocket equation. Following this, an atmospheric model was utilized to find aerodynamic forces on the vehicle. The flight of the vehicle was modeled using a time stepping force balance that accounted for the mass exhausted from the motor and the thrust of the motor, drag, and gravity in order to find the acceleration at a

designated time. Velocity was found from the integration of acceleration, and so forth for altitude. It is key to note that all thrust was modeled to be purely axial, all aerodynamic forces were axial, and likewise with body forces from gravity. After a motor had burnt out, a coasting period was modeled, if required by the input parameters of the mission, by the same procedure just without thrust of the motor. Once separation occurred, the inert mass of the first stage was subtracted from the vehicle's total mass, and the second stage followed the same procedure to find acceleration on the vehicle. This process resulted in the time history data for vehicle mass, dynamic pressure, net force, acceleration, velocity, altitude, atmospheric conditions, Mach, along with others derived from these. It is important to note that the coefficient of drag used in this model was variable and had critical Mach numbers of 0.7 and 1.3, which affected the vehicle most as it was going through Mach 1. After all of these calculations took place, the final altitude was compared to the input parameter for the desired altitude, and if the margin of error was not met, the process would be repeated with an updated delta V for the mission. Therefore this method can be thought of as a modified ideal rocket solution, since at its core it uses the ideal rocket equation to find the mass of the vehicle, but it iterates on this value to find a solution that incorporates forces other than the vehicle's thrust.

### 3.4 Mass Estimation and Sizing System

Once the propulsion team generated point designs using ranges of parameters, it was decided that further steps were necessary to visualize and analyze the selected designs, as well as generate the inputs needed to evaluate the designs using the 6 degree of freedom (6DOF) model, which will be discussed in detail in Section 3.5. The goal of this script is to determine whether point designs can fit the propulsion analysis' inert mass requirement, while doing preliminary structural analysis to ensure these materials and geometries pass minimum safety factor requirements.

#### 3.4.1 General Operation and Information

The program takes inputs from the Pareto analysis, as well as from preliminary mass and location estimates for the vehicle subsystems. Using the inputs gathered from these sources, the program then does the basic geometric layout of the rocket, generating lengths, wall thicknesses, and a design that can then be visualized with the help of tools such as OpenRocket and CAD software. The program also calculates key physical characteristics of the rocket, the center of mass and mass moment of inertia over the duration of the flight.

In order to simplify analysis, some assumptions about the rocket were made, which are covered in Table 10. The design generated contains the position and mass of all aerostructures and internal components from both stages. These include the nosecone, the sustainer airframe, the sustainer fins, the interstage, the booster airframe, and the booster fins. Internal components include the motor, the forward closure, the nozzle, the recovery subsystem, the despin subsystem, and the avionics subsystem.

The program also performs primary column buckling and local column buckling analysis on the sustainer airframe. This is done assuming the airframe is a fixed-free column; however this will change once the detailed design of the rocket is done. Currently this check is simply a “sanity check” so to speak, just as a qualifier for further analysis on each point design.

<b>Current Assumption</b>	<b>Justification</b>
All point designs are sub-minimum diameter	The sub-minimum design, when compared to their minimum, and other counterparts for such high powered applications, offered more benefits in mass and space saving.
All point designs use metallic airframes	Sub-minimum diameter rockets require their airframes to be pressure vessels, and the team does not have the capability to make composite overwrapped pressure vessels in-house.
All point designs use four fins for each stage	This assumption was made in order to perform first-order analysis; in the future, fin characteristics will be optimized by the 6DOF and prior art.
All point designs have a 5:1 Von Karman nosecone	Based on prior art; for other high powered rockets the 5:1 Von Karman design was commonly used.
Point designs do not have igniters, RF-transparent sections, nozzles, fasteners, or couplers	These components are a part of the detailed design, as such to reduce complexity, they were left out of the analysis.
All point designs' internal rocket components' dimensions and masses are static	These components are a part of the detailed design, as such to reduce complexity, they were left static in this analysis
All point designs' internal components are modeled as cylinders	In order to simplify for the first order analysis, as well as generalize for the wide range of point designs generated, the internal subteams provided us with simplified representations of their sub-systems

Table 10: Mass estimation and sizing assumptions

### 3.4.2 Analysis

The Pareto analysis provided the diameters of both stages, the maximum expected operating pressure (MEOP) of both motors, the mass of the motors as a function of time, the maximum drag force, and the maximum acceleration of the rocket. Additional inputs were also given in the form of material properties, and geometric properties.

The majority of the analysis was performed on the airframes, as the dimensions and stability of the airframe drive the viability of the point design.

Starting with the airframes, wall thickness of each stage was calculated using the MEOP of both motors and the thin wall hoop stress formula. The length of the motor is calculated using the propellant mass, the propellant density, and the internal diameter of the airframes. The forward closure was modeled as a uniformly loaded circular disk with clamped edges, and thickness was backsolved from the corresponding formula. The length was calculated by simply adding the length of the motor, the internals, and the bulkheads together, with some amount of room for error. The mass of the airframe and the bulkheads was calculated by calculating the volume of each and multiplying by material density. The script has three types of column buckling included, with two relevant criteria per airframe. The first, the primary buckling instability can be modeled by either the Euler or Johnson buckling formulas. The script chooses one over the other based on the slenderness ratio of the airframe and calculates the associated buckling stress. The third form of analysis is local buckling. The formula was obtained from NASA's SP 8007 manual [3], and used to calculate the critical local buckling stress.

To estimate inert masses, a simple method was used. For aerostructures, we calculated the volume of each component and multiplied by material density. For the internal components, the internal subteams were consulted on generalized masses and dimensions for each sub system that could be applied to all point designs. The motor mass was given by the Pareto analysis outputs, and is represented as a function of mass over the time duration of the flight.

The script calculates the center of mass of the rocket as a function of time, based on the motor mass time history, and was verified at the beginning and end of motor burns using OpenRocket. It also calculates the moment of inertia of the vehicle in its three principal dimensions. This was verified using SolidWorks models of point designs.

### 3.4.3 Results

After the Pareto analysis determined a significant number of viable point designs, the structures script was used to further narrow down this number. Most point designs were discarded because they could not meet inert mass requirements, while others were deemed to have motors that would be beyond our team's manufacturing capabilities. We used the 1DOF model to simulate all designs with an altitude ceiling of 150 km, however, the 6DOF model was not ready to validate or update this parameter. 6DOF validation of these point designs will likely bring down their flight ceiling significantly, and the extra altitude provides a mass budget excess that can be used in detailed design.

The materials and geometries used in the conceptual designs are primarily outlined in Section 7,

Variable	Minimum Value	Maximum Value
Inert Mass	14.39 kg	18.39 kg
Propellant Mass	28.73 kg	34.58 kg
Stage 1 Diameter	4.5 in	5.5 in
Stage 2 Diameter	4.0 in	4.75 in
Burn Times	6.1 sec	9.1 sec
Inert Mass Fraction	63%	67%
Delta V Split	35%	42.5%
Max. Mach Number	6.5	8.0

Table 11: Design space determined by the structures sizing process

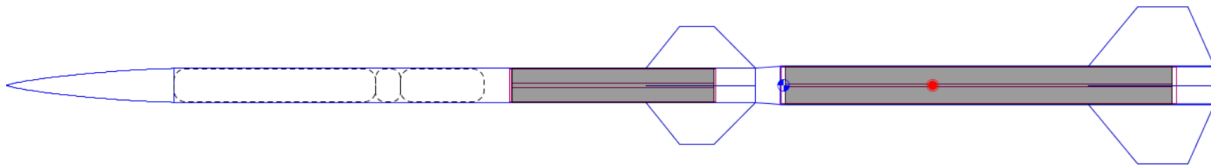


Figure 4: The 4"-4.5" design, shown in its expendable configuration

but the materials (aluminum, titanium, steel) were chosen for their availability, manufacturability, thermal resistance, and strength, while geometries were chosen based on prior art and manufacturability. Following the structures analysis and its simplifying assumptions, the design space determined viable point designs were found within the bounds in Table 11.

As stated in SR.4, the team wishes to have an expendable first stage. This appears viable examining prior spaceshot launches, but confirmation is needed. Sizing has established that viable point designs exist with first stages that are not recoverable, such as the 4.5 to 4 inch rocket in Figure 4. Additionally, viable point designs exist for fully recoverable rockets, such as the 5.5 to 4.75 inch rocket in Figure 5.

Throughout the rest of this report the work required to arrive at this design space will be presented. All of the work requiring dimensions and masses was done with the 4 to 4.5 inch expendable rocket, as this design represents the team's Minimum Viable Product (MVP). Once the 6DOF can evaluate the design space, then additional analysis will be performed to ensure that the assumptions and Pareto analysis still hold true.

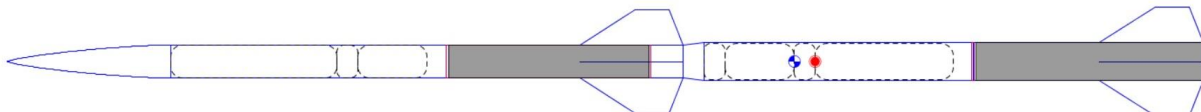


Figure 5: The 4.75"-5.5" design, which can reasonably be flown with either a recoverable or expendable first stage

### 3.5 Trajectory Analysis Model and Statistical Methods (6DOF)

Once a thorough primary design analysis is complete, the rocket must be simulated. To conduct more thorough analysis of the point designs identified by the initial sizing process, HA developed a six degree of freedom (6DOF) model, to simulate the flight of a design to a much higher level of accuracy. We decided to progress directly from a 1DOF to a 6DOF, since building an intermediate 3DOF would not have been easily adaptable into a 6DOF. This model will be refined as the program develops, and will eventually be used to determine the confidence interval on the rocket's apogee, and the landing ellipse where each stage will touch down.

The 6DOF model we developed runs in MATLAB Simulink. All the aerodynamic data is generated by a 1997 version of Missile DATCOM. While the most updated versions of this software are export controlled, the 1997 version is approved for public release and uncontrolled. Aerodynamic tables are generated in DATCOM; a table corresponds to a single rocket geometry over a range of altitudes, Mach numbers, combined sideslip and angle of attack, and roll angles. The 6DOF numerically integrates the dynamic equations of motion corresponding to both position and orientation.

The 6DOF models the rocket's motion in three spatial dimensions and their respective rotational modes as a result of in-flight forces, namely, thrust, gravity, and aerodynamics. A full attitude representation is given with respect to a geodetic frame, which has its third basis vector pointed at the center of the Earth. It also models motion relative to a rotating Earth and the included effects. The 6DOF requires an initialization script consisting of initial conditions for all relevant differential equations, atmospheric effects, Earth effects, an aerodynamic reference table for all stability derivatives, and design-specific variables: these are mass histories, MOI histories, center of mass, and thrust curves for both stages.. Once the simulation has run, a post-processing script provides trajectory visualization. Additionally, the simulation has the capability for dispersion analysis (currently only for apogee dispersion with a confidence ellipsoid) but only if the proper covariance is available. The simulation primarily uses discrete integration.

#### 3.5.1 Strengths and Shortcomings

The 6DOF as it exists currently is not in its final state; there are a number of refinements planned for future semesters. However, analyses done for this report still contain the somewhat simplified assumptions of the current 6DOF. In Table 12, the assumptions made by the current model are enumerated, along with the planned improvements, when relevant.

A strength of our model is its flexibility in rocket geometry; we can completely specify the geometry, and must only generate a new aerodynamic table with Missile DATCOM. We can also track any variable or any group of variables against each other using the MATLAB Simulink data inspector and scopes for real-time analysis. While this will be very useful as the detailed design of the vehicle converges, the breadth of the design space in these initial stages can be daunting. Since a single aerodynamic table generation takes upwards of a half hour, we are reluctant to generate many tables; instead we are working on how to appropriately and reasonably interpolate inside of the tables for reasonably small design changes. This process is not trivial and will take time and input from others to achieve.

<b>Current Assumption</b>	<b>Explanation / Planned Improvement</b>
Wind/discrete gusts not considered	We plan to use the wind/gust model built into Simulink
The rocket geometry is currently axisymmetric	This simplifies the dynamic model and the workload for the structures team without any significant loss in fidelity
The simulation stops at apogee	In the near future, we will model the parachute deployments and descents, including drift
Staging is perfect	We may add randomly-varying moments and forces on the stages at separation
Staging is instantaneous	DATCOM cannot simulate the aerodynamic properties of two bodies in proximity; within the 6DOF, we will continue to neglect the dynamics of staging and focus only on the body of primary analysis
Spin stabilization and de-spin are not modeled	As the stability analyses develop, this capability will be added to the 6DOF
Thrust curve does not vary (constant thrust during burn)	As the design of the motors develops, realistic error will be injected into the thrust tables to model real variance of solid motors
Thrust is perfectly aligned through the body primary axis	We will add random variability in the direction of the thrust, to simulate minor misalignments of the motor in the airframe
Simulation starts right off the rail (neglects complex dynamics on the rail)	Since the dynamics of the rocket on the rail are very important to the overall trajectory, we are working to develop and integrate a rail model into the 6DOF with friction and added noise

Table 12: Summary of current 6DOF assumptions

### 3.5.2 Stability

An important task for the 6DOF is to ensure the vehicle is suitably stable at all phases of the flight. Many rockets with similar missions spin-stabilize; this is a possibility we are still evaluating. In the future, we will simulate flights with canted fins, for example, and compare the stability to flights with un-canted fins. It is likely that the vehicle will spin some amount even without canted fins, due to manufacturing tolerances, and this is also something that will need to be characterized.

We plan to perform basic transient stability analyses on the aerodynamic coefficients throughout the flight. As some of the coefficients behave like damping terms in a classical mass-spring-damper system, we observe decaying sinusoidal motion in the stability derivatives with respect to time. Analyzing parameters like rise time, peak time, steady state, overshoot, and other factors can allow us to assess the raw stability of the system in the context of converging to a steady state, such as a small (preferably near-zero) angle of attack and sideslip angle, steady rolling motion, and small pitching/yawing oscillations. Beyond this, our team is currently working on a rigorous stability analysis methodology that will allow us to analyze a design or compare it to an ideal case. Additionally, the transonic flight regime will be scrutinized to a high degree as it is a key area of interest regarding flight stability. From there, specific CFD cases can be defined and investigated.

### 3.5.3 Statistical Methods

For higher-fidelity results, a single simulation per configuration will be insufficient. To properly characterize the influences of the many unknown components of the vehicle's flight, we will need to perform hundreds or thousands of flights with the same configuration, only varying the noise and sources of error. We expect the most significant sources of noise in a real flight to be

- Wind / turbulence
- The launch rail, and the forces it puts on the vehicle
- Manufacturing tolerances in the vehicle, especially the fins
- Variance in the motors, in terms of total impulse, the particular thrust curve, and the axis of thrust
- Large and quick disturbances in the turbulence of transonic flight
- Staging interactions

Moving forward, the primary metrics we will characterize probabilistically will be the apogee, and the landing locations for each stage. With the planned improvements in Table 12 implemented, we will be able to run Monte-Carlo type analyses to determine confidence intervals on these two metrics. Currently, a chi-squared analysis is in place based on very basic covariance data to determine a “confidence ellipsoid,” wherein the rocket is expected to be at apogee with 95% confidence, for example.

### 3.5.4 Results

Currently, no definitive results from a two-stage spaceshot capable rocket (using point-design geometries from the Pareto analysis and fin configurations from preliminary structural analysis) due to some aerodynamic issues likely stemming from the static force and moment contributions. However, in the absence of these static contributions, full trajectories can be plotted with the

inclusion of staging. Because a trajectory without the (very important) static force and moment contributions is not a true representation of the vehicle's stability, in combination with the fact that in the absence of the static contribution, the dynamic contribution becomes quite small (due to the scaling by the inverse of the velocity) and ultimately does not impact the trajectory by much. Therefore, until this issue can be resolved, no “true” spaceshot trajectories can be provided. The other issue is generating accurate moments of inertia data — as the motor burns, the moment of inertia will change, as will the center of mass. This, as well as the changing center of pressure, can change the stability of the rocket as measured without the changing moments of inertia.

In the case of designs from which realistic aerodynamics can be generated, plots of all relevant dynamic parameters can be made. This includes: all aerodynamic forces and moments, angle of attack and sideslip angle (and their respective derivatives), body velocity and acceleration components, altitude, downrange and crossrange distance, mass, thrust, angular velocity about the principle body axes, Euler angles (yaw, pitch, roll) and their respective derivatives with respect of the geodetic frame, Mach number, and center of pressure.

### 3.5.5 Validation

Since this flight model is designed entirely by students (with the exception of the aerodynamics, from Missile DATCOM), it is important to ensure the results produced are accurate to real-life performance. At this early stage, only rough validation has been performed, since the model is still a work in progress. However, we have sought to “check our work” as we go. For example, the model in its current state can run neglecting all aerodynamic forces, to test the dynamics alone. Simple trajectories have been validated with hand calculations of projectile motion. We separately tested and verified our blocks for Newton’s second law, Euler’s law, our quaternion/DCM models for attitude dynamics, and Earth effects. Since complete rigid body dynamics were validated some time ago, we moved forward with aerodynamics implementation. It then becomes much less trivial to assess the validity of the aerodynamics. We trust Missile DATCOM to give sound aerodynamics data in the range of dependencies specific earlier based on body geometry, fin setup, nosecone, and some other inputs, however, validation is still required. We have some open source flight simulations to compare against such as RASAero and RocketPy which both have valid aerodynamic models, however, data on some of the dynamic stability derivatives is more limited compared to the static ones.

A more concrete form of validation will be through existing flight data. We plan to simulate other rockets, and compare the simulated parameters of the flight with the true values. We hope to use both past PSP flights, as well as other vehicles’, especially in the high-altitude regime.

We have also explored the possibility of doing tests on the actual vehicle to empirically determine the aerodynamic coefficients. We are evaluating the benefits and drawbacks of using a supersonic blowdown wind tunnel in the future to accomplish this. Since this would be a significant amount of time in the future, we have no detailed plans for this at the moment. One important benefit would be increased assurance of the stability of our rocket in sensitive flight regimes. However, it would require a significant effort on our part to design and manufacture a scale model and ensure it is dynamically similar to the real flow we are interested in analyzing. We would also need to develop a run matrix, and analyze the data that comes out of the wind tunnel test. We have not yet made any

serious proposals for use other than an interest presentation.

## 4 Propulsion

### 4.1 Introduction

The key responsibility of the propulsion system is to propel the rocket to the Kármán line utilizing two separate stages, each having their own individual propulsion systems (PRO.1 and PRO.2). Quantitative requirements that each motor will need to fulfill are being determined through Pareto analysis and the 6DOF model. The two point designs and the results of our analysis determine the specific aspects of the propulsion system. The team will thoroughly verify the ability of the propulsion system to complete the mission through simulation and testing. Each stage will contain its own ignition motor made of the same formulation as the main motor. While the first stage ignition will be manually activated by the mission control room, the second stage will be ignited by the avionics system on the second stage.

The formulation for each of the rocket motors and igniters is based on NATO propellant research [19] and will be carefully mixed and manufactured at Purdue University's propulsion laboratory — Maurice J. Zucrow Laboratories. Through direct coordination with Zucrow, the propulsion team will construct a robust test stand in order to evaluate the performance of propulsion mechanisms and their interactions with other systems.

Throughout the research, design, manufacturing, and testing process, the team recognizes that it is paramount that safety is placed first, and is taking proper precautions to ensure this. We realize the inherent dangers of working with solid propellants and will work with experienced researchers to ensure the process is as safe as possible.

### 4.2 Performance

Two different point designs are currently being considered for the two-stage propulsion system based on system integration between the first and second stages. Currently, the primary difference between each design is the motor diameter. Variations and optimizations of the fuel grain geometry, the shape of the burning surface of the solid motor, will be determined after a point design is selected. Each point design was simulated based on each motor utilizing a BATES grain geometry (shown in Figure 6) with sub-minimum motor diameter. A CAD mockup is shown in Figure 7. The quantitative requirements of performance for each design to achieve its mission were found through the thrust profiles from the 1DOF model and  $\Delta V$  outputs from the Pareto analysis. The first design considered has a first stage with an external diameter of 4.5 inches and a second stage with an external diameter of 4 inches. The second design consideration has a first stage with an external diameter of 5.5 inches and a second stage with an external diameter of 4.75 inches. The performance of each design is displayed in Table 13.

### 4.3 Ignition

Ignition of both stages will be achieved through small ignition motors in their respective forward bulkheads (PRO.1.2, PRO.2.2). These ignition motors will be made of a faster-burning propellant than the main motors with a smaller-scale nozzle and casing to account for the change in atmospheric conditions at high altitudes. The igniters themselves will be ignited with a small pyrotechnic ignition

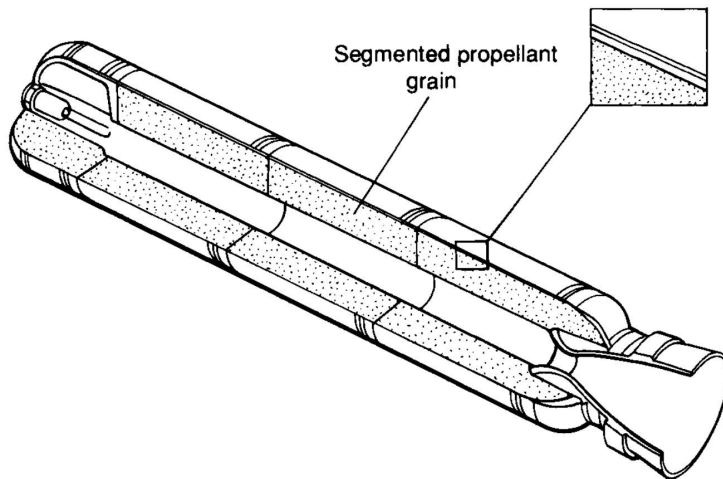


Figure 6: Section view of a segmented BATES grain (from [22])

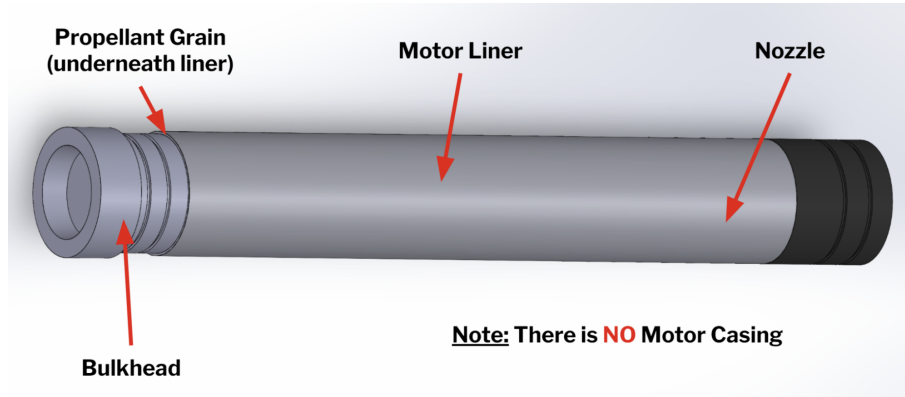


Figure 7: CAD mockup of a sub-minimum diameter BATES motor assembly

<b>4" - 4.5" Design</b>				
Burn Time (s)	$\Delta V$ (km/s)	$\Delta V$ Split (Stage 1)	Impulse Requirement (N·s)	
6 - 9	3.7 - 3.8	42.5%	Total	~ 80 000
			Stage 1	~ 60 000
			Stage 2	~ 20 000

<b>4.75" - 5.5" Design</b>				
Burn Time (s)	$\Delta V$ (km/s)	$\Delta V$ Split (Stage 1)	Impulse Requirement (N·s)	
7 - 9	3.4 - 3.5	35%	Total	~ 100 000
			Stage 1	~ 56 000
			Stage 2	~ 44 000

Table 13: Quantitative propulsion results of the Pareto analysis for both point designs

Hazard	Mitigation
Unwetted micrometric and nanometric metals pose an aerosol inhalation hazard	Any fine (micron) powders should be added inside of the ZL6 fume hood. Add metals and fine oxidizer close to the binder surface and wet thoroughly by hand stirring.
Unwetted micro-metals pose an electrostatic discharge ignition hazard	Wear wrist ESD grounding straps during weighing and addition of micrometals.
Ammonium perchlorate exposure can cause kidney and thyroid damage	Use a ceiling mounted high-volume draft fan operating at 100% flowrate during the entire mixing procedure.
Isocyanates used as curatives are highly neurotoxic and are an inhalation hazard	Use low vapor pressure isocyanate. Any isocyanate will be weighed out and added to the mixing bowl within the ZL6 fume hood.
Skin absorption of propellants can be toxic to operator	Wear appropriate nitrile gloves and safety glasses for the entire procedure. In case of contact, flush out the area of the skin with water and follow propellant material safety data sheets for further instructions.
Ignition of propellant in bowl during mixing	Mixing will be conducted away from any flammable materials. No smoking or open flames will be permitted in the mixing cell.
Waste presents fire and toxicity hazard	Dispose of any excess propellant or contaminated material through Purdue's REM.

Table 15: Hazards present in the mixing process, and mitigation plans

charge. Ignition of the first stage will be controlled via a wired connection to the control room. A manual key will be used for safety to inhibit unplanned ignition. The second stage will ignite via on-board avionics. This will be disarmed on the pad and remotely armed via an actuator with a physical key in the airframe. The actuator will be able to arm and disarm the second-stage ignition system remotely.

When the second stage ignites, a burst disk will be applied on the nozzle to keep atmospheric pressure in the combustion chamber. While optimal separation is through drag separation, if an event occurs where this does not happen, stages will separate using the thrust from the second-stage motor. This will be discussed further in Section 6.3.

#### 4.4 Manufacturing

Motors will be mixed at Zucrow Labs, in building ZL6 using the Hobart 20 qt dough mixer. All fine powders will be measured in a fume hood with wrist ESD grounding straps to prevent ignition. Pants, lab coats, nitrile gloves, and eye protection will be worn during every stage of the mixing process. Solids will be carefully wetted in increments. Propellant will be vacuum processed after mixing/before casting to evacuate air bubbles. Propellant will be pourable and cast into Kraft paper

tubes around a removable mandrel to form the grain shape. Paper tubes are used for inhibition of the outer surface. Grains will be cast longer than needed and cut to the exact length for propellant consistency. Grains will be glued into the phenolic motor insulator, and the grain faces will be cut concavely to prevent accidental face inhibition.

All mixing operations will be performed under the supervision of Tim Manship or an approved Zucrow graduate student. All waste propellants and chemicals will be disposed of in accordance with the Purdue Radiological and Environmental Management (REM) requirements [10]. Hazards and mitigation relevant to the mixing procedure are discussed in the Table 15.

## 4.5 Testing

The objectives of the testing process will be to confirm the safe operation of the propulsion system and to verify its ability to meet our performance requirements. The first phase of testing will be propellant formula characterization. The second phase will include the creation of a test stand in direct collaboration with Zucrow Laboratories and motor testing of our propellant. The test stand design will incorporate elements found in industry and academic test stands to maximize safety and simplicity. The team will utilize an iterative testing process where small-scale tests are conducted to confirm prior analysis and modeling before building upon the data to create larger-scale and more comprehensive tests.

Propellant formula will be characterized through pressure bomb strand-burning analysis to obtain the burn rate coefficient and exponent. This testing will be completed under existing safety procedures at Zucrow Laboratories and manufacturing of strands will be completed safely as outlined in our manufacturing section. Example safety procedures are provided in Appendix E. Along with strand burning, tensile testing of propellant dog bones will help confirm the propellant formulation exhibits the required mechanical properties to complete the mission, such as the propellant's tensile strength.

After small-scale propellant testing, a subscale single-grain Bates motor cast with our propellant will be tested to confirm predicted chamber pressures and thrust based on modeling and simulation. Finally, full-scale motors will be tested before launch to confirm that systems work nominally on a large scale and are capable of achieving the required total delta V (PRO.1.1.4, PRO.2.1.4) and thrust profile. Effects of the propulsion system on other subsystems will be tested to confirm that heat generated by the motors does not deteriorate the integrity of the rocket structure. Additional tests will indicate how quickly and effectively the second-stage igniter can accept the fire signal from the avionics system.

A horizontal test stand will be used to experimentally verify the thrust (delay, duration, and maximum) and chamber pressure values predicted by the simulations subteam. The majority of solid motors in industry are tested horizontally as this is typically safer in the event of a test stand failure. Mounting motors horizontally eliminates the need for any actions to be performed on an elevated surface because the entire motor is close to the ground. This simplifies testing setup and limits the time spent in close proximity to energetics. Solid motor performances are also not significantly affected by gravity, so it is not necessary for the team to create a vertical test stand which simulates the proper launch orientation.

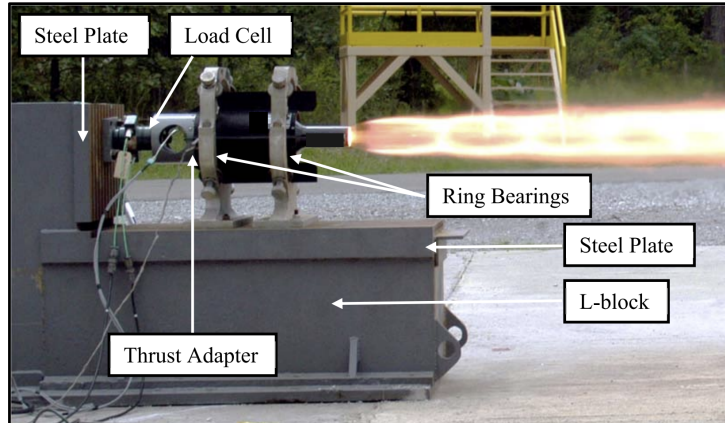


Figure 8: Solid rocket motor firing from a mobile L-block (from [8])

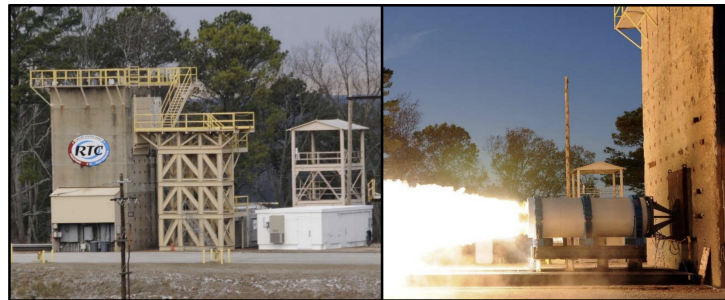


Figure 9: Solid rocket motor firing from a fixed L-block (from [8])

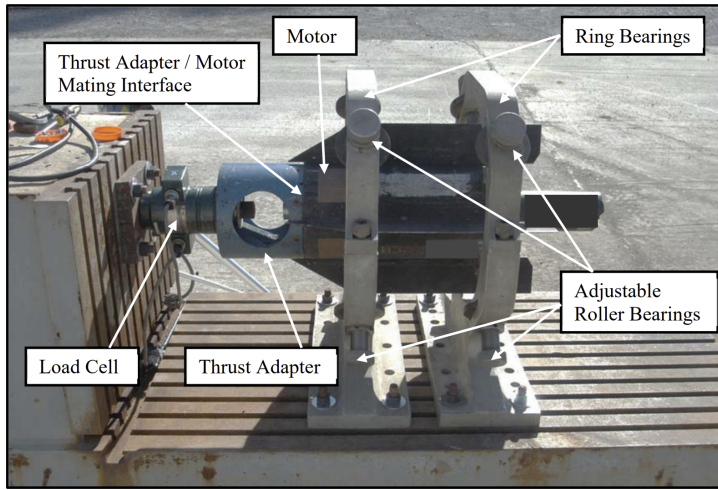


Figure 10: Ring / roller bearing arrangement used for leveling and centering (from [8])

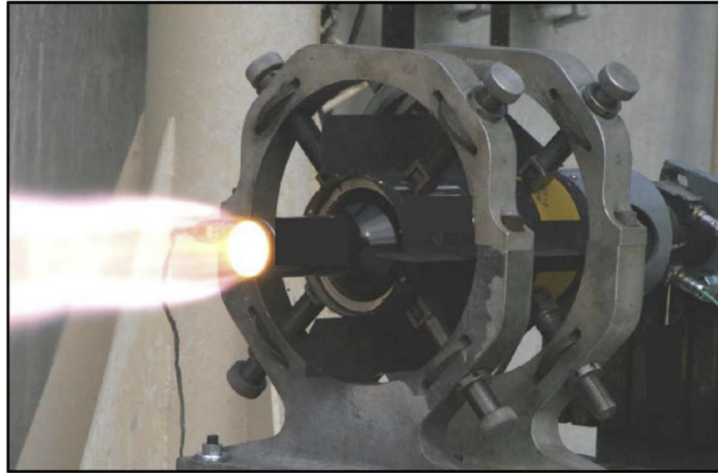


Figure 11: Typical static motor firing (from [8])

To verify the safety of our testing systems, research has been conducted into prior test stand designs that are centered around an I-beam assembly. One of the more well-documented I-beam test stand designs is that of the University of Alabama Huntsville. The university has created two similar L-block designs, with the key difference between them being that one features a mobile L-block (Figure 8) while the other features a fixed L-block (Figure 8). The mobile L-block is employed when testing small, tactical-size motors and can be placed at several different locations within their facility campus depending on the test objectives. By contrast, the fixed L-block is a monolithic reinforced concrete/rebar block that is embedded up to 50 feet below grade and surrounded by a concrete apron, which acts as the horizontal “L” face. The main component of the horizontal face is a rail system based around an I-beam that can accommodate motor-firing carts of different sizes. The vertical “L” face is reinforced with concrete and a large, 6-inch-thick steel plate to support the motor and handle high thrust forces during firing [8].

Prior to motor installation, the L-block is prepared with measurement tools suited for the motor

being fired. The appropriate load cell, thrust adapter, ring bearings, and various other specific attachment hardware are installed (Figure 10 and Figure 11). Next, a mock motor of the proper dimensions is installed to ensure preliminary centering and leveling with the centerline of the load cell and thrust adapter. Installing a motor in the system involves using adjustable cylindrical roller bearings which contact the motor case and allow free axial motion of the motor. Following this initial process, a live motor is installed in place of the mock motor, with the centering and leveling fine-tuned (involving close monitoring of the distribution of light around the motor in the interface between the thrust adapter and the motor) before the motor is seated into the thrust adapter and bolted in place. After arming the motor, all testing operations personnel must return to the control room to begin the static fire. Safety is further ensured through FEA determination of the maximum yield stress beforehand. Strain gauge-based canister load cells measure the motor thrust by means of electrical signals, with a larger signal correlating with a larger thrust force [8].

In addition to rigorous verification of the design of our test systems, we must verify the safety of our procedures. We will refer to existing Zucrow Laboratories procedures to create new procedures for motor assembly and hot-fire. Alongside instructions needed to conduct the test, the procedures will include appropriate PPE to be used; potential hazards and mitigation, such as limiting smoking and open fires near flammable objects; and lastly any additional procedures needed in case of a safety incident such as an occurrence of fire on the test setup. Any fire will not be fought. Instead, the building will be evacuated and emergency contacts will be approached. Hazards specific to each test will have additional safety requirements, given in Table 17, Table 19, and Table 21.

Currently, any procedures created are provisional as designs are not finalized. All procedures will be revised accordingly to any design changes. Before any testing is conducted, safety procedures will be verified by Tim Manship and Scott Meyer. Additionally, subject matter experts Dr. Stephen D. Heister and Prof. Mark Grubelich will actively provide any feedback as they deem necessary. All members who will conduct tests shall fulfill Zucrow Laboratories training requirements that will be provided by Tim and Scott in addition to reviewing each test procedure.

## 4.6 Analysis and Simulation

As safety is of paramount concern, structural Finite Element Analysis (FEA) will be used during the design of the test stand and motor to ensure designs meet all safety requirements. FEA results combined with hand calculations will be used to determine bolt preloads, torques, and show that all components can handle expected loads scaled by safety factors while retaining a positive safety margin. The FEA models will be created and run using Siemens NX Nastran.

Once vehicle sizing has been completed, motor grains will be designed to match the optimal thrust vs time profile for the flight. Two Blackburn simulation programs are planned to be used for grain design. The initial design will be completed using BurnSim, a commercially available burnback program. Once an adequate base grain design has been determined, an in-house optimization program will be used to refine the geometry to its final state. The program is based on work done by Magni Johannsson [14] but will use different simulation programs. The optimizer will combine an NX (CAD-based) surface regression program with a MATLAB-based ballistic modeling script for thrust and pressure calculations, and a derivative-free local optimization program called NOMADS.

Hazard	Mitigation
Snap ring assembly	Wear safety glasses and work gloves when installing snap rings. Cup tensioned snap ring with hands while installing and point snap ring away from people.
Mounting brackets are heavy and may pose a hazard when suspended	Require a minimum of two people to lift any heavy objects.
Early, unintended ignition of test motor	Keep ignition circuit isolated until the motor is ready for testing. Keep any flames or heat sources away from propellant grains.
Catastrophic motor failure	Ensure all testing is conducted remotely, with appropriate stand-off distances or bunkers in place. Fire suppression systems must be easily accessible.

Table 17: Hazards present during hot fire testing, and mitigation plans

Hazard	Mitigation
Toxic chemicals, aerosol sprays	Use aerosol sprays in well-ventilated spaces and avoid breathing in aerosolized mist.

Table 19: Hazards present during dog bone testing, and mitigation plans

Hazard	Mitigation
Failure of pressurized parts	Test will be operated remotely from a control room.
Ignition of energetics during handling and preparation	Use small sample sizes (<5g) and wear PPE.
Post-experiment residue exposure	Purge pressure vessel with an inert gas after experiment.

Table 21: Hazards present during pressure vessel and Crawford bomb testing, and mitigation plans

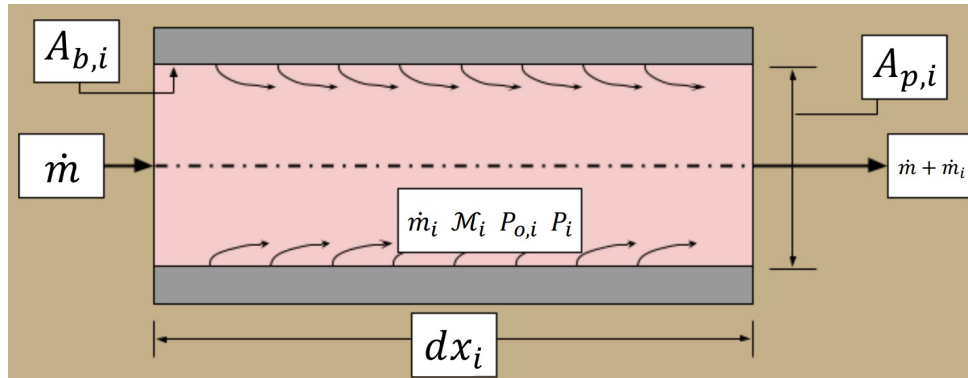


Figure 12: Diagram of the control volume for solid rocket motor combustion analysis

The dual program approach will be used due to the runtime of each program and the lack of documentation on the calculation methods used by BurnSim. The quick run speed of BurnSim allows for rapid iterations of geometry with reasonable results before transitioning to our own ballistic code. Our code takes longer to run, but provides thrust and pressure results with more confidence as we know how calculations are being done.

## 4.7 Combustion Modeling

In order to properly model the internal combustion of a motor, relations were derived based upon quasi-one-dimensional flow relations and by utilizing a mass and momentum balance. This particular method tracks discrete elements in the combustion chamber as a function of time. By selecting the system to be the port of the motor, conservation of mass can be used as mass input from the propellant grain, and mass output through the nozzle of the rocket. This understanding along with isentropic relations builds the foundation of this model and is able to track the combustion processes to occur.

The core of this model revolves around discretized segments of the grain into a large number of elements, of which a sample element is shown below. In the schematic, each element adds a certain amount of mass to the exhaust gas in the port of the element, which then changes the total pressure, static pressure, and Mach number which leads to compressibility effects in the fluid. The amount of mass that is being added to the flow is dictated by the surface area of the propellant, which can be modeled as a function of web, while the Mach number is affected by the port's cross sectional area.

The key advantage of splitting each segment into elements is the ability to track the exhaust gas property changes as a function of axial distance down the motor, and by time. When run until termination of the program, this ability to track per element allows for the compilation of data as a time history for a simulated burn of the motor. This allowed for our team to match certain qualities of a motor to things such as grain geometry and chamber pressure, chamber pressure and thrust as a function of time, and other key propulsive performance metrics.

The initial head pressure conditions are estimated with the Steady State Lumped Parameter model, shown in Equation (1), which is then used to iteratively find a quasi-transient head chamber pressure. The program then steps axially through the elements of each segment and updates the

Symbol	Meaning
$a$	Burn rate coefficient
$A_b$	Burn surface area
$A_t$	Throat area
$c^*$	Characteristic velocity
$\gamma$	Ratio of specific heats
$n$	Burn rate exponent
$M$	Mach number
$R$	Specific gas constant
$\rho$	Density
$T_c$	Chamber temperature

Table 22: Symbols used in the equations in this section

flow properties as it goes, using Equations 2 through 5. Once the last element has been run, a mass balance is performed to check the amount of mass accumulated in the port to the theoretical mass that should have accumulated as dictated by Equation (8). If the two values of mass were within a tolerance of one another, then a time step equal to half of the chamber time constant was taken which updated the geometry of the grain with the appropriate web based on the local stagnation pressure at each element. Additionally, NASA CEA was utilized to find local exhaust properties of each element based on the chamber pressure. When an element “burned out” meaning there was no more exposed propellant that had a surface area, then that element was treated as a slot. Each slot was modeled as a single element that had a stagnation pressure loss as found in [12]. The program would terminate when all of the elements have burned to their maximum web or the stagnation pressure at the head of the motor was less than 200 psi (chosen to show the ending of the burn). The model algorithm structure can be found in Figure 13.

The algorithm solved the following equations as a system of equations for each element, via the following process.

1. Solve Equation (2) for the mass input of that segment using the assumption that static and Mach number are the same as for the previous element
2. Solve Equation (3) for stagnation pressure using the previous element’s Mach number
3. Solve Equation (4) for static pressure using the previous element’s Mach number
4. Solve Equation (5) for Mach number implicitly
5. Resolve Equation (4) with updated Mach number for static pressure
6. Resolve Equation (3) with updated Mach number and static pressure for stagnation pressure
7. Resolve Equation (2) with updated stagnation pressure

The algorithm was tested with the solid rocket boosters of the Space Shuttle as shown modeled in Figure 14, which slightly altered the grain geometry of the Space Shuttle by replacing the 11 pointed star with a cross pattern in section A-A. The given burn rate coefficients to St. Robert’s law, were estimated to be  $a = 0.038 \frac{\text{in}}{\text{s} \cdot \text{psi}^n}$  and  $n = 0.35$ . The Space Shuttle propellant used was 69.6

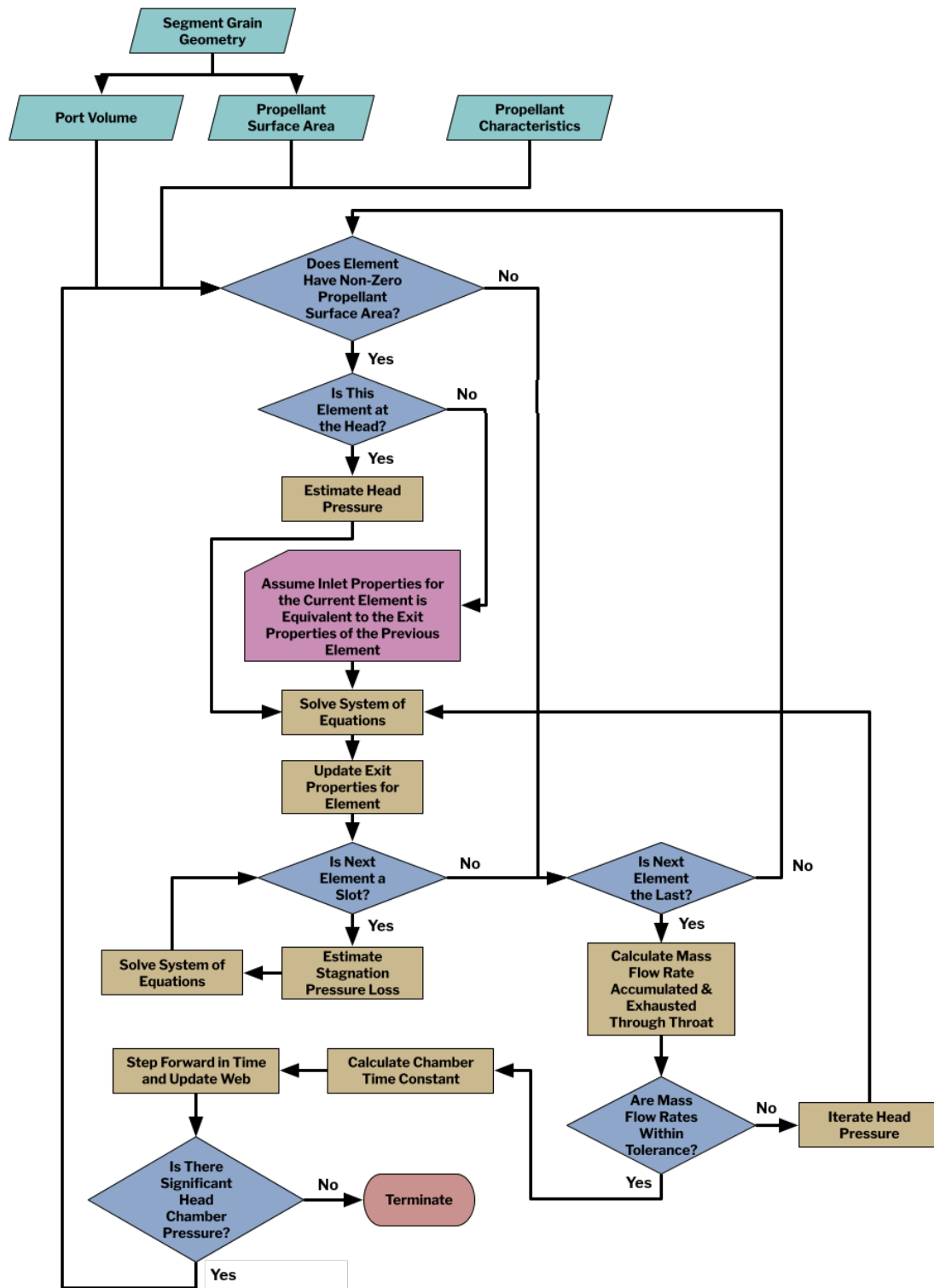


Figure 13: Flow chart representing the ballistic model algorithm

$$P_0 = \left( \frac{a\rho A_b c^*}{gA_t} \right)^{\frac{1}{1-n}} \quad (1)$$

Steady lumped parameter model (estimate head pressure)

$$\dot{m}_i = a P_{o,i}^n \rho A_{b,i} \quad (2)$$

Continuity equation

$$P_{0,i} = \frac{P_{i-1}}{1 + \gamma \mathcal{M}_i^2 \left( \frac{\dot{m}_i}{\dot{m}} \right)} \quad (3)$$

Momentum Equation

$$P_i = \frac{P_{0,i}}{\left( 1 + \frac{\gamma-1}{2} \mathcal{M}_i^2 \right)^{\frac{\gamma}{\gamma-1}}} \quad (4)$$

ISENTROPIC pressure relation

$$\dot{m}_i + \frac{\dot{m}_i}{2} = \left( \frac{\mathcal{M}_i P_{0,i} A_{p,i}}{\sqrt{\frac{RT_c}{\gamma}}} \right) \left( 1 + \frac{\gamma-1}{2} \mathcal{M}_i^2 \right)^{\frac{-\gamma-1}{2(\gamma-1)}} \quad (5)$$

Average mass flow; is solved for Mach number ( $\mathcal{M}_i$ )

$$\dot{m}_{in} \sum_{i=1}^n \dot{m}_i \quad (6)$$

Mass accumulation

$$\dot{m}_{out} = \frac{g P_{0,n} A_t}{c^*} \quad (7)$$

Mass ejected through the throat

$$\frac{dm}{dt} = m \left[ \frac{dP_{0,n}}{dt} \left( \frac{1}{P_0} \right) + \frac{dV}{dt} \left( \frac{1}{V} \right) \right] \quad (8)$$

Theoretical mass flow rate accumulated in the combustion chamber

$$\frac{dm}{dt} = \dot{m}_{in} - \dot{m}_{out} \quad (9)$$

Actual mass flow rate accumulated in the combustion chamber

$$\tau = \frac{\rho_g V}{\dot{m}_{out}} \quad (10)$$

Chamber time constant (amount of time to expel entire exhaust gas and replace;  $\sim 0.1 - 0.15$  seconds)

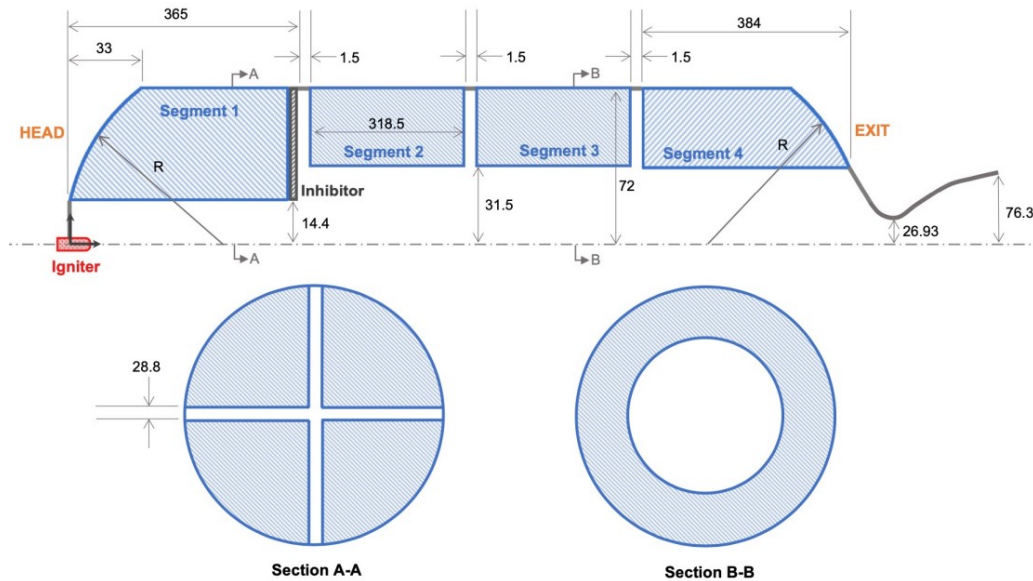


Figure 14: Cross section of model shuttle solid rocket booster, with different grain geometries highlighted

wt% Ammonium Perchlorate, 16 wt% Aluminum, 14 wt% Polybutadiene acrylonitrile (PBAN), .4 wt% Iron(III) Oxide.

After the convergence of the system of equations and termination, certain compressible flow losses can be seen from the results of the program as shown by Figure 17. As the motor burned, the Mach number decreased, shown in Figure 16, which led to less total pressure loss, and ultimately less entropy generation. The port area dictates the flow's Mach number which if high enough, leads to compressible effects and erosive burning. This is typically around Mach 0.3.

While the thrust profile of the model was similar when compared to the published data from the Space Shuttle, some key differences are noticeable. This is because the actual booster had an 11-pointed star grain geometry whereas the model uses a simple cross geometry. Additionally, erosive burning was not accounted for due to the relatively low Mach throughout the port. However, the magnitude of thrust for the max Q range between 20 - 75 seconds is highly comparable between the model and the actual results.

It was found that Mach number decreases in the slot elements due to stagnation pressure loss and the increase in cross sectional area while Mach Increases down the port due to heat and mass addition.

Rate of the mass flow rate accumulation changes as a function of time for each segment due to the surface area of the segment changing. It can be seen comparing the initial slope visually to the slope after a period of time that segment 1 burns regressively since its slope decreases with time and segments 2-4 burn progressively since their slope increases with time. As the segments burn axially in the slotted regions, the slotted region grows, and no mass is accumulated in that region.

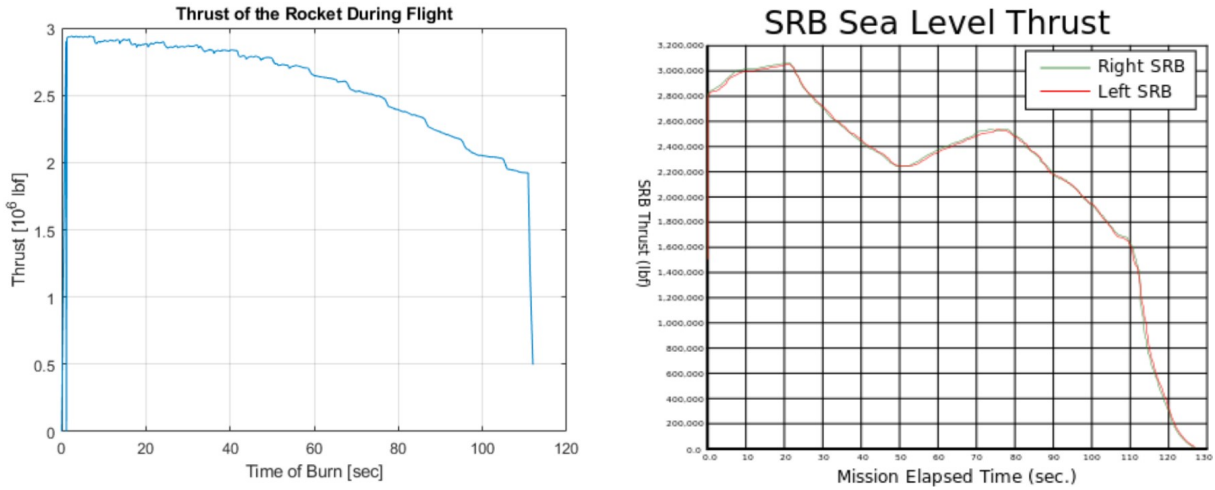


Figure 15: Thrust curve produced by our model, compared to the true thrust curve of the Space Shuttle SRBs

Ultimately by using the Space Shuttle as a case study, and comparing it to real data, we are able to build confidence in our ballistics code. In the future this program will be utilized to match grain geometries to chamber pressure profiles from selected point designs. There are a near infinite number of grain geometries to fit a pressure curve, but using intuition on manufacturability and prior art on geometries we will hopefully be able to deduce what the geometry could look like. Furthermore, this model will be used after Bates testing has been done with our chosen propellant in order to update burn rates, chamber pressure, and thrust as a function of time. With more accurate data, in the future this model could be improved by adding an erosive burn rate modifier by using Green's model  $r = aP_c^n(1 + kM)$ , where  $k$  is found experimentally.

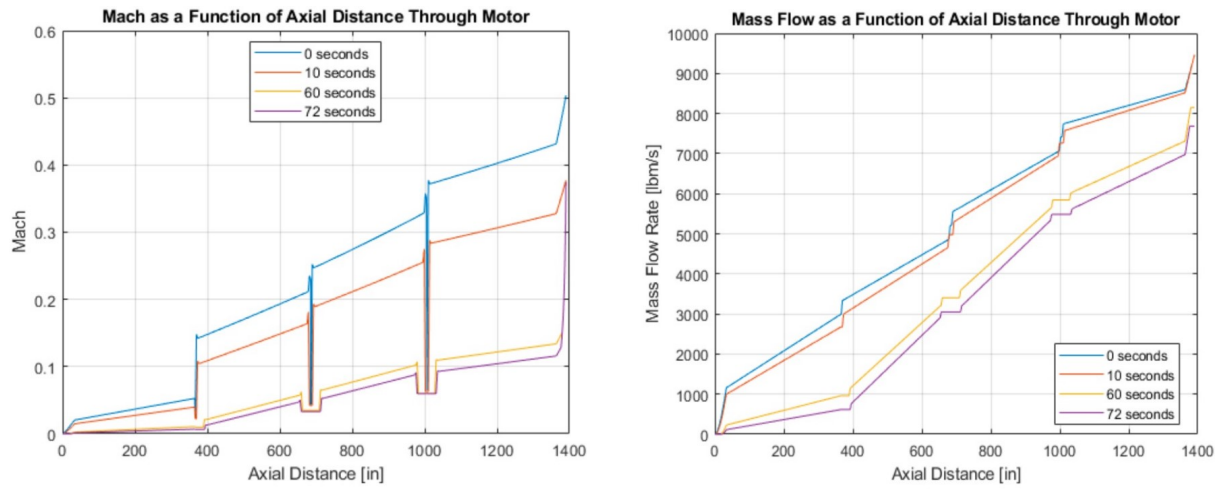


Figure 16: Mach number through each element's port, and mass flow through the motor

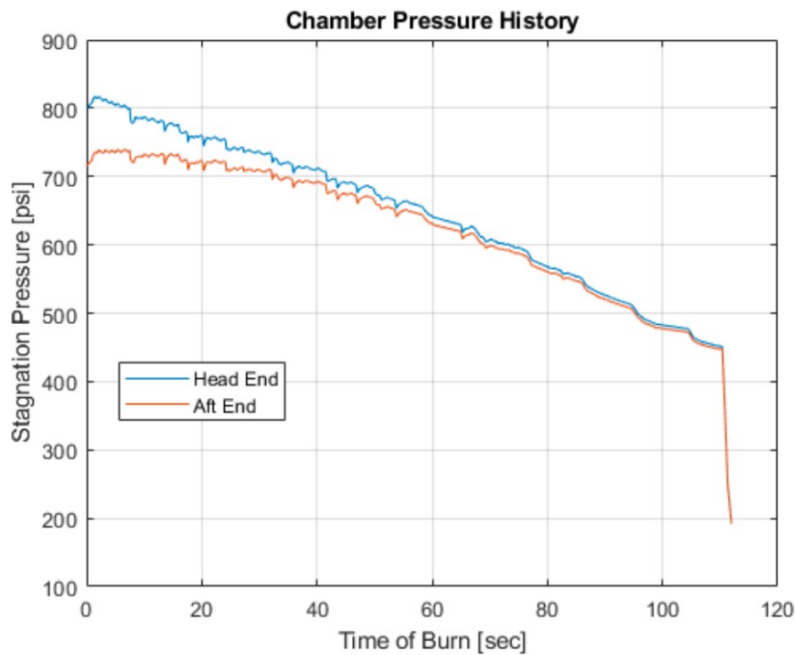


Figure 17: Model chamber pressure

## 5 Avionics

### 5.1 State Estimation and Apogee Determination

Considering the team's overarching goal of reaching the altitude of 100 km, an important responsibility of the avionics system is to verify the apogee reached by the vehicle. The objective of the flight will not be achieved without high confidence that the vehicle has reached the target altitude. Being able to verify the rocket's apogee (AVI.1) will be achieved through a culmination of different data in order to account for the highly dynamic environment throughout the spaceshot. During the flight, the avionics system will record several different datastreams, and an algorithm will combine all the data collected to estimate the state of the rocket (AVI.1.1). This data will be stored onboard and recovered to allow a more accurate apogee verification after the flight (AVI.1.2).

#### 5.1.1 System Architecture

The avionics system will consist of both Commercial Off-The-Shelf (COTS) and Student Researched and Developed (SRAD) components. There will be both a primary and backup flight computer for redundancy on the vehicle. The current plan is to use the SRAD flight computer as the primary flight controller, with one or more COTS computers as backups. This setup is preferred because the SRAD computer allows for more customization of hardware and software to better match the overall profile of the flight. The SRAD computer will gather and store data from multiple sensors, estimate the rocket's current state, trigger staging and recovery events, and possibly transmit data to the ground. It will also allow all the raw sensor data to be stored for analysis on the ground. However, extensive development and testing of the SRAD flight computer is still in progress. It may be determined after testing that higher customization of the SRAD board does not outweigh the reliability and flight heritage of commercially available options. In this case, the SRAD system will primarily record data for post-flight analysis, while a COTS computer will be the primary controller for the flight.

One COTS flight computer option under consideration is the AltusMetrum Telemega<sup>5</sup>. This computer includes a GPS, Inertial Measurement Unit (IMU), and barometer. It has the ability to trigger staging and recovery events, based on altitude and attitude data, only triggering flight events when the programmed conditions are met. It also can transmit telemetry to the ground. However, it does have limitations. Due to COCOM regulations<sup>6</sup>, its GPS will provide data at altitudes greater than 50 km or velocities greater than 500 m/s. While this computer has Kalman filtering and could work on a 100 km flight, it has many limitations, as is further discussed in Section 5.1.2. Finally, its telemetry downlink antenna only has a range of about 12 km, which is much less than the distance traveled throughout the flight.

By using the SRAD flight computer, GPS data could be obtained up to 80 km<sup>7</sup>, and a more precise accelerometer and barometer could be used. It would also have custom software to match

<sup>5</sup>The Altus Metrum Owner's Manual can be found at [this link](#).

<sup>6</sup>Due to government regulations, commercially available GPS units will not provide data while they are above 60,000 ft (18 km) MSL and traveling faster than 1000 knots (500 m/s). Some manufacturers enforce both limits, while others only use one, and some use the speed limit with varying height limits.

<sup>7</sup>The ublox MAX-M10S is capable of this altitude, per its [data sheet](#).

the mission of the rocket. This includes more specific conditions for triggering events, an improved Kalman filter that uses the predicted mass and aerodynamic profile of the rocket, and storing all the raw sensor data and GPS satellite pings for post-flight analysis.

The discussion until now has been about the avionics system on the second stage. If the first stage of the vehicle is expended, it will require no avionics system, but if it is recovered, it will have its own avionics bay, which would likely be entirely COTS components to reduce complexity. A COTS system onboard the first stage would serve the simple purpose of parachute deployment. Because of the lower altitude, flight speed, and reduced flight complexity, an SRAD system would be unnecessary, and only serve to increase complexity and chance of failure. Whether or not the first stage is expended, the stage separation and ignition will be controlled by the second stage avionics system. Therefore, regardless of which design is used for the space shot, the design of the second stage avionics system will be unaffected.

### 5.1.2 Data Fusion Algorithm

In order to provide telemetry and trigger flight events, the SRAD flight computer must know the current state of the rocket throughout the flight. “State” includes the rocket’s position, velocity, and attitude on all 3 axes. To do this, the computer will take measurements from three different sensors: a 6-axis IMU, a barometric pressure sensor, and a GPS. These sensors all have their own benefits and limitations, and their individual reliability will change throughout the flight. While GPS might provide the most accurate measurement of position, it will not be available for the entirety of the flight. Due to COCOM regulations, the GPS receiver will not provide data when moving faster than 500 m/s and/or above a set altitude, dependent on the specific module. Even without these restrictions, a GPS may have trouble obtaining a lock during the highest-speed portions of the flight. Additionally, there could be radio frequency (RF) interference from parts of the rocket, limiting the GPS signal transmission. We are aware of rockets operating in similar flight regimes experiencing these issues; USC’s Traveler IV spaceshot did not have a GPS lock for the majority of the flight, and Derek Deville’s Qu8k, despite carrying four different GPS modules, failed to maintain a lock.

The other two data streams are flawed as well. A pressure sensor, sampling the ambient air pressure, can be used to estimate the rocket’s current altitude. This requires adding holes to the airframe to equalize the pressure in the avionics bay with the external ambient pressure. However, shock waves from traveling at supersonic speeds can interfere with the ambient pressure readings. Additionally, pressure readings will become ineffective once the atmospheric pressure decreases below 10 mbar (25-30 km MSL). The 6-axis IMU measures acceleration and rotational rates. This data will need to be integrated to get a measurement of state, and this causes error to build up over time. Finally, all of these sensor measurements will have some level of noise which will decrease their precision.

In order to obtain the best state estimate from multiple measurement sources, a sensor fusion algorithm is needed. This sensor fusion algorithm will be some version of a Kalman filter, likely an Extended Kalman Filter (EKF). A Kalman filter combines a measurement with a predicted value, and outputs the estimated state along with a measurement of the uncertainty. An EKF works for non-linear systems, which include systems with multiple measurement inputs. Although some COTS computers (such as the Telemega) use Kalman filtering, they are limited since they do not have any

information about the flight profile or the aerodynamic characteristics of the rocket, so they fall back on a simpler physical model. An EKF run on the SRAD computer can provide a more accurate estimate, because the state update function can account for the thrust, mass, and drag profile of the rocket. This sensor fusion algorithm is currently being developed and tested using MATLAB and Simulink, as discussed in the testing section.

In addition to the onboard state estimation, the raw sensor data and GPS satellite pings from the flight will be saved for post-flight analysis on the ground. The data will be analyzed with more accurate methods that may be too computationally expensive to run during the flight. This will allow the apogee to be estimated with more precision.

### 5.1.3 Testing

The flight computer's software algorithms are currently being developed in MATLAB Simulink, and will go through software in the loop testing in Simulink to validate them prior to flight. First, the 6DOF simulation will provide a theoretical flight path of the rocket. State data from this flight path is then converted into sensor data that would be generated by the computer's sensors. This includes adding noise to the sensor outputs and matching the frequency and range of the sensor. This simulated data is then sent to the Simulink flight computer prototype. The flight computer's state output can then be compared to the simulation output to judge the accuracy of the state estimation algorithm. This allows changes to be made to the algorithm to find optimize the estimate. This method will also be used to test the flight logic. Many potential failure modes can be tested to verify that the flight computer makes the correct decision in each scenario.

For verifying firmware functionality, we will unit test all sensor and hardware drivers extensively using fakes, which are essentially simplified software models of the corresponding devices. Unit tests will be written both for native desktop hardware as well as the target boards to balance ease of development and accuracy. Unit tests will use a hardware abstraction layer that calls into faked models of the hardware to allow seamless testing without hardware being available. We are also currently investigating doing hardware in the loop testing. However, due to the complexity of implementing such a system and the diminishing increase in failure scenarios being tested, we intend to pursue this only if we have extra time, and will not make this a limiting goal on our timeline.

Finally, the flight computer will be tested as a passive data recorder on many flights before it is the primary computer on any rocket. Its state estimation will then be compared to data from other COTS flight computers on the rocket to determine its accuracy.

## 5.2 In-Flight Events

As previously discussed, the spaceshot vehicle will have two stages with a recoverable upper stage. During the flight, this requires a stage separation and ignition followed later by a recovery system deployment. The avionics system will be in charge of sending the activations for these flight events (AVI.2 and AVI.3). The activation conditions of these events need to be carefully verified before the rocket is permitted to proceed to the next stage of flight (AVI.2.1, AVI.3.1, MEC.3, and PRO.1.2.1.2), and this process will be completed by the avionics' onboard state estimation algorithm. After this verification occurs, the signal will be sent to activate the relevant subsystems on the rocket (AVI.2.2 and AVI.3.2).

In order to ensure the flight events happen in the correct order, the SRAD flight computer will keep track of the current phase of flight. These phases can only happen in the intended order. Transitions between phases will be triggered when conditions using the rocket's position or acceleration data are met. These phases include: on the pad; first stage burn; first stage coast; second stage burn; second stage coast; and descent. There are specific conditions that must be met for transitioning between phases and triggering events which are based on altitude, acceleration, and/or attitude. For example, the second stage can only be ignited when the rocket is pointing less than a set angle from vertical. If this condition isn't met, there is an option for a second stage abort scenario. A more detailed summary and flowchart of phases and transition criteria is available in Appendix D. This flight sequence is modeled using Simulink and Stateflow, which can be compiled into C and run on the flight computer.

### 5.2.1 Safety

To ensure the safety of everyone working on the rocket, we intend to employ several subsystems that will ensure that energetic materials are not inadvertently triggered in unsafe situations or before they are expected to.

In order to prevent triggering of the motor or recovery hardware while the rocket is assembled, all avionics hardware will have a hardware power cutoff controlled by switches that will not be enabled until the rocket is vertical. We are currently exploring two primary cutoff schemes. The first is a WiFi switch, which can be opened and closed over a wireless connection. This is a device we have used in the past, and it has performed very reliably. However, the switch does not automatically give an indication of its state. A simple solution might be to wire a buzzer in-line. The second option that we are exploring is a mechanical pin, which arms the avionics when pulled out of the rocket. This might require a larger mechanism, along with a hole in the airframe, but it is conceptually simpler than the WiFi switch, and it gives a clear visual indication of its state.

Two systems to arm the flight computer that we are not pursuing are magnetic switches and key switches. On previous launches, we have used magnetic switches, but they have shown consistent reliability issues. Key switches embedded in the body of the rocket come with many of the benefits of the pin, but there is more structural complexity. Additionally, if the keyway protrudes from the vehicle at all, there are aerodynamic concerns.

We also plan to include software or hardware lockout timers that will ensure that staging or recovery doesn't occur during early stages of the flight where potentially anomalous sensor data is expected (high acceleration and transonic regimes). On SRAD flight computers and programmable COTS boards, we intend to use time based software lockouts as we believe that the primary points of failure are the state estimation algorithms, which a software lockout at the flight logic level should be able to mitigate.

Finally, a similar system will be used to disable send stage motor ignition after a certain time period. This is to ensure that in the case of a second stage abort, it is safe to later approach and recover the rocket without fear of the second stage motor (which would still be loaded) accidentally being ignited. To minimize complexity, we intend to have an electromechanical system trigger a digital timer on launch that then cuts off a relay or transistor after the prescribed time (i.e. the system is prevented from igniting the second stage motor after five minutes have passed beyond

the detected launch).

### 5.3 Downlink

It is critical that the team is able to locate the rocket after the flight is completed and the rocket has touched down (AVI.4). In order to achieve this, the rocket will use GPS data so the recovery crew can have accurate coordinates of the landed vehicle (AVI.4.1). Due to potential GPS limitations, the rocket will transmit the GPS data throughout the flight as it is received (AVI.4.2). This will allow the recovery crew to have accurate GPS readings of position and velocity for as long as possible, being able to estimate the final ground location if needed.

While it would be ideal to have live telemetry throughout the entire flight, it is most important to have a signal on the descent portion so that the rocket can be tracked for recovery. One significant challenge of live telemetry is getting a RF signal out of the airframe, which is likely to be metal. To solve this problem, the avionics bay will be inside an RF transparent section of the airframe. The length of this section of airframe will likely need to be at least the length of any antennas inside of it. This will also allow the GPS receivers to receive GPS signals. Even with this section, there may be other sources of interference to the antennas during flight. Also, the orientation of the antennas may affect their signal range. To ensure a strong signal on the descent, an antenna may be attached to the parachute or shock cord so that it leaves the body of the rocket after parachute deployment.

There are multiple COTS GPS modules that can transmit telemetry to the ground. One option is the Multitronix Kate-3 GPS Tracking System. This system apparently does not have a GPS altitude limit, but it does still have the COCOM speed limit of 500 m/s. It also includes an accelerometer, but this has a limit of 50G, which may be less than the forces experienced during flight. Because of this and its lack of a barometer, it is currently not planned to be used for triggering staging and recovery events. However, it may be used as the primary telemetry system since it can transmit telemetry to a range of 150 km.

On the other hand, an SRAD solution could be more adaptable to our specific needs. On the rocket, we could transmit telemetry using simple FM transmitter modules like the popular Radiometrix HX1 (but likely at higher frequencies) used in high-altitude balloons, or higher power XBee modules. We could experiment and research a wider range of frequencies, protocols, and data rates in order to find a solution that maximizes range and reliability. This would also give us the options to test different antennas to maximize range while decreasing space use. Antennas will need further research and guidance as they have many tradeoffs, especially in the rocket. We want to try to maximize range, but the rocket's antennas should also be omnidirectional to allow reception in any position the rocket may land. Additionally, we should try to limit the size of the RF transmissible airframe section, since it will decrease the overall structural integrity of the vehicle. On the ground we could use a combination of omnidirectional and directional antennas to allow flexibility in how we track the rocket. This could include a simple custom ground station with a software defined radio (SDR). This custom ground station would make it easier to use different antennas and also allow us to tune into different frequencies.

## 5.4 Payload

To satisfy our stakeholder requirements (SR.5), the spaceshot vehicle will have a payload, which will not be essential to the successful flight of the vehicle. The payload will include a camera, but if there is more available mass and volume, we hope to include additional items. To support additional payload mass, as well as general overruns in component design, the vehicle is being sized with an apogee of 150km, well above our true target.

The camera system will, at a minimum, consist of a single camera looking radially out of the second stage. This imposes a requirement on the vehicle to de-spin if it is spin stabilized, so that good imagery can be captured (MEC.1). The detailed design of the camera bay is beyond the scope of this review, but we expect the hole cut in the rocket to remain uncovered, as opposed to being blocked by a transparent window. The specific model of camera to be used will be based primarily on reliability and flight heritage; based on a brief study of comparable-performance amateur rockets, GoPro cameras seem to be the leading candidate.

If the payload subsystem is allocated more mass and volume than a single camera requires, we plan to add additional components to the payload. Ideas under consideration include

- A camera inside the recovery bay, watching the deployment of the parachute
- A thermal camera inside the nosecone, to characterize the thermal loading
- A collection of COTS avionics boards, so we can later publish their performance on such an extreme flight
- A biological experiment, as minimal as a Petri dish, to explore the effects of a zero-g environment
- A LEGO Minifigure of the Star Wars character Mace Windu, which has flown on all previous HA flights

The specific components of the payload subsystem will be determined by PDR, once the actual mass and volume constraints are solidified.

## 5.5 Durability

While actively collecting, calculating, and transmitting data, the rocket will undergo very high accelerations and pressures. The avionics systems need to be able to survive these intensities throughout the flight with a successful recovery (AVI.5). To ensure this survivability, the system will be prepared to withstand certain forces, vibrations, and thermal environments (AVI.5.1, AVI.5.2, and AVI.5.3).

For the design of the SRAD board, we do not expect to have major problems with structural loading, since soldered and especially surface mounted (SMT) components should be able to handle forces well beyond what the rocket is expected to experience. However, we are considering potting the SRAD board to ensure any larger components like capacitors do not break off. We need to further investigate the viability and benefit of doing this. One potential issue with potting the board is that heat produced by the board may be trapped, leading to it overheating. However, we expect the power draw of our board to be low, so this issue is unlikely to be a problem. Another concern is that the barometer may get blocked from reading the ambient pressure. This issue requires more

investigation into the specifics of potting.

For testing performance under acceleration, we are planning a test in which we will attach the board to the wheel of a vehicle, and drive it to simulate a 200g load on the board (the maximum our planned linear accelerometer would be able to measure). This acceleration is likely much higher than any sustained forces during the flight, but there should be little to no cost to additionally verifying that the board can work up to those accelerations.

The biggest problem we anticipate is vibration causing breakage of connectors and wires going to and from the board. Our current plan of mitigating this is soldering as many connections as possible before assembly, and using latching connectors for any final connections. In addition, for the final flight we will try to use SMT components as much as possible, including for the storage media. We currently do not have a good way of testing the impact of this problem or the efficacy of our solutions, but we will continue to look into leveraging resources at Purdue and beyond to determine if we can perform useful vibration testing.

The final consideration related to avionics durability is thermal resilience. Many of the components we will be using have a maximum temperature rating as low as 85 degrees Celsius. Early thermal estimates show internal air temperatures in the avionics bay exceeding that value. It is not possible for us to take any action on this front until the structural design of the vehicle and the thermal analyses become more developed.

## 6 Mechanisms

### 6.1 Recovery System

As discussed earlier in this report, we are currently unsure whether the first stage of the space-shot vehicle will be expended. For this reason, we are designing systems to safely recover both stages (MEC.2), with the understanding that the first stage recovery system may be removed in the future.

For the second stage of the rocket, descent speeds are not to exceed 50 feet per second above 1000 feet in altitude, and must not exceed 20 feet per second below 1000 feet to keep the more sensitive structures of the vehicle intact (MEC.2.2). Under the assumption that the booster stage also needs to be recovered, it has a similar set of requirements, though the allowable velocities will be some amount higher since it is expected that the first stage will be more durable and more able to withstand a hard landing (MEC.2.1). Depending on the booster recovery design selected, this velocity will likely range between 20 and 40 feet per second.

The recovery systems for each stage will deploy from a single airframe separation in each of their respective airframes (MEC.2.1.2 and MEC.2.2.2). Prior to separation, each of the airframe sections will be held together through the use of nylon shear pins. The booster recovery system will deploy from a break in the airframe between the motor and the staging interface. The sustainer recovery system will deploy from a break above avionics and below the nosecone. Due to the high altitude of both recovery deployments, a simple separation mechanism will be used to break apart the airframe (MEC.2.1.2.1 and MEC.2.2.2.1). The specifics for this device are found later in Section 6.2.

#### 6.1.1 First Stage Recovery

Two minimal recovery designs for the first stage are being considered, in case it is determined that the first stage must not be expended. Line diagrams for all the recovery schemes discussed in this report are provided in Appendix C, for further reference. The first design consists exclusively of a separation mechanism, one line of shock cord approximately twice the length of the booster, and a mid-sized parachute. This option is intended to be extremely compact and lightweight to allow for minimal design work by the structures and avionics teams. As only a single chute is used for this design, descent speeds will be much higher than the ideal 15 to 20 feet per second below 1000 feet. Descent speeds will likely range between 30 and 40 feet per second for the entirety of the descent to prevent excessive drift from the stage's apogee. The landing impact for the booster will be more forceful than what a typical recovery system would result in, but we currently expect the booster to be tough enough to withstand the conditions without severe damage. Since no valuable payload is onboard, this rough landing is deemed acceptable.

The second parachute option we are considering is a "Sombrero". This device is a mini-parachute attached to the canopy cords, which is able to freely slide up and down, allowing the main chute to unfurl roughly depending on its position. Early estimates indicate this system could use only five times the rocket length in shock cord compared to the nine times used by a conventional drogue-main setup. Acquiring one may be difficult, as the "Sombrero" is a patented device created by Butler Parachutes. They do offer custom orders for parachute systems, but pricing is unknown

and requires further inquiry. Another option would be to manufacture a similar system in-house, but that leads to risk of the device being of poor quality and failing during use. This parachute system offers a great way to reduce mass and volume, but it is difficult to source or manufacture.

While the two recovery systems are similar, they each pose their own advantages and disadvantages. The single chute alone is by far the simplest, most reliable, lightest, and cheapest method, but it has the booster landing at a high velocity of 30 to 40 feet per second. This will undoubtedly damage the booster to some extent, but it is likely to remain in one piece. Also, it is not likely to bury itself in the launch range, allowing for it to be easily located and retrieved. The sombrero avoids a hard impact, but it is significantly more difficult to manufacture, is far more expensive, and adds more mass to the rocket. Further research will be conducted into both systems to choose an ideal option.

### **6.1.2 Second Stage Recovery**

There are also two options for second stage recovery systems. Line diagrams for these options are provided in Appendix C. The first option is the most massive as it requires 8-9 times the length of the sustainer in shock cord. However, currently it is deemed the most reliable method, and the team has the most experience with this system as similar recovery designs have been used for two of our previous flights. This method uses a traditional drogue-to-main parachute scheme. At apogee, the separation mechanism separates the single sustainer airframe break and deploys the drogue parachute, also releasing the main parachute bundled in a parachute bag. A single line of shock cord will run from the drogue parachute to the rocket body where it is attached by use of a tender descender. A tender descender is a simple device that holds two quick links together until a black powder charge that was previously contained within the device detonates in response to a signal from the avionics computers. This line connecting the drogue to the tender descender will carry all of the chute tension above 1000 feet in altitude. During descent, the drogue will slow the rocket down to acceptable speeds around 50 feet per second before the system reaches 1000 feet in altitude. Shock packs, various devices that reduce the high forces of parachute deployment or snatch force, will be implemented throughout the system to limit stress on mechanical mounting structures during descent.

Running parallel to the tender descender to drogue shock cord during the entirety of the descent above 1000 feet will be a secondary set of shock cords which connect the main chute to both the drogue chute and the rocket body. This shock cord will use a different mounting location than the tender descender. Above 1000 feet, this system will be in slack, and the main parachute will be contained within its bag. At 1000 feet, the tender descender holding the force of the drogue chute will separate, transferring the path of tension through the shock cord connected to the main chute. This tension will rapidly remove the main chute from its bag as the rocket body falls away from the drogue parachute. As the path of tension will transfer from the rocket, to the main, and then to the drogue, the upward force of the drogue will help to quickly inflate the main parachute. The deployed main parachute will then bring the rocket descent speed down to a gentle 15 to 20 feet per second.

For the sustainer stage recovery, the second recovery option that is being researched is reefing parachutes. This system consists of a main chute that can be variably deployed by temporarily fixing

the shroud line length via a reefing ring. Essentially, this system allows the single parachute to act both as the drogue and the main chute. This system would greatly decrease the amount of shock cord required to roughly four times the length of the rocket and entirely eliminate the need for a drogue chute, saving valuable mass and volume. Also, if only one chute is used, it would reduce the snatch force the rocket would experience, compared to deploying a chute in the standard fashion. However, as a team, we lack experience using this system and creating or sourcing a reefed chute has an unknown price tag or level of reliability.

After researching several reefing options, the following are being considered:

1. Single reefing ring: simplest option, but not too predictable especially at high altitudes.
2. Double reefing ring configuration: Using friction, we can delay the opening process of the parachute. We still need to further study this option.
3. Active reefing process: Using a triggered event from avionics to loosen or drop the reefing ring, allowing the chute to expand from a drogue to a main at a specified altitude. This option requires significantly more research.

As it contains 8 to 9 times the length of the rocket in shock cord, two chutes and a tender descender, the first recovery method mentioned, is by far the heaviest and least space-efficient option. However, this is the option the team has the most experience with, is more reliable, and is easier to manufacture and assemble. The reefing method will take up approximately half of the volume of the first option, immediately making it a strong contender. Various methods of reefing will continue to be explored and tested, but at this time the reliability and feasibility of this much more compact method is still in question.

## 6.2 Separation Mechanism

Due to the high altitude required of the recovery deployments for both stages of this vehicle, traditional black powder airframe separations are not viable. These simple systems require atmospheric pressure to both fill the airframe with compressed gas and provide a medium for heat transfer to ignite nearly all of the black powder used in the initial charge. In the low pressure environments in which this rocket will require an airframe separation, another solution is needed (MEC.2.1.2.1 and MEC.2.2.2.1). As recovery systems using tender descenders will not require their use above 1000 feet in altitude, the operation of tender descenders will not be impacted by these same concerns.

Many rockets flying at these high altitudes use a compressed CO<sub>2</sub> separation system for airframe separation. This technique was researched, but CO<sub>2</sub> canisters and the various systems used to release the gas and separate the airframe are rather bulky, heavy, and relatively complicated which could lead to various points of failure. Since two separation systems could be required for the rocket, this method was deemed unsatisfactory. Instead, a simple black powder piston-like device was designed. A preliminary CAD model of this device is shown in Figure 18. This device consists of a mounting plate, a compartment of O-ring sealed atmosphere within a piston like chamber, a pushing plate, and a firebolt.

A firebolt is simply a bolt that has had a hole drilled through it to allow for the passage of e-match electronic ignitors through the bolt. These e-matches are then sealed within the bolt through the

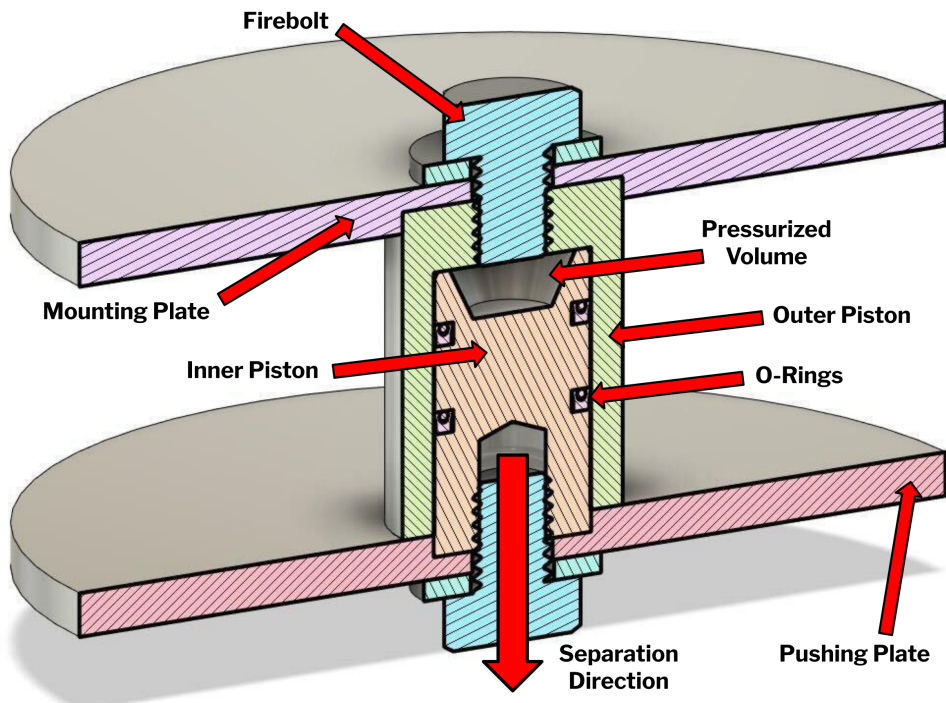


Figure 18: CAD model of the preliminary piston-based separation device

use of epoxy and a small sealed container of about 0.5 grams to 1 gram of black powder is placed around the ignitor tip of the e-matches. The exact amount of black powder will be determined through on the ground testing of the system long before launch. The threads of the bolt can be wrapped with pipe sealant and placed within the device to form a proper seal, leaving the black powder on the inside of the separation mechanism and the e-match leads on the other end. These leads will be connected to the avionics computers which will then be able to ignite the black powder at a specified time or altitude. As the black powder is contained within a small pocket of atmospheric pressure at any altitude, proper ignition is possible and the separation mechanism will separate itself and the airframe of the rocket in the process.

To actually achieve separation of the airframe, the black powder ignition will force the inner piston upwards relative to the rocket. This movement will be transferred to the airframe coupling through the use of the pushing plate. Since the coupling is attached to the upper half of the airframe and the mounting plate of the separation mechanism is attached to the lower airframe, this force will push the airframe apart.

Two separation mechanisms will be included in the entire rocket if the first stage is required to be recovered: one in the booster stage and one in the sustainer. In both cases, the separation mechanism will be located directly below the parachute bay and above the avionics bay. This allows for easy and safe wiring of the firebolt to the avionics computers. During final rocket assembly, the connection of the two halves of the piston will be the final step, leaving any accidental ignition of the black powder free to expand safely without causing harm to the assembly team or equipment.

### 6.3 Inter-Stage Mechanism

An essential part of the rocket's flight is the clean separation of the two stages between their burns. Since a failure to separate would very likely lead to catastrophic mission failure, it was decided that a stage separation mechanism would need to be developed to satisfy MEC.3.

After preliminary development and research, we concluded that the main separation mechanism should be as simple as possible. The optimal time to separate, based on minimizing the loss of velocity due to drag, is when the two stages would naturally drag-separate, i.e. the drag on the first stage "pulls" it off the second stage. However, we are unable to simulate the complex aerodynamics of two free bodies in proximity. Thus, the separation scheme we propose is as follows.

1. The first stage burns out
2. The optimal time of separation occurs. Depending on the aerodynamics of the vehicle, this may occur immediately after first stage burnout. Additionally, the stages may not naturally drag-separate at this point
3. If the stages do not naturally drag-separate, we will ignite the upper-stage motor, to "hot-separate" the stages
4. Either from the hot separation, or after a short coast after drag-separating, the second stage burn begins

We considered using a mechanism to retain the stages together until the ignition of the upper stage. Shear pins were the leading candidate for this. However, there are potential stability concerns with hot-separating with shear pins. Specifically, if one shear pin breaks even a fraction of a second before the others, a strong moment will be put on the vehicle, disturbing it from its trajectory while the second stage motor is firing. This is unacceptable, so we decided the two stages would simply be nested into each other geometrically, with only a small amount of friction to overcome to stage. Using this separation scheme allows the rocket to be reduced in mass, as no extra mechanism is required in order for the stages to separate. This also saves on cost, as no extra materials are needed. Additionally, it would still keep the second stage stable during separation, allowing the second stage to continue on course as predicted.

A concern of ours with this scheme is that the uncertainty of the natural drag separation leads to imprecision in our simulation. However, we plan to mitigate this by running simulations where the stages drag-separate immediately after burnout, and simulations where the stages remain together until the second stage ignition.

### 6.4 De-Spin Mechanism

While many rockets with similar missions to ours spin-stabilize, we are not yet able to determine if we will need to. While that uncertainty exists, we have been examining the feasibility of de-spin systems. To satisfy other needs of the mission, namely recovery and payload concerns, the vehicle must be rolling at a rate no higher than 60 revolutions per minute when it reaches apogee (MEC.1). At this point, our analysis has assumed a very large range of possible initial spin rates, between 50 and 1000 revolutions per minute. Of course, as the stability analyses develop, this range will be tightened. After researching the common options for despin, the mechanisms that the team considered were yo-yo despin, cold gas thrusters, hot gas thrusters, and a reaction wheel system.

Yo-yo despin is achieved by wrapping two cables, each attached to a mass, around the rocket. A release mechanism allows the cords to unwind at the desired time, allowing the masses to spread out to the full length of the rope which increases the rocket's moment of inertia. When the cords are fully extended, they release from the vehicle, carrying a significant amount of angular momentum. Additional optimizations can be done, such as using cables with elasticity, but our preliminary analysis was done with the most basic model. Yo-yo despin is relatively simple, and requires only a small amount of mass and volume.

Cold and hot gas thrusters operate on similar principles. Two small nozzles are aimed tangentially to the airframe, and exhaust gasses are ejected, slowing the rotation of the vehicle. Cold gas thrusters are fuelled by a tank of compressed gas, typically nitrogen or carbon dioxide, while hot gas thrusters use small solid rocket motors to generate the exhaust gas. For both cases, we considered only passive systems with fixed amounts of impulse; a more complex system might, for example, close the valve between the tank and the nozzles when the rotation rate slows sufficiently.

Finally, a reaction wheel would also be capable of reducing the spin of the vehicle by using a motor to spin a flywheel inside the stage. The angular momentum of the stage as a whole would be transferred to the flywheel alone. However, unlike the other three designs considered, this system is actively controlled, requiring a microcontroller to drive the motor. Also unlike the other three, this system does not actually discard the angular momentum of the vehicle, so the flywheel must continue to spin until landing.

Analyses were performed for each of these candidates. The results of these analyses were condensed into the decision matrix shown in Table 23. Each system was ranked on eight metrics, each on a scale from 1, the worst, to 10, the best. These metrics are generally simple to understand, such as cost and mass, but some have more nuance. The explanations below clarify our interpretation of each metric.

- **Testability:** Ease with which a test rig can be built with similar dynamics to the flight despin mechanism. A higher number indicates that we believe that the design would be easier to test in a meaningful way.
- **Reliability:** How infrequently the system fails in the flight environment.
- **Precision:** How frequently the despin mechanism is able to reduce the spin within the acceptable range. A higher number indicates the system is more consistently capable of slowing the vehicle to zero spin, regardless of initial spin, while a lower-ranked system would leave the vehicle spinning more often.
- **Simulability:** The accuracy of a simulation of the system. A higher number indicates a system that can be modeled with very high accuracy.

Based on this evaluation, yo-yo despin is the most optimal method. It is not the most highly rated method in every category, but is the best overall. Assuming that spin-stabilization is required, the team's de-spin method of choice to ensure successful parachute deployment will be the yo-yo method.

While parameters of the rocket are currently in flux this early in the design process, using the current estimates available, performance for the yo-yo despin mechanism can be calculated. We conducted a literature search for the governing equations for yo-yo despin. Equations from four

Metric	Weight	Yo-yo	Cold Gas	Hot Gas	Reaction Wheel
Mass	5	6	2	9	1
Volume	5	8	1	9	3
Reliability	8	8	6	5	8
Cost	5	9	2	8	3
Testability	8	10	6	8	10
Precision	7	8	1	1	10
Manufacturability	8	9	3	7	5
Simulability	7	8	2	2	9
<b>Totals:</b>		443	166	311	352

Table 23: Decision matrix for the de-spin mechanism

sources ([4], [6], [17], and [20]) were determined to be equivalent, under the following assumptions, drawn from those sources:

- Cables unwind at a constant rate
- Cables are massless
- Despin masses are point masses
- System is perfectly conservative
- Gravitational effects are negligible
- Cables are released when radial (see Figure 19)
- Rocket rotation is perfectly on-axis

Figure 20 shows the required cable length, as a function of the yo-yo mass, to de-spin the vehicle completely. This analysis makes conservative assumptions: a stage dry mass of 10 kg, distributed as a cylindrical shell, and a 4 inch diameter. The relationship proves the feasibility of this mechanism for our mission.

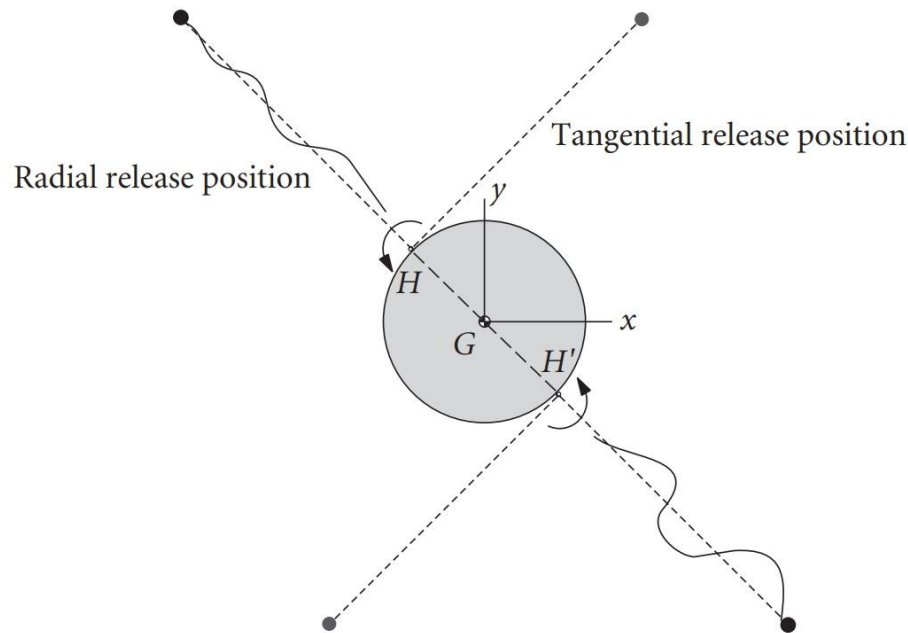


Figure 19: Comparison of radial and tangential release for a yo-yo despin system (from [4])

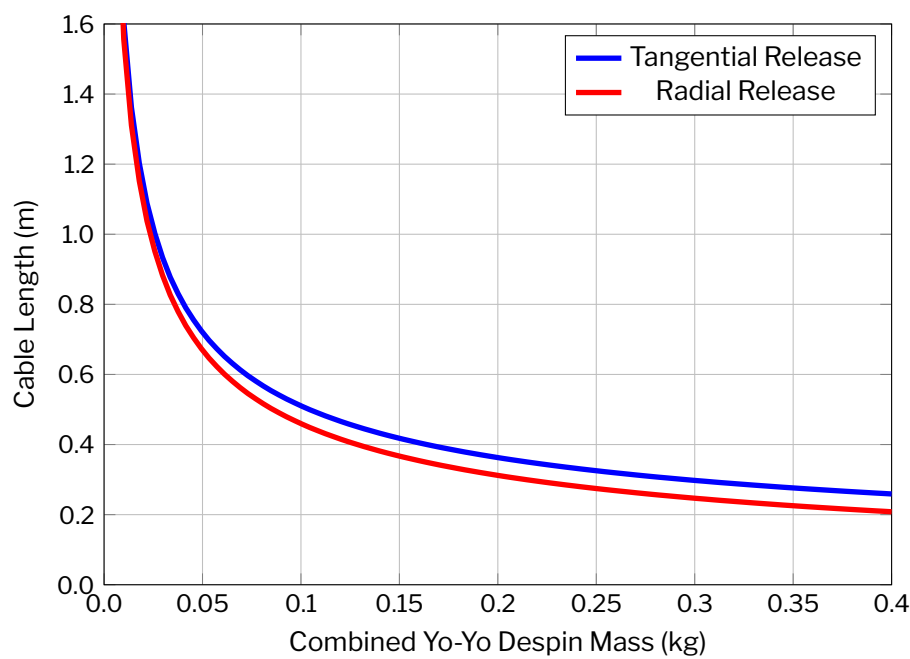


Figure 20: Tradeoff between yo-yo despin masses and cable length

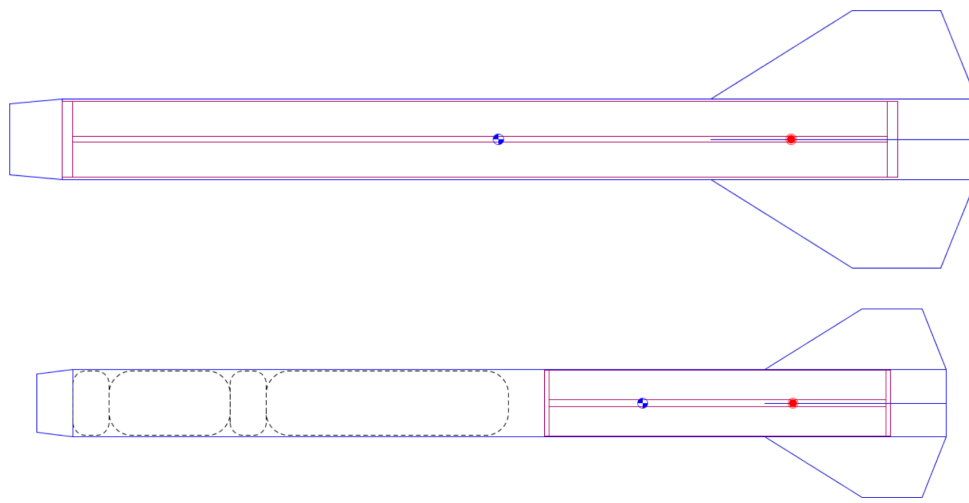


Figure 21: Basic models of the 4.5" expendable first stage (top) and the 5.5" recoverable booster (bottom)

## 7 Structures

### 7.1 First Stage

The first stage must be able to withstand the structural and thermal loading that it will experience during the flight (STR.2.2.1, STR.2.2.2). As discussed previously, it is yet undetermined if the first stage may be expended. An expendable first stage will not need an avionics or recovery system, which would significantly reduce the weight of the stage and the design complexity. However, a recoverable booster stage is still under consideration and included in this review.

#### 7.1.1 First Stage Airframe

Based on the sizing results, the optimal diameters for the first stage airframe are between 4.5" and 5.5". For the recoverable 5.5" airframe, aluminum and titanium were considered and studied by our team. Since the recoverable first stage option slightly exceeds the mass budget estimated by the structure's sizing script, titanium as a material for the first stage was eliminated. In addition, the heating effects on the booster stage are not as significant as the sustainer stage, making aluminum a valid decision for the first stage. That airframe diameter makes buying or machining the tube feasible. A 1/4" thick aluminum 6061 tube is available that satisfies safety factor requirements (STR.2.3).

For the 4.5" expendable option, aluminum is still the leading option for the airframe material. Since all point designs are sub-minimum diameter, the airframe will act as the motor casing. Aluminum is the best material that can withstand the internal pressure and the heating effects expected on the first stage during flight. A 1/8" wall thickness Aluminum 6061 tube is available that satisfies safety factor requirements.

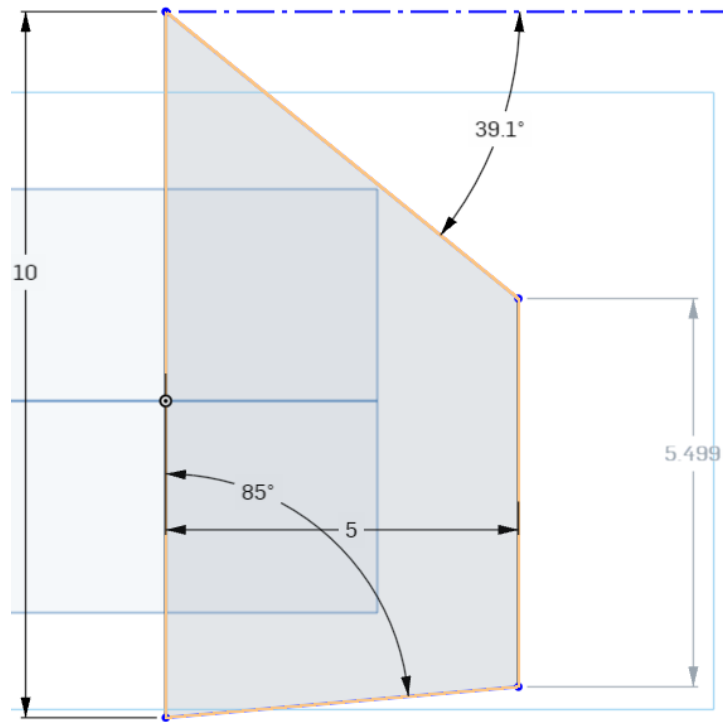


Figure 22: "Combo Bonus" fin geometry

### 7.1.2 First Stage Fins

For preliminary sizing of lower fins, off-the-rail stability margin, fin flutter velocity and ease of manufacturability were evaluated. Fin flutter is a serious design concern at supersonic speeds, as when speeds increase, the likelihood of the fins vibrating at their resonance frequency and breaking increases as well.

Three fin options were created based on research of prior art. The current leading candidate fin geometry, dubbed "Combo Bonus", consists of a geometry as depicted in Figure 22, with a thickness of 2 mm of titanium (STR.1.4). The projected number of fins is 4, in order to manage the center of pressure while minimizing the necessary size of fins, as larger fins are more susceptible to fin flutter (STR.1.3).

The thickness of the fins was chosen to be 2 mm to reduce the chance of fin flutter while keeping the fins relatively light. 2 mm thick fins allow for fin flutter stability with the thinnest fins possible, based on the analysis below. The tip chord was chosen to determine the size of the fins (STR.1.7). The leading edge is the most important factor, as a 39.1 degree leading edge maximizes the safe velocity without fin flutter [21] (STR.1.10). The edge opposite to the leading edge was chosen at 85 degrees, to increase stability by reducing the length of the root chord slightly.

Fin flutter velocity as a function of altitude was calculated to evaluate the feasibility of the "Combo Bonus" design, using Equation (11). An Openrocket file of the 4.75" - 4" expendable rocket point design was used to vary the fin geometry and evaluate the off-the-rail stability margin. A stability

$$V = \frac{a}{\sqrt{P}} \sqrt{\frac{G}{\left[ \frac{1.337(AR)^3(l+1)}{2(AR+2)(t/c)^3} \right]}} \quad (11)$$

Fin flutter velocity equation (from [13])

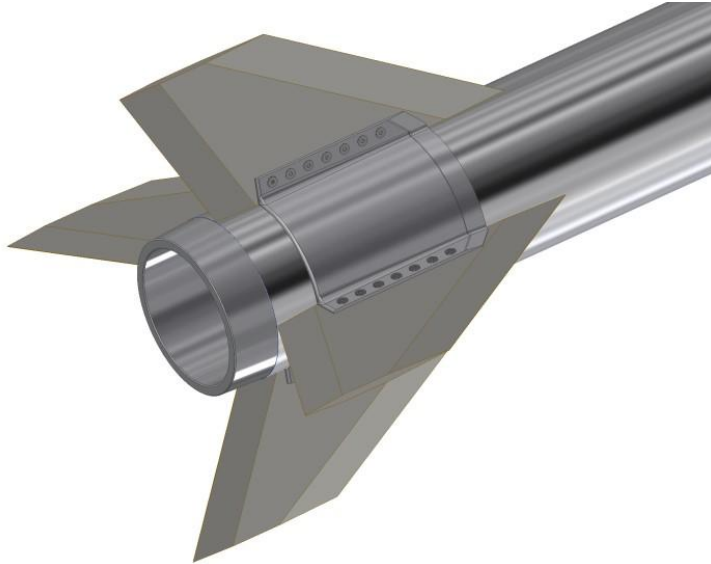


Figure 23: Princeton SpaceShot fin can CAD (from [15])

caliber of above 1.5 is generally recommended for high power rockets.

Many different considerations were made regarding fin attachment methods. It is important to select a method that can withstand the high structural and thermal loads the rocket will be subjected to (STR.4.2.1, STR.4.2.2). An additional complication comes from the sub-minimum diameter airframe: no through-the-wall methods near the pressure vessel are feasible, and welding was deemed too risky. The main methods of attachment considered were a customized fin can, a fin bracket attached to the nozzle walls, and a leading edge hoop attachment with lower edge bracket. The customized fin can was well demonstrated by the Princeton SpaceShot vehicle [15]. The quarters of the fin can are manufactured individually and then a high temperature epoxy is applied to join the quarters together to create a cohesive fin can, shown in Figure 23. This method provides liberty in choosing materials as well as high structural integrity, however it requires a long manufacturing process.

While it is impossible to drill into the airframe where the motor pressure vessel is, the airframe furthest aft, near the nozzle, is not a pressure vessel. The fin bracket method takes advantage of this by drilling into the nozzle casing to create brackets bolted into the nozzle casing that line the rocket body up to the leading edge of the fins. The fins are then attached to this bracket on the edge closest to the rocket body.

Another option is to have a leading edge hoop with a lower edge bracket, aimed to make the fins more stable with only a small amount of additional manufacturing. The idea behind this design is to



Figure 24: Fins attached using bolts and brackets (from [1])

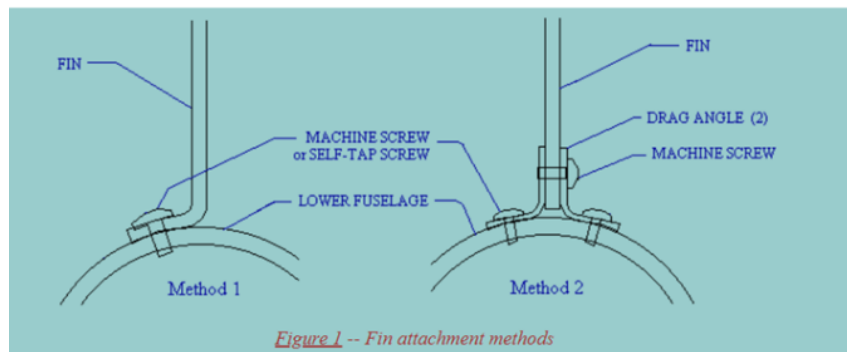


Figure 25: Fin bolted at the bottom of motor casing (from [16])

take advantage of the 5 inch nozzle throat section to secure the fins to the body similarly to the fin bracket method. Then, to ensure the fins remain stable even at the leading edges, the band will secure the other end around the combustion chamber.

The pictures below show examples of possible fin attachment methods. In Figure 24, bolts are used to attach the fin trailing edge to the bottom of the motor casing and brackets to attach the fin root chord. From Figure 25, the second method is preferable – two brackets bolted to the bottom of the motor casing (with the fin between the brackets). The optimal method for mounting and bolt configuration will be determined in the future through analytical structural analysis and FEA.

The fin attachment methods discussed in this section are equally applicable to the fins on both stages, since both stages are sub-minimum diameter.

### 7.1.3 Interstage

The current interstage design is currently unrefined, as this design review is being held early in the design process. For the sake of sizing, it was assumed to be a conical section three inches tall (STR.3.3). The wall thickness and material was kept constant with the first stage airframe (STR.3.4). Buckling and compressive safety factors were not calculated for this review as they can be assumed to be higher than the first stage airframe, as the structure is a short truncated cone with

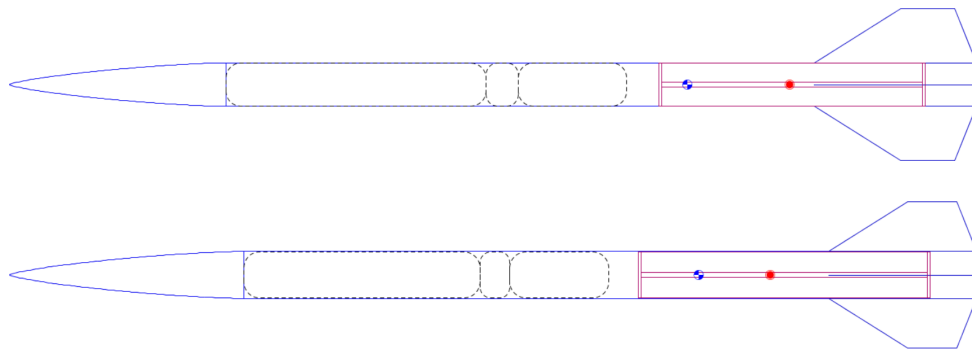


Figure 26: Basic models of the 4" (top) and 4.75" (bottom) second stage designs

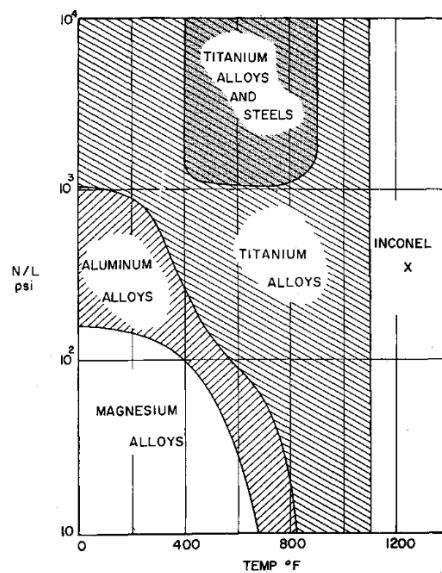


Figure 27: Material efficiency chart for stiffened cylinders in compression [9]

lower inertial loads than the first stage (STR.3.2.1, STR.3.2.2).

## 7.2 Second Stage

### 7.2.1 Second Stage Airframe

The point designs for the second stage airframe have diameters from 4" to 4.75" with a thickness of 0.05" (STR.5.1, STR.5.3). Those diameters have been selected through the sizing process, and the thicknesses were selected based on the available titanium tube sizes. Even with the 0.05" thick tubes, the titanium airframes passed our first-order buckling and hoop stress analysis with safety factors over 3 (STR.5.2.2). Additionally, titanium was shown to be able to withstand the highest thermal loads of the materials considered (STR.5.2.1), and was shown to be effective at high Mach numbers in prior art. Titanium was selected for the sustainer since it maintains most of its strength for temperatures of over 800K, unlike aluminum [9].

### 7.2.2 Avionics Bay

A section of the airframe on the second stage must be designed to accommodate the avionics system, which requires RF transparency so downlink can occur (AVI.4). This requirement rules out materials like metals or carbon fiber for this section. The material selected for this section is fiberglass reinforced plastic. Based on our team's current, limited knowledge of electromagnetic wave propagation analysis, the height of the transparent section was set at 14 inches. Whether this is sufficient or excessive will be determined through future research and testing.

The main issue with a fiberglass avionics bay, as shown by the high altitude rocket created by University of Canterbury, is heat (AVI.5.3). They mitigated the heat transfer to their RF transparent fiberglass section using a phenolic ablative resin that was externally applied to the tube [5]. The phenolic is also RF transparent, and does not interfere with RF transparency.

In addition to RF transparency, the avionics system requires sampling holes, which allow the pressure inside the vehicle to equalize with the continuously changing ambient pressure, so the barometer can sample the pressure accurately (AVI.1.1). The quantity and size of the sampling holes mainly depends on the diameter of the avionics bay. Thermal concerns caused by the sampling holes are still being researched. There may need to be some structure inside the vehicle that the incoming air must pass through before interacting with the avionics boards, to protect them.

### 7.2.3 Second Stage Fins

Taking into account fin flutter and a stability caliber of about 2.6, the following preliminary geometry for the second stage fins is as follows:

- Root Chord: 15" (STR.4.6)
- Tip Chord: 4" (STR.4.7)
- Height/Semi Span: 4" (STR.4.8)
- Sweep Length: 8.66" (STR.4.9)
- Sweep angle: 65.2° (STR.4.10)

The fin flutter velocity can be determined using the same methods as in Section 7.1.2. The Mach number corresponding to the flutter velocity ranges from Mach 4.01 to 5.64 for an altitude range of 10K - 30K feet, and from 40K - 80K feet, the flutter velocity ranges from Mach 6.96 to 18.18. Currently, the rocket is predicted to reach high supersonic speeds (Mach 4); therefore flutter is only a concern until an altitude of about 40 - 50K feet and not higher, once flutter velocity is significantly greater than rocket's velocity. Ideally, a factor of safety of 2 is needed for the fins. If the flutter Mach number doesn't meet this requirement throughout the rocket's velocity profile, the fin geometry parameters will need to be changed. This would include reducing the aspect ratio, and increasing fin thickness (STR.4.4), which is currently estimated to be ~0.1 inches [13].

It should be noted that the upper fin geometry is dependent on lower fin geometry (in terms of center of pressure and resulting stability margin off-the-rail), among other considerations such as thermal and structural loads (STR.4.2.1, STR.4.2.2). Currently, titanium is being considered for the upper fins due to its low thermal conductivity and because the sustainer stage is likely going to be made of titanium.

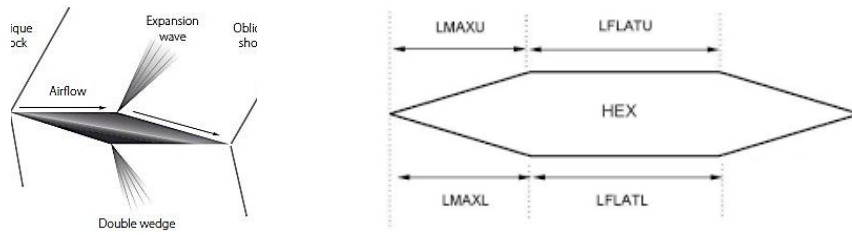


Figure 28: Double wedge airfoil cross section and hexagonal airfoil cross section

Metric	Weight	Double Wedge	Hexagonal
Cost	7.5	7	7
Manufacturability	10	1	10
Ease of Design	5	2	7
Success Rate	15	8	9
Performance	12.5	9	8
<b>Totals:</b>		305	422.5

Table 24: Decision matrix for the fin cross-section geometry

The hexagonal design is by far the most realistic and feasible cross-sectional geometry for the second stage fins. Both cross-sections included in the matrix have hypothetically similar costs, assuming the same materials are used (a conventional airfoil was not considered due to extremely poor performance and high failure rate at supersonic speeds [2]). The double wedge has superior flight performance and there are examples of it being used in real-world applications (see Figure 2). However, after discussing with the manufacturing lead, it was determined that the double wedge would be next to impossible to manufacture compared to the hexagonal design. Combine this with only small marginal differences in the drag characteristics of the two cross-sectional geometries, as well as the fact that the hexagonal shape provides slightly better stability in flight, the hexagonal cross-section is easily the best choice for the upper fins.

#### 7.2.4 Nosecone

For the preliminary sizing of the nosecone, several different geometries and their individual performances across several Mach numbers were evaluated. The nosecone should cause the least amount of drag possible (STR.6.7) and should also be able to survive the expected thermal (STR.6.2.1, STR.6.3.1) and structural loads (STR.6.2.2, STR.6.3.2) at all speeds. Based on this research, it was determined that although power series nosecones have the lowest drag coefficients above the transonic region, the Von Kármán profile with a fineness ratio of 5:1 had superior performance in the transonic region and thus may be the best choice (STR.6.1).

The expected steady state temperature at the nosecone tip will be around 1350K, based on flight at Mach 5.7 at 40,000 ft [7]. To account for such temperatures, the nosecone must be made out of titanium to maintain its high strength. Aluminum, for example, would lose 90% of its strength if it were exposed to these temperatures. At flight to around Mach 4.5, titanium and its alloys would be

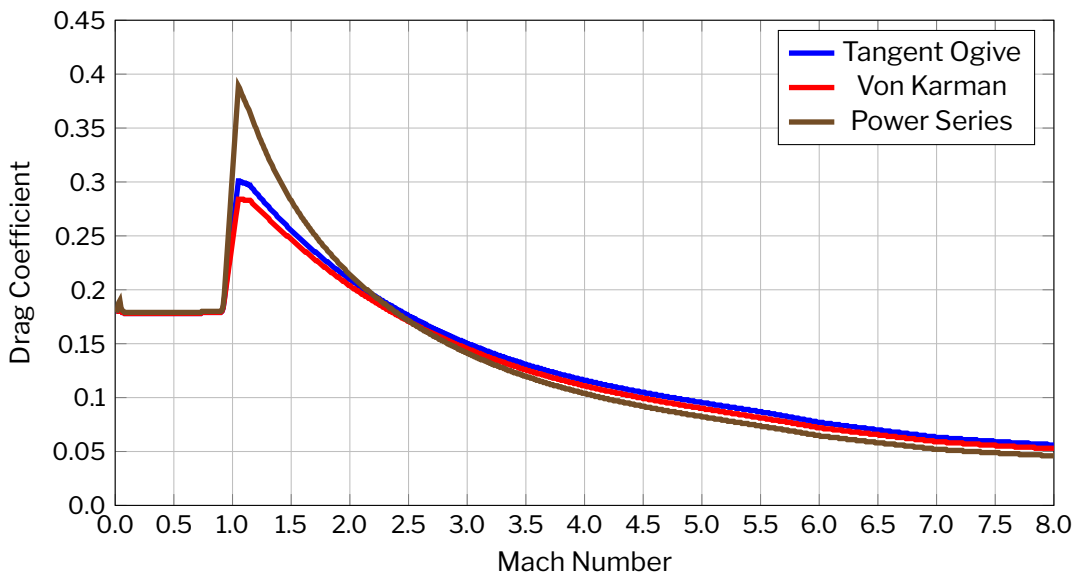


Figure 29: Comparison of drag coefficients for different nosecone shapes

the preferred material to survive the thermal and structural loads, while at speeds up to Mach 5.7, alloys such as Inconel must be used to survive [7]. The tip of the nosecone will either remain as titanium or be made out of Inconel. That decision will be driven further flight modelling and a more accurate maximum Mach number.

The manufacturability of the nosecone material is extremely important to consider given the need for machining. Titanium, while extremely durable and heat resistant, is also expensive and difficult to machine with traditional subtractive manufacturing techniques. Inconel is similar, with high strength and temperature resistance making it extremely difficult to machine.

There are several criteria to be considered when deciding on a nosecone shape. Primarily, it is desired to have the lowest coefficient of drag during all periods of flight in order to minimize energy lost to drag. However, because the rocket is expected to fly through a range of speeds, the coefficient of drag must be considered in several regimes. The first is subsonic speeds, lower than Mach 0.8; the next, transonic flight at Mach 0.8 to Mach 2.0; then supersonic flight from Mach 2 to Mach 5; and finally hypersonic flight at speeds above Mach 5.

As depicted in Table 25, the best option currently for the shape of the nosecone is a Von Karman nosecone with a fineness ratio of 5:1 (STR.6.5). The values in the design matrix are the minimum drag across the three designs, divided by the drag of the particular design. RASAero was used to obtain reliably comparable data for the coefficient of drag up to Mach 8, with the results shown below. The decision matrix did not take into account the manufacturability as the differences in manufacturability are considered to be negligible. In addition, the thermal load difference is not taken into account due to insignificant differences in different designs (based on [18]).

Metric	Weight	Power Series	Von Karman	Tangent Ogive
Min. Drag Subsonic ( $M < 0.8$ )	5	0.99394	1.0	1.0
Min. Drag Transonic ( $0.8 < M < 2$ )	15	0.86123	1.0	0.96630
Min. Drag Supersonic ( $2 < M < 5$ )	15	1.0	0.96993	0.93326
Min. Drag Hypersonic ( $M > 5$ )	10	1.0	0.89271	0.83619
<b>Totals:</b>		62.888	63.476	61.855

Table 25: Decision matrix for the nosecone geometry

## 7.3 Thermal Analysis

The thermal analysis progress coming into this review has consisted of researching prior art for rockets or aircraft that either went above the Kármán Line or achieved high Mach numbers. For each of these vehicles, we sought common factors that determined success at high temperatures.

### 7.3.1 Nosecone

For the nosecone, different materials were considered for different Mach speeds. For higher Mach number, a graphite/polyimide composite structure has an advantage of high structure efficiency at higher temperature, up to about Mach 4. For flight to about Mach 4.5 without external insulation, titanium structure and its alloys are preferred. Up to Mach 5.7 without external insulation (about 2000°F), super nickel alloys such as Inconel, Rene, Hastelloy, and Haynes must be used. Above Mach 5.7 the superalloys require either external insulation or active cooling [2]. This suggests that if a rocket is built with the performance expected, the nosecone would either need to be a short blunted Inconel tip attached to a high temperature metal nosecone using state-of-the-art materials, or a lower temperature composite nosecone coated with an ablative material.

### 7.3.2 Airframe

Materials considered for the airframe included titanium alloys, aluminum alloys, carbon fiber, and fiberglass. Additional research on prior art was done on rockets such as Traveler IV and Into the Black II, and aircraft such as the X-15 and SR-71 Blackbird. When it comes to the temperatures the airframes of the rockets would experience, there was very little data on the specific temperatures of the airframes themselves, but we can assume that they would experience at maximum the same temperatures of the nosecone. There is data available for the maximum temperature of the nosecone, which at Mach 5 is approximately 1750 K. However, the temperature distribution for the airframe will be lower than that of the nosecone (an example can be seen in Figure 30) which is why materials such as titanium are still viable for this vehicle. Based on this research, titanium alloys would work best for the rocket, as it is the best material available to withstand very high Mach numbers and temperatures. Aluminum and carbon fiber would also be viable for the first stage as they can withstand the temperatures experienced at lower Mach speeds and are cheaper to produce than titanium. Fiberglass can also be used as a RF-transparent section but should not be used as a primary material for the airframe.

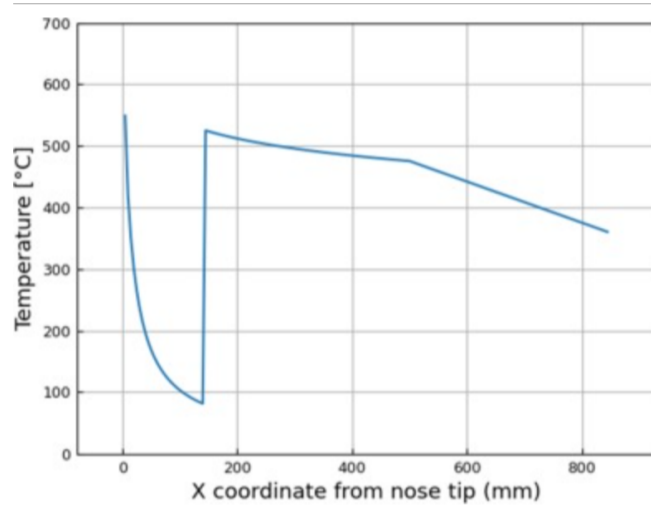


Figure 30: Temperature as a function of distance down the vehicle. From Into the Black II ([5]).

## 8 Next Steps

### 8.1 Highest Risks

In this section, the highest risks of the program are explored. These program risks represent aspects of the spaceshot program that are highly uncertain, carry a significant amount of timeline variability, are on the critical path, or are difficult to test or verify accurately. These risks are essential areas our team will focus on in the future, including methods to reduce the program risk when possible.

The highest program risk related to the propulsion subsystem is currently the duration of the process of designing a new test stand and getting it approved by Zucrow personnel. In the past, as part of propulsion design reviews with Zucrow, we have gone through several design iterations of our test stand. Designing a new test stand, especially if designed in conjunction with Zucrow to replace the broken test stand in the T-cell, means another developmental cycle that needs to be compliant with Zucrow's standards. This could set back testing full scale. Both stages on the spaceshot vehicle will need powerful solid motors that are not usually tested at Zucrow so getting approval for designs will not be as straightforward as we might like. Additionally, the second stage ignition cannot be adequately tested in a high-Mach regime during ground or subscale trials. The true conditions will be experienced for the first time on the spaceshot launch.

The primary risk surrounding avionics is the inability to completely verify the functionality of either an SRAD or COTS flight controller under the conditions they will be subjected to during a spaceshot. We were unable to find data on previous launches of the more popular COTS boards that go as high as this, which means that despite their proven track record at lower altitudes, they may not be as reliable when operating at these extremes. Furthermore, although we intend to verify the SRAD boards' functionality with extensive modeling and unit testing, any full tests can only be done using simulation models that may or may not be accurate. On the hardware side of things, iteration is going to be expensive and time consuming due to needing custom PCBs. This problem is exacerbated by the ongoing chip supply issues, which may necessitate substitutions and thus redesigns over longer periods of time.

The highest risk items within the recovery systems consist of potential designs for both the sombrero (first stage) and reefing (second stage) parachute schemes. Neither of these parachute designs can be adequately tested during ground or subscale trials, meaning they will only experience the conditions presented by spaceshot on the final launch day. This makes it difficult to determine proper descent speeds across the significant distance from which the stages will be falling. This in turn makes the prediction of landing locations for both stages incredibly difficult. Also, since neither of these designs are widely used, there is a nonzero chance that both systems will have to be manufactured in-house. This could lead to significant challenges as extremely precise manufacturing is required involving parachute lines, something we have no prior experience with. These concerns could lead to prolonged manufacturing and testing times if not handled properly.

Primary risks associated with the separation system come mainly in the form of prolonged development time. The first prototype is currently being manufactured and will need to pass a

number of tests before the design can be continued. Mainly, the mechanism must be able to hold atmospheric pressure in a near vacuum similar to flight conditions and burn at least 80% of black powder detonated in vacuum separation tests. Failure for the system to achieve these goals would likely lead to the need for major redesigns and significantly prolonged development time.

Additionally, the inter-stage mechanism carries a significant amount of uncertainty, because testing stage separation in a spaceshot-accurate environment is near impossible. The greatest risk associated with the de-spin mechanism is likely a significant increase in system complexity compared to the existing conception of the design. As the detailed design of the mechanism gets fleshed out, the complexity will increase, bringing the reliability down.

When it comes to the structures of the vehicle, our concerns greatly depend on the expected maximum Mach numbers the rocket will travel at. According to the 1DOF developed, the maximum speed is expected to be around Mach 8, though this estimate is likely conservative, and will be refined with the 6DOF. At such speed, several sections of the rocket need to be thermally insulated like the avionics bay. The sampling holes will serve as points of direct heat flux into the avionics bay, putting the electronics at risk. Proposed solutions include insulating the avionics bay with ablatives. Mimicking the heat flux at Mach 8 to test our solutions will be a difficult task and results will be inconsistent. Failure to accurately test the design will lead to several design changes and possibly a prolonged schedule.

Of course, there are significant program risks a level above each subsystem. Integration of components and inter-system dependencies will not be a smooth process, and will slow timelines down. For the spaceshot attempt itself, along with any high-altitude test flights, there is complexity in regulatory approval, coordination with launch sites, transportation of the vehicle and its motors cross-country, and the transportation of the members of the launch crew to the launch site. We are already exploring the logistics of these events, with the objective of minimizing the associated program risk.

## **8.2 Testing Capabilities**

The overall purpose of conducting testing is to prove that certain aspects of the system fulfill the outlined requirements. Tests are designed to return data showing that the part being tested is capable of the required functions for the overall rocket to function. During test operations, safety is of course our top priority, and we work with our advisors as well as the facilities we work at to develop and practice safe procedures.

Like any team, we do not have an unlimited capability to test our system. Often times, there are high-risk systems that we are not able to test with high fidelity, which is a difficult combination. This section is intended to summarize the capabilities that our team has for testing. As far as test flights, we are very capable of flights less than roughly 10,000 ft; these flights can be conducted locally. However, high-altitude test flights are very difficult for us, due to the distance to launch sites where such flights could occur. Our long-term plans for such tests are very much undetermined at the moment, but for the sake of practicality, we hope to minimize the systems that can only be tested on such flights.

Our team is very lucky to work at Zucrow Labs, where we have the ability to manufacture and test

## Next Steps

---

motors. Hot-fire testing at Zucrow will be an important step as we approach our spaceshot attempt. We will be able to fully characterize the motors we will fly on, which will be included in our 6DOF to most accurately predict the parameters of the flight. Also, the better we can characterize the motor, the more accurate the state estimation algorithm running on the avionics board will be. While a simplified model of the motor in the avionics software would not likely lead to a mission failure, the better the motor model, the more accurate the in-flight estimation of state, and the more precisely the in-flight events can be triggered. An additional component of the propulsion system is the method by which the second stage motor will be ignited at a high altitude. A leading candidate to solve this problem is a burst disk. An upside of this design is the relative ease of testing it; an unloaded motor with a burst disk could be vacuum tested.

As was discussed earlier in Section 5.1.3, testing of the avionics system will develop over time. The core component of the avionics system, the state estimation algorithm, will receive software in the loop testing. Simulated flight data will be generated by the 6DOF, noise will be injected as the flight data will be passed through sensor models, and the state estimation algorithm will determine the parameters of the flight, which will be compared to the true data directly from the simulation. This will allow us to finely tune the parameters of the state estimation algorithm to perform well with flights like the spaceshot. We are also investigating hardware in the loop testing; however, it may be the case that the amount of time and effort required for this would outweigh the benefits. Finally, for all test flights, the avionics board will fly, at least passively. This will help us characterize the performance of the board and algorithm together, as well as reducing “unknown unknowns”. The other significant component of the avionics system we will test is the downlink. Once transmitters, receivers, and antennas are selected, we plan to perform ground testing, but simply moving the components far apart, as well as flight testing. However, these flights will not be very accurate in simulating the flight, particularly in terms of altitude, so more investigation is needed.

We are relatively confident in our ability to test the mechanisms of the spaceshot vehicle. A draft of the separation mechanism is already being manufactured, with plans to fly in the spring semester. We are also able to perform higher-fidelity testing of this device on the ground. We are exploring testing the mechanism in a vacuum chamber to verify its performance during the spaceshot flight. The despin mechanism will also be somewhat straightforward to test on the ground with a spinning test rig. The parachutes and associated systems will be tested on lower-altitude test flights, which we are able to perform locally, and without significant overhead (as would be required for a high-altitude flight), though the conditions during these flights will not be able to replicate some aspects of the spaceshot launch. Unfortunately, the inter-stage mechanism will be very difficult to accurately test without a two-stage flight, which by their nature are more complex and risky than single-stage flights. The very simple design for the inter-stage we are pursuing helps to mitigate the lack of associated testing capabilities.

Testing of the aerostructures comes in two types: first, structural testing. We are confident in our abilities to characterize the structural characteristics of the vehicle through structural testing. Much more difficult, however, is testing the aerothermal loading the vehicle will experience. We are exploring testing options in this realm, but the design will likely need large safety factors for thermal loading, because the phenomenon is difficult to test, and to characterize in general.

### 8.3 Timeline

Next semester, we plan to make headway into the design of the vehicle. In particular, we plan to re-fly one of our existing vehicles (to roughly 5000 ft), primarily to test the stage separation mechanism, though the SRAD avionics board will be passively on board as well. However, we do not expect to hold another design review in the spring. Preparing for a design review stretches the limited resources of our team. We will work to balance the benefits a design review brings, especially in the form of feedback from reviewers, with the costs of holding one. For this reason, we plan to spend the spring semester entirely focused on design and testing, with our Preliminary Design Review tentatively expected to be held next fall. After that, we expect to hold a Critical Design Review, and finally a Flight Readiness Review, though naturally those reviews are much further out.

## Appendix A Acronyms and Glossary

### Acronyms

Term	Definition
CAD	Computer Aided Design
CDR	Conceptual Design Review
CEF	Characteristic Evaluation Function
CO <sub>2</sub>	Carbon Dioxide
COTS	Commerical Off the Shelf
DATCOM	Data Compendium
DOF	Degree of Freedom
EKF	Extended Kalman Filter
FAA	Federal Aviation Administration
FEA	Finite Element Analysis
FM	Frequency Modulation
GPS	Global Positioning System
HA	High Altitude (see PSPHA)
IMU	Inertial Measurement Unit
MEOP	Maximum Expected Operating Pressure
MSL	Mean Sea Level
NASA	National Aeronautics and Space Administration
PDR	Preliminary Design Review
PEPC	Purdue Engineering President's Council
PESC	Purdue Engineering Student Council
PPE	Personal Protection Equipment
PSP	Purdue Space Program
PSPHA	Purdue Space Program High Altitude
PZL	Purdue Zucrow Labs
RF	Radio Frequency
SDR	Software Defined Radio
SMT	Surface Mount Technology
SRAD	Student Research and Development
SRR	System Requirements Review

## Glossary

Term	Definition
1DOF	1 degree of freedom model for simulating the flight of a rocket
6DOF	6 degree of freedom model for simulating the flight of a rocket
BurnSim	Simulates motor profile and performance
COCOM Limit	Limits placed on GPS sold in the US. Shuts off GPS if the speed and height thresholds are met
Delta V ( $\Delta V$ )	Change in velocity. Often used as velocity needed to reach height in terms of impulse
MATLAB	Mathworks computing program with built in functions and user created function
Missile DATCOM	Program developed by the US Airforce that generates an aerodynamic table based off vehicle parameters
OpenRocket	An open source rocket modeling programs that allows the user to assemble an amateur rocket and simulate it with an in house 6DOF program
Siemens NX	CAD program developed by Siemens
Simulink	Mathworks block diagram enviornment that allows modeling of functions in different blocks and connect them to each other

## Appendix B System Requirement Tables

Some of these requirements are dependent on whether or not we expend the first stage. Requirements that only exist if the first stage is recovered are marked with a \*, and requirements that only exist if the first stage is expended are marked with a †.

### B.1 Internal Stakeholder Requirements

Req. ID	Requirement	Rationale
SR.1	The rocket shall reach 100 km mean sea level.	To fulfill our mission statement of reaching space, which the 100km mark is widely regarded as the boundary.
SR.2	The rocket shall have two powered stages.	To learn from the complexity of the separation mechanism and develop valuable learning experience, and become the first successful two stage spaceshot rocket built by a student team.
SR.3	The rocket shall have one or more motors created by students at Purdue Zucrow Labs.	To involve a student designed propulsion on a PSP rocket.
SR.4	The upper rocket stage shall be recoverable <sup>8</sup> .	To be able to study the effects of high speed flight on all parts of the rocket on the ground.
SR.5	The rocket shall carry a payload non-essential to rocket performance.	We want to put an object inside the rocket that is meaningful to the team and launch it to space. It should not be a critical part of the vehicle.
SR.6	The rocket development shall follow systems documentation.	This is a requirement meant to address some of the documentation shortcomings of our previous PSP rocket teams. Documentation tends to be lacking, and whenever a core member leaves the team, limited knowledge gets transferred, resulting in having to start certain research from the beginning. This will also standardize the explanation of the function of a system across the teams and pass on our knowledge to future teams and groups.

### B.2 External Stakeholder Requirements

#### B.2.1 Federal Aviation Administration

Req. ID	Requirement	Rationale
EX.1.1	There shall not be a 90 person per square mile population area within a quarter range of vehicle targeted height.	To minimize public danger or property damage in case of rocket veering off course.
EX.2.1	Certificate of Authorization shall be approved by the FAA.	To confirm that rocket operational area will not endanger the public or interfere with air traffic.

<sup>8</sup>If we are not able to expend the first stage, this requirement would extend to both.

EX.3.1	The rocket shall not reach above 150km.	Above 150km, the vehicle would no longer be classified as an amateur rocket and would be subject to a different set of FAA requirements.
EX.4.1	Form 7711-2 shall be approved by the FAA.	To confirm that rocket operational area will not endanger the public or interfere with air traffic.

## B.2.2 Purdue Zucrow Laboratories

Req. ID	Requirement	Rationale
EX.2.1	Purdue Zucrow Laboratories shall set high level requirements based on our mission profile.	They can approve mixtures dependent on our mission instead of a strict standard.

## B.2.3 Launch Sites

Certain launch sites have additional requirements due to company policy or local regulations. These are blanket requirements that we have extrapolated from reading different launch sites and are reasonable enough to impose as a team wide requirement.

Req. ID	Requirement	Rationale
EX.3.1	The team shall design its own launch rail.	Most launch site operators requested for us to use our own rails due to the SRAD motor possibly damaging their blast plates.

## B.3 Functional Requirements

### B.3.1 Flight-Critical Requirements

These are the minimum requirements needed for our rocket to fly successfully.

Req. ID	Requirement	Rationale	Traced From
DEF.1.1	Rocket stages shall have fundamental flight articles.	These are the minimum components for a stage of our rocket to be considered a stage.	SR.1
DEF.1.1.1	The stage shall have an airframe.	Core structural part of a rocket that houses subsystems.	SR.1
DEF.1.1.2	The stage shall have a motor.	Being a two stage powered rocket, all stages will have a motor.	SR.2

## System Requirement Tables

DEF1.1.3†	The stage shall have a recovery system.	To safely recover the stage.	SR.4
DEF1.1.3.1†	To be able to study the effects of high speed flight on all parts of the rocket on the ground.	The recovery system will be actively controlled for safety.	SR.4
DEF1.2	The lower stage shall have the required flight articles to be the first stage.	Lower stage may contain components that are not required on other stages.	SR.1
DEF1.2.1	The lower stage shall have fins.	Passively-stabilized rockets like ours usually require fins to remain stable throughout the flight.	SR.1
DEF1.3	The upper stage shall have the required flight articles to be the first stage.	Upper stage may contain components that are not required on other stages.	SR.1
DEF1.3.1	The upper stage shall have fins.	Passively-stabilized rockets like ours usually require fins to remain stable throughout the flight.	SR.1
DEF1.3.2	The upper stage shall have a nosecone.	Rockets usually require a nose cone to remain stable throughout the flight.	SR.1
DEF1.3.3*	The upper stage shall have a recovery system.	This stage travels to apogee and would be able to physically confirm height and performance.	SR.4
DEF1.3.3.1*	Stages with a non-autonomous recovery system shall have an avionics system.	The recovery system will be actively controlled for safety.	SR.4
DEF1.4	The vehicle shall have a staging mechanism between stages.	This allows the stages to separate.	SR.2
DEF1.5	The vehicle shall ignite the upper stage motor.	The second stage motor is ignited by the rocket itself as there will be no external mechanism for rocket ignition.	SR.1, SR.2

### B.3.2 Recovery Requirements

Requirements for a successful recovery.

Req. ID	Requirement	Rationale	Traced From
DEF2.1	The upper <sup>9</sup> stage shall be recoverable.	The upper stage travels through the entire stage of the flight and records it.	SR.4
DEF2.1.1	The upper stage touchdown velocity shall be less than 20 ft per second.	The stage must touch down slow enough to prevent significant damage.	SR.4

<sup>9</sup>Both stages if they must both be recovered

DEF.2.1.2*	The lower stage touchdown velocity shall be less than 20 feet per second.	The stage must touch down slow enough to prevent significant damage.	SR.4
------------	---	--	------

### B.3.3 Non-Flight Critical Requirements

Requirements not necessarily required for the vehicle but fulfills a stakeholder requirement

Req. ID	Requirement	Rationale	Traced From
DEF.3.1	The vehicle shall have a payload.	Satisfies the payload requirement, and gained data is directly useful as visual proof of rocket location.	SR.5
DEF.3.2	The vehicle shall determine its apogee.	To confirm that the rocket has reached the target apogee.	SR.1
DEF.3.3	The vehicle shall identify its location.	For easier post launch recovery.	SR.4
DEF.3.4	The vehicle shall check its state before igniting second stage.	Implied required safety feature for any two stage rocket.	EX.1.1, EX.1.2, EX.1.4

## B.4 Systems Requirements

In this section, the requirement from which any given requirement is derived from is by default its numerical parent; i.e. requirement PRO.1.2.1 is derived from PRO.1.2. Exceptions and special cases will be noted explicitly. Also, at this early stage in the design process, some specific parameters in requirements are still undetermined. They are given as “BLANK”.

### B.4.1 Propulsion

Req. ID	Requirement	Traced From
PRO.1	The rocket shall have an upper stage propulsion system	DEF.1.1.2
PRO.1.1	The rocket shall have an upper stage motor	
PRO.1.1.1	The upper stage motor shall be made from a solid propellant	
PRO.1.1.1.1	The propellant formulation shall be TS - 78	
PRO.1.1.2	The upper stage motor shall be made of BLANK fuel grains	
PRO.1.1.2.1	The first fuel grain will have BLANK geometry	
PRO.1.1.2.2	The second fuel grain will have BLANK geometry	
PRO.1.1.3	The upper stage motor shall have a nozzle	
PRO.1.1.3.1	The nozzle shall have a converging angle of BLANK	

## System Requirement Tables

PRO.1.1.3.2	The nozzle shall have a diverging angle of BLANK	
PRO.1.1.3.3	The nozzle shall have a retainer	
PRO.1.1.3.4	The nozzle shall have an ablative casing made of graphite	
PRO.1.1.4	The upper stage motor shall produce a total Delta V of BLANK	
PRO.1.2	The upper stage motor shall have an igniter	
PRO.1.2.1	The igniter will activate via a pyrotechnic charge	
PRO.1.2.1.2	The charge will accept signal from avionics to activate	DEF.1.5
PRO.1.2.2	The igniter will have an ignition motor activated by the charge	
PRO.1.2.2.1	The igniter formulation shall burn faster than the main motors	
PRO.1.2.3	The igniter shall operate at BLANK pressure	
PRO.1.2.4	The igniter shall be encased in the bulkhead	PRO.1.1, PRO.1.2
PRO.1.2.4.1	The bulkhead will withstand a chamber pressure of BLANK	
PRO.2	The rocket shall have a lower stage propulsion system	DEF.1.1.2
PRO.2.1	The rocket shall have a lower stage motor	
PRO.2.1.1	The lower stage motor shall be made from a solid propellant	
PRO.2.1.1.1	The propellant formulation shall be TS - 78	
PRO.2.1.2	The lower stage motor shall be made of BLANK fuel grains	
PRO.2.1.2.1	The first fuel grain will have BLANK geometry	
PRO.2.1.2.2	The second fuel grain will have BLANK geometry	
PRO.2.1.3	The lower stage motor shall have a nozzle	
PRO.2.1.3.1	The nozzle shall have a converging angle of BLANK	
PRO.2.1.3.2	The nozzle shall have a diverging angle of BLANK	
PRO.2.1.3.3	The nozzle shall have a retainer	
PRO.2.1.3.4	The nozzle shall have an ablative casing made of graphite	
PRO.2.1.4	The lower stage motor shall produce a total Delta V of BLANK	
PRO.2.2	The lower stage motor shall have an igniter	
PRO.2.2.1	The igniter will activate via a pyrotechnic charge	
PRO.2.2.1.2	The charge will accept signal from the control panel to activate	
PRO.2.2.2	The igniter will have an ignition motor activated by the charge	
PRO.2.2.2.1	The igniter formulation shall burn faster than the main motors	
PRO.2.2.3	The igniter shall operate at BLANK pressure	
PRO.2.2.4	The igniter shall be encased in the bulkhead	PRO.2.1, PRO.2.2
PRO.2.2.4.1	The bulkhead will withstand a chamber pressure of BLANK	

### B.4.2 Avionics

Req. ID	Requirement	Traced From
AVI.1	The avionics shall verify the rocket's apogee.	DEF.3.2
AVI.1.1	The avionics shall use gathered data to estimate altitude.	
AVI.1.2	The avionics shall store the altitude data throughout the flight.	
AVI.1.2.1	The avionics system shall write gathered and calculated data to the system memory.	
AVI.2	The avionics shall activate the recovery system at the proper time.	DEF.1.1.3.1
AVI.2.1	The avionics shall determine the moment of recovery activation.	
AVI.2.1.1	The avionics shall use an algorithm to determine moment of recovery activation.	
AVI.2.2	The avionics shall output a high voltage recovery activation signal	
AVI.3	The avionics shall activate the stage separation and second stage ignition at the proper time.	DEF.1.5, DEF.3.4
AVI.3.1	The avionics shall determine the moment of separation and ignition.	
AVI.3.1.1	The avionics shall use an algorithm to determine moment of separation and ignition.	
AVI.3.2	The avionics shall output high voltage separation and ignition signals.	
AVI.4	The avionics shall locate the rocket after the flight.	DEF.3.3
AVI.4.1	The avionics shall gather location data.	
AVI.4.1.1	The avionics shall gather GPS data.	
AVI.4.2	The avionics shall transmit the rocket location data.	
AVI.4.2.1	The avionics shall have an antenna capable of transmitting the relevant data.	
AVI.5	The avionics systems shall be durable enough to safely fly on the vehicle.	DEF.1.1.3.1, DEF.1.5, DEF.3.1, DEF.3.2, DEF.3.3, DEF.3.4
AVI.5.1	The avionics shall withstand the projected forces during flight.	
AVI.5.2	The avionics shall withstand the projected vibrations during flight.	
AVI.5.3	The avionics shall withstand the projected thermals during flight.	
AVI.6	The avionics shall have a payload	DEF.3.1
AVI.6.1	The avionics shall have an outward recording camera throughout the flight.	
AVI.6.2	The avionics may have additional payload(s).	

### B.4.3 Mechanisms

Req. ID	Requirement	Traced From
MEC.1	The rocket shall despin to no more than 60 revolutions per minute.	DEF.2.1
MEC.1.1	The rocket shall have a despin mechanism.	
MEC.1.2	The despin mechanism shall deploy at a specific altitude.	
MEC.2	Both stages <sup>10</sup> of the rocket shall be recoverable.	DEF.1.4, DEF.2.1
MEC.2.1	The first stage shall descend with a slower velocity.	
MEC.2.1.1	The first stage of rocket shall have a recovery system.	
MEC.2.1.2	The airframe of the first stage of the rocket shall separate.	
MEC.2.1.2.1	The separation mechanism shall be capable of operation without significant ambient pressure.	
MEC.2.2	The second stage shall descend at no more than 20 ft/s below 1000 ft, and no more than 50 ft/s above 1000 ft.	
MEC.2.2.1	The second stage of the rocket shall have a recovery system.	
MEC.2.2.2	The airframe of the second stage of the rocket shall separate.	
MEC.2.2.2.1	The separation mechanism shall be capable of operation without significant ambient pressure.	
MEC.3	The two stages of the rocket shall separate at a predicted or commanded time.	DEF.1.4, DEF.2.1
MEC.3.1	The rocket shall have a separation mechanism between the first and second stages.	
MEC.3.1.1	The inter-stage separation mechanism shall not significantly disturb the trajectory of the second stage.	

### B.4.4 Structures

Req. ID	Requirement	Traced From
STR.1	The rocket shall have fins on the lower stage.	DEF.1.2.1
STR.1.1	The lower fins shall be a BLANK shape.	
STR.1.2	The lower fins shall survive BLANK stage of flight.	
STR.1.2.1	The lower fins shall withstand BLANK temperatures.	
STR.1.2.2	The lower fins shall withstand a compressive load of BLANK.	
STR.1.3	There shall be BLANK fins.	
STR.1.4	The lower fins shall be BLANK inches thick.	

<sup>10</sup>Only the second stage if the first may be expended.

STR.1.5	The lower fins shall have a BLANK cross section.	
STR.1.6	The lower fins shall have a BLANK inch root chord length.	
STR.1.7	The lower fins shall have a BLANK inch tip chord length.	
STR.1.8	The lower fins shall be BLANK inches high.	
STR.1.9	The lower fins shall have BLANK inches of sweep length.	
STR.1.10	The lower fins shall have BLANK degrees of sweep angle.	
STR.1.11	The lower fins shall be BLANK inches from the bottom of the lower airframe.	
STR.2	The rocket shall have a lower airframe.	DEF.1.1.1
STR.2.1	The lower airframe shall have a diameter of BLANK inches.	
STR.2.2	The lower airframe shall survive BLANK stage of flight.	
STR.2.2.1	The lower airframe shall withstand BLANK temperatures.	
STR.2.2.2	The lower airframe shall withstand a compressive force of BLANK.	
STR.2.3	The lower airframe shall be BLANK inches thick.	
STR.3	The rocket shall have an interstage.	DEF.1.4
STR.3.1	The interstage shall have a diameter of BLANK inches.	
STR.3.2	The interstage shall survive BLANK conditions.	
STR.3.2.1	The interstage shall withstand BLANK temperatures.	
STR.3.2.2	The interstage shall withstand a compressive load of BLANK.	
STR.3.3	The interstage shall be BLANK inches high.	
STR.3.4	The interstage shall be BLANK inches thick.	
STR.4	The rocket shall have fins on the upper stage.	DEF.1.3.1
STR.4.1	The upper fins shall be a BLANK shape.	
STR.4.2	The upper fins shall survive BLANK stage of flight.	
STR.4.2.1	The upper fins shall withstand BLANK temperatures.	
STR.4.2.2	The upper fins shall withstand a compressive load of BLANK.	
STR.4.3	There shall be BLANK fins.	
STR.4.4	The upper fins shall be BLANK inches thick.	
STR.4.5	The upper fins shall have a BLANK cross section.	
STR.4.6	The upper fins shall have a BLANK inch root chord length.	
STR.4.7	The upper fins shall have a BLANK inch tip chord length.	
STR.4.8	The upper fins shall be BLANK inches high.	
STR.4.9	The upper fins shall have BLANK inches of sweep length.	
STR.4.10	The upper fins shall have BLANK degrees of sweep angle.	
STR.4.11	The upper fins shall be BLANK inches from the bottom of the lower airframe.	
STR.5	The rocket shall have an upper airframe.	DEF.1.1.1
STR.5.1	The upper airframe shall have a diameter of BLANK inches.	

STR.5.2	The upper airframe shall survive BLANK stage of flight.	
STR.5.2.1	The upper airframe shall withstand BLANK temperatures.	
STR.5.2.2	The upper airframe shall withstand a compressive force of BLANK.	
STR.5.3	The upper airframe shall be BLANK inches thick.	
STR.6	The rocket shall have a nosecone.	DEF.1.3.2
STR.6.1	The nose cone shall be a BLANK shape.	
STR.6.2	The nose cone tip shall withstand BLANK stage of flight.	
STR.6.2.1	The nose cone tip shall withstand BLANK temperatures.	
STR.6.2.2	The nose cone tip shall withstand a compressive force of BLANK.	
STR.6.3	The nose cone body shall withstand BLANK stage of flight.	
STR.6.3.1	The nose cone body shall withstand BLANK temperatures.	
STR.6.3.2	The nose cone body shall withstand a compressive force of BLANK.	
STR.6.4	The nose cone shall be BLANK thickness.	
STR.6.5	The nose cone shall have BLANK fineness ratio.	
STR.6.6	The nose cone shall have a BLANK inch base diameter.	
STR.6.7	The nose cone shall have a minimized coefficient of drag.	

## Appendix C Recovery System Line Diagrams

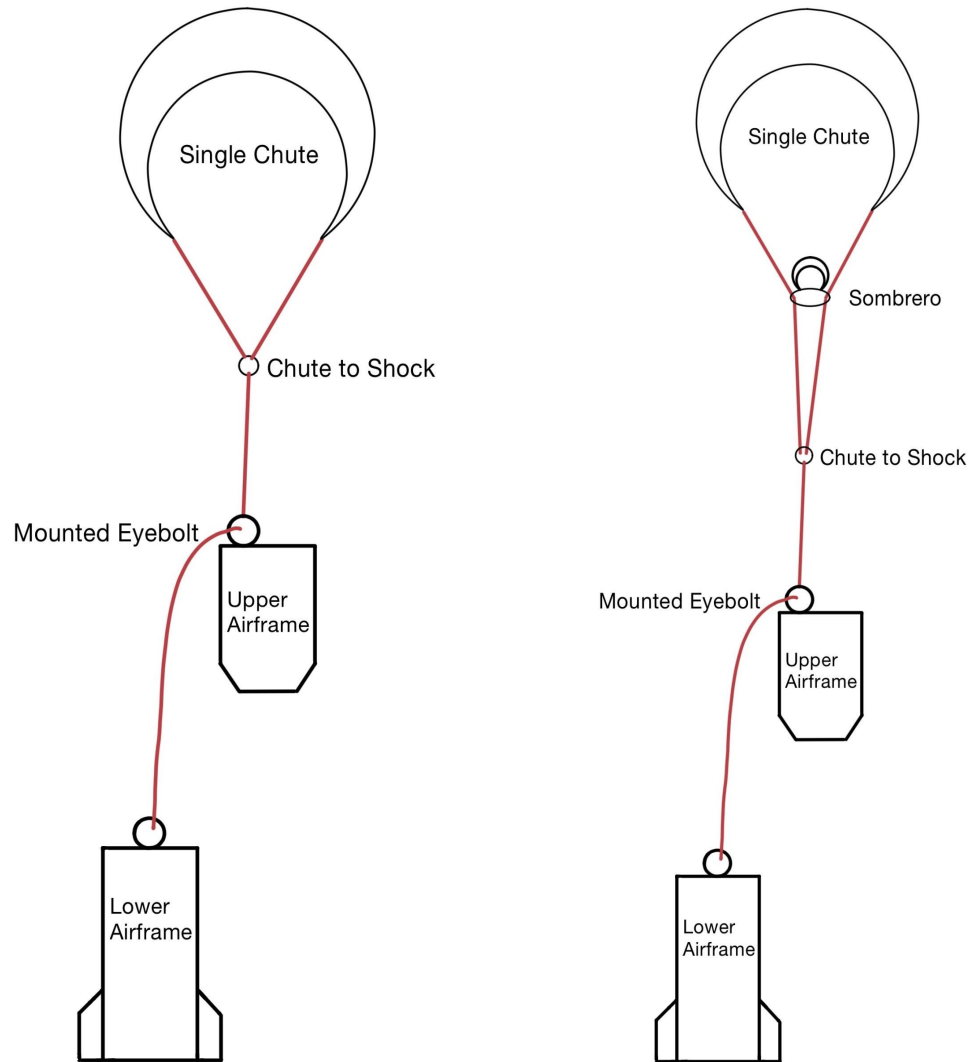


Figure 31: Two recovery schemes for the first stage: on the left, a single parachute, and on the right, the "Sombrero"

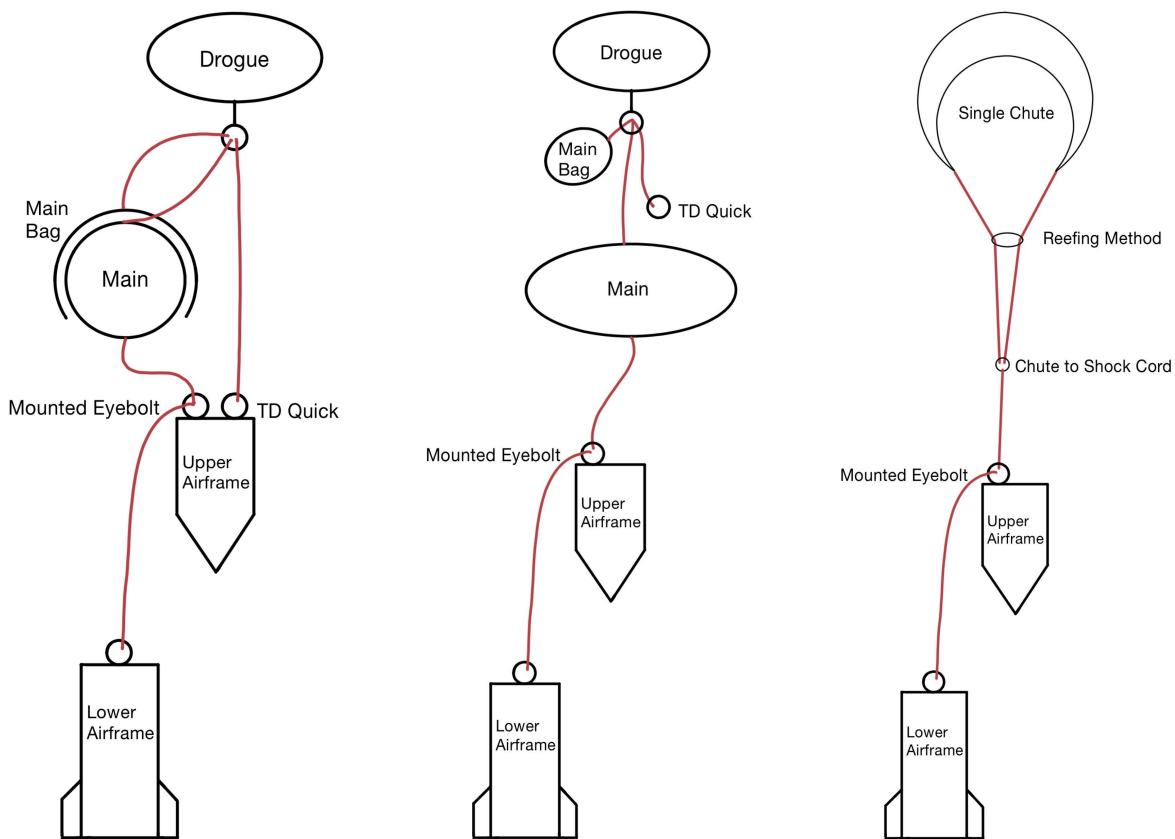


Figure 32: Two recovery schemes for the second stage: the left two images show the dual-deploy with the drogue deployed, and with the main deployed; on the right, the reefing chute design

## Appendix D Avionics In-Flight Event Overview

### Flight Mode

The computer will track changes through the following phases of flight. Each phase will be represented in a Stateflow model. These states and their transitions may change slightly as the design of the vehicle changes over time.

#### On the Pad

This phase happens when the computer is powered on and the rocket is vertical on the rail. All sensor calibrations should happen during this phase. During this phase the computer will be checking the accelerometer data to check for liftoff, but not recording the data yet.

#### First Stage Burn

One liftoff is detected by the accelerometer the computer enters the first stage burn phase. During this phase it is measuring and recording acceleration data at the highest frequency possible. It will also be measuring and recording data from all other sensors, and sending it to the state estimation algorithm. Additionally, the first stage lockout countdown begins as soon as the rocket enters this phase. No events (e.g. stage separation/ignition/parachutes) can be triggered until the first stage lockout countdown has reached 0.

#### Combined Coast/Staging

After the primary motor has burned out and the first stage lockout has ended, the computer will enter the staging phase.

**Hot Separation:** If a “hot separation” method is used, the rocket will separate stages by igniting the second stage motor while the two stages are still together. This could be used in combination with/as a backup to drag separation.

**Passive (Drag) Separation:** If a passive separation method is used, the two stages will not be held together. They may naturally separate after first stage burnout, due to drag on the first stage. This method may include a separation detection circuit. If this does not naturally occur, a hot separation will occur, assuming the conditions are still met.

**Active Separation:** If an active staging method is used, a mechanism will hold the stages together until commanded to separate. We do not expect to use this method.

#### Second Stage Ignition

Second stage ignition can only occur if the following conditions are met:

- Rocket is above a certain altitude
- Rocket is not tilted more than a certain threshold from vertical
- Stage separation has been triggered (if applicable)
- A set time delay since stage separation has passed (if applicable)

If all these conditions are met, second stage ignition will occur. If they are not met, the computer will skip to the apogee detection phase without igniting the second stage.

### **Second Motor Burn**

The computer enters this phase upon detection of the second stage igniting (from accelerometer data). Upon entering this phase the second stage lockout countdown will start. If ignition is not detected within a certain number of seconds after it should have happened, the computer will skip to the apogee detection phase, without starting the timer.

### **Coast/Apogee Detection**

In this phase, the computer will use data from the state estimation to detect when the rocket has passed apogee.

### **Drogue Deploy/Descent**

After apogee has been passed and any active lockout timers have ended, the drogue chute will deploy.

### **Main Deploy/Descent**

Once data from the state estimation function shows that the rocket is under the main deployment altitude, the main chute will be deployed.

### **Touchdown**

Once the rocket is on the ground stop, it will stop recording data, safe itself, and shut down.

## **Flowchart of Phases**

The state flow diagram is shown in Figure 33. Each rounded box is a flight phase (Stateflow state). The phase will help the State Estimation determine which prediction model to use. Each parallelogram box is an event that needs to be triggered. These could be their own states or just happen upon entering/exiting the previous/next state. The circles show different options that depend on the rocket configuration (stage and separation method). See Table 38 for transition criteria for each arrow. In the table, yet-undetermined parameters are left as “BLANK”.

### **Lockout Timers**

The purpose of the lockout feature is to prevent an early parachute deployment or staging event. This feature will prevent the rocket from igniting any charges until a predetermined amount of time since motor ignition. The time will either be a hardcoded value added when the software is loaded on, or set by the user before launch. Simulations should provide an estimate of how long the lockout timer needs to be. There will be a separate timer for the first and second motor burns. If the second motor doesn't light, the second lockout will not happen, to allow recovery events to happen regardless of whether or no ignition is successful.

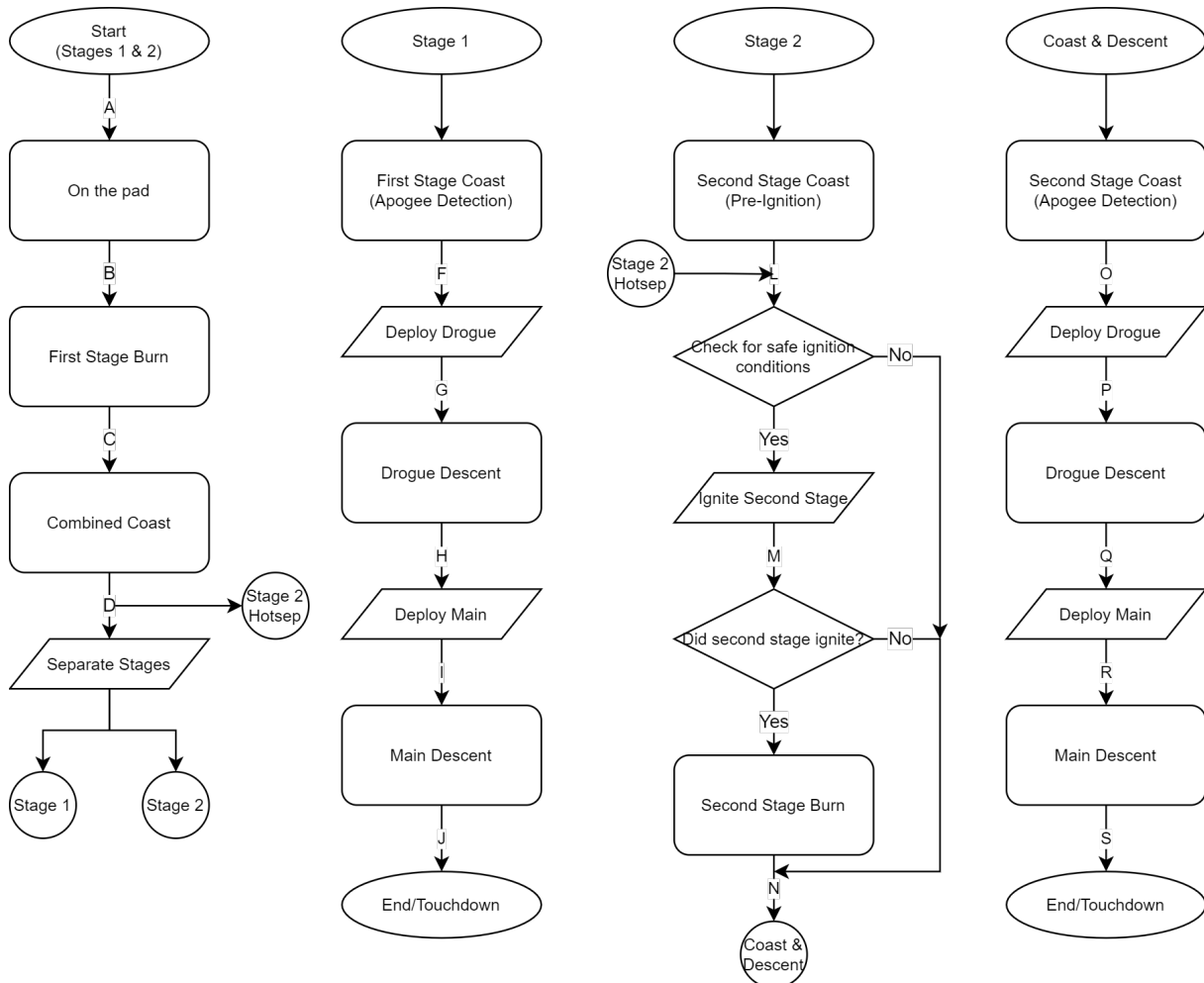


Figure 33: The preliminary avionics flight event logic stage flow diagram

<b>Transition Label</b>	<b>Criteria</b>	<b>Transitions To</b>
A	The rocket is vertical on the launch rail. This means the pitch angle is $90 \pm \text{BLANK}$ degrees.	On the Pad
B	The accelerometer detects positive acceleration in the vertical direction greater than BLANK m/s <sup>2</sup> for longer than BLANK milliseconds.	First Stage Burn
C	After first stage burnout: The accelerometer detects acceleration in the vertical direction less than BLANK m/s <sup>2</sup> for longer than BLANK milliseconds.	Combined Coast
D	The first stage lockout timer has reached 0, and the stage separation altitude and/or time delay conditions are met	Separate Stages or Check Ignition Conditions (for stage 2 hot-sep)
L	Ignition Conditions <ul style="list-style-type: none"> <li>• Altitude is greater than BLANK</li> <li>• Rocket is not tilted more than BLANK degrees from vertical</li> <li>• All time delays/lockouts have passed</li> </ul> If conditions are not met within BLANK seconds, skip to Second Stage Coast	Ignite Second Stage or Second Stage Coast
M	The accelerometer detects positive acceleration in the vertical direction greater than BLANK. If this is not detected within BLANK seconds after attempting to ignite the second stage, skip and continue to second stage coast.	Second Stage Burn
N	From successful ignition: The accelerometer detects acceleration in the vertical direction less than BLANK	Second Stage Coast (Apogee Detection)
F/O	The rocket has passed apogee: vertical velocity is negative, BLANK seconds since apogee have passed, and the second stage lockout timer has reached 0	Deploy Drogue
G/P	Immediately after drogue deployment is triggered	Drogue Descent
H/Q	The altitude is less than BLANK	Deploy Main
I/R	Immediately after main deployment is triggered	Main Descent
J/S	The rocket velocity is $0 \pm \text{BLANK}$	Touchdown

Table 38: Avionics state flow model transitions

## Appendix E Propulsion System Safety Procedures

### E.1 Example Procedure for Crawford Bomb Testing

#### Pressurized Combustion of Energetic Materials in Crawford Bomb

1. NOTE: The “two person rule” applies to this procedure. A second researcher should be nearby and aware of experimental procedures being conducted. During sample preparation, other researchers may occupy the test cell while wearing appropriate PPE (safety glasses, nitrile gloves).
2. During equipment setup and sample preparation, other researchers wearing appropriate PPE (safety glasses) may occupy test cell.
3. Prior to conducting experiments, check the condition of the experiment (corrosion on ignition leads, integrity of windows, o-ring and gasket seals, and ensure window fixture bolts are tight). Replace or repair any damaged consumables prior to testing.
4. Setup any diagnostics required (video camera(s), spectrometers(s), etc.).
5. Turn on room draft fan (~50% flowrate setting)
6. Ensure electrical ignition power supply is off
7. Place prepared energetic pellet in test article fixture
8. Affix nickel-chromium ignition wire to energetic pellet and ignition wire leads
9. Test electrical continuity of ignition circuit
10. Tightly screw test fixture into the bottom of the combustion vessel
11. Attach pressurant gas inlet tube to test fixture
12. Attach electrical ignition leads to electrical feedthrough wires
13. Prepare diagnostics for data acquisition trigger
14. Evacuate personnel from the test cell and close test cell door
15. Place “Do Not Enter” sign over test cell door knob
16. Pressurize combustion vessel to 100 psi.
17. Enter test cell to audibly check for gas leaks.
  - (a) If a gas leak is identified, depressurize the vessel, re-enter, and tighten leaking fitting or seal.
18. Evacuate personnel from the test cell and close test cell door
19. Place “Do Not Enter” sign over test cell door knob.
20. Pressurize combustion vessel to test pressure.
21. Ignite energetic material by turning on and ramping power supply current.
22. When combustion is complete, depressurize combustion vessel using solenoid actuated vent line.
  - (a) If solenoid actuated vent line is clogged (slow depressurization), vent with the manual vent valve and replace vent line filters prior to next test.
23. After venting to ~100 psi, purge vessel with inert gas (~10 seconds) to exhaust combustion products.
24. Depressurize vessel and re-enter test cell. Other personnel may also reenter the test cell at this time

## E.2 Example Procedure for Hot Fire Test

### Dual Propellant Pseudo Motor Procedures

#### Fuel Grain Sample Preparation

1. WEAR Proper PPE (long pants, closed toed shoes, lab coat, safety goggles, nitrile gloves)
2. GATHER driver grain and target grain sticks from propellant magazine
3. CUT 5" section from driver grain stick
4. BORE a 1/4" hole through the center of the driver grain with a drill bit by hand, ensure hole is centered
5. MEASURE the maximum and minimum length and diameter of the driver grain (mm)
6. WEIGH the driver grain (g)
7. COAT both sides of the driver grain with 5 minute epoxy, and let cure for more than 10 hours
8. APPLY masking tape to outer diameter of driver grain to match OD of driver grain with ID of driver grain pipe nipple
9. CUT 1.25" long section from target grain stick
10. REMOVE cardboard insulator from target grain
11. MEASURE the maximum and minimum length and diameter of the target grain (mm)
12. WEIGH the target grain (g)
13. STORE unused driver and target grains in propellant magazine, as well as prepared grains if not immediately running test operations
14. DISPOSE properly of all waste and propellant shavings

#### Test Area Setup

1. CLEAR test area
2. OPEN garage door
3. TURN ON NO<sub>2</sub> sensor
4. ASSEMBLE unistrut extensions to stand B in the T Cell
5. ATTACH MI BNC cables to channel 1 and 3 of the oscilloscope. Attach trigger BNC cable to channel 4.
6. TURN ON oscilloscope
7. INPUT correct Oscilloscope settings:
  - (a) Hit "Acquire" and ensure "Mode" is "Hi-Res" and "Samples" is "1M"
  - (b) Ensure Channels 1, 3, and 4 are visible
  - (c) Ensure the termination of channels 1 and 3 is 50Ω and channel 4 is 10MΩ
  - (d) Change the vertical resolution of channels 1 and 3 to 1mV and channel 4 to 10V
8. SET UP microwave interferometry system in t-cell by positioning it on support material and attaching power brick and MI BNC cables
9. CONNECT MI BNC cables to Microwave Interferometer
10. PLACE test warning signs outside t-cell in full view
11. ENSURE Silver SCSI Cable which goes to the NI SCXI 1001 Chassis is connected to the back of the DAQ PC
12. TURN ON DAQ PC
13. TURN ON NI Chassis

14. OPEN NI Measurement & Automation Explorer. Open “Devices and Interfaces” -> NI PCIe-6351 -> NI SCXI-1001. Click “Reset” and ensure it was successful.
15. START LabView data acquisition system
16. OPEN main vi (Tcell\_main.vi)
17. RUN main vi
18. LOAD CONFIG -> Control Wiring -> DARPA Control
19. LOAD CONFIG -> Data Wiring -> DARPA DAQ 3
20. OPEN Schematics -> Darpa tmotor.vi
21. START acquiring LabView data
22. VERIFY power supply is turned OFF and ignition cables are disconnected from power supply and shunted
23. VERIFY security cameras are turned on
24. RECORD feed from camera channels 1, 3, and 4. Using the mouse hanging from a hook on the server rack, right click, hit “Main Menu”, click the crossed hammer and screwdriver (2nd from the right), click “Storage”, on the “Record” tab, ensure that 1, 3, and 4 are set to “Manual”.  
Click OK and right click to remove menus
25. RECORD ambient temperature (deg F). Use www.weather.gov w/ zipcode 47907
26. RECORD atmospheric pressure (mb) and humidity (%). Use www.weather.gov w/ zipcode 47907

### T-Motor Assembly

1. INSPECT all components for structural impurities
2. CUT EPDM rubber to fit the shape of the cross fitting
3. APPLY five minute epoxy to EPDM rubber, fit into the cross fitting, and let cure
4. APPLY three wraps of Teflon tape to all male pipe threads
5. INSERT driver grain into the long pipe nipple
6. ATTACH cap to end of 5" pipe nipple
7. TIGHTEN cap to end of nipple a turn and a quarter greater than hand tight
8. ATTACH driver grain assembly to cross fitting
9. TIGHTEN driver grain assembly into cross fitting
10. INSERT teflon cone into target grain plug
11. APPLY five minute epoxy to target grain plug, and insert alumina disk
12. INSERT target grain into target grain plug
13. ATTACH target grain assembly into cross fitting
14. TIGHTEN target grain assembly into cross fitting
15. RECORD nozzle throat diameter (mm)
16. INSTALL o-ring onto nozzle and lubricate with vacuum grease
17. INSERT nozzle into 2.5" pipe nipple
18. ATTACH nozzle cap onto pipe nipple and ensure o-ring seat
19. TIGHTEN nozzle cap
20. ASSEMBLE burst disk
21. TIGHTEN burst disk
22. ATTACH 1/4 NPT tee-connector to instrumentation plug
23. FILL 1/4 NPT pipe nipple with high temperature oil

24. APPLY vacuum grease to pipe nipple
25. ATTACH pressure transducer and burst disk to 1/4 NPT tee-connector
26. TIGHTEN instrumentation to 1/4 NPT tee-connector
27. ATTACH instrumentation plug to cross fitting
28. TIGHTEN instrumentation plug to cross fitting
29. THREAD two e-matches through nozzle throat
30. CUT OFF finger from pair of nitrile gloves and fill with 0.25g of excess propellant shavings from sample prep
31. ATTACH igniter bag to end of ematch and insert into port of driver grain
32. APPLY nitrocellulose lacquer in a flat coat on the top of the target grain and attach the ematch
33. ATTACH nozzle assembly to cross fitting across from driver grain assembly
34. TIGHTEN nozzle assembly
35. ATTACH instrumentation assembly to cross fitting across from target grain assembly
36. TIGHTEN instrumentation assembly with pressure transducer facing towards driver grain assembly
37. VERIFY all connections have been sufficiently tightened
38. ALIGN T-motor assembly to mounting plate
39. ATTACH T-motor assembly to mounting plate, sliding U bolts around the target grain and instrumentation assembly ports in the cross fitting
40. TIGHTEN the U-bolts to the mounting plate
41. ATTACH full T-motor assembly to unistrut stand with nozzle facing outside of test cell
42. CONNECT pressure transducer to DAQ (AI-11)
43. CONNECT teflon waveguide to target grain plug

### **Run Test Operation**

1. TURN ON microwave interferometry system
2. CENTER signal from microwave interferometry on oscilloscope
3. SET scale on oscilloscope to 40.0s
4. VERIFY microwave interferometry is sending signal by running hand along teflon waveguide and observing large signal change on the oscilloscope
5. TURN ON the system relay panel in the control room (Flip the large red switch on the front of the server rack)
6. VERIFY proper readings from pressure transducer and load cell
7. SET UP blast plate behind T-motor assembly to protect other hardware
8. TURN ON fan in t-cell with exhaust facing outside of test cell
9. VERIFY warning signs outside of test cell are still up
10. PLACE signal LED in view of security camera
11. ATTACH igniter leads to e-matches in parallel
12. SET timer for five minutes
13. PRESS “single” on oscilloscope. NOTE: AFTER THIS STEP MI DATA WILL ONLY BE COLLECTED FOR FIVE MINUTES. IF TIME TO TEST EXCEEDS FIVE MINUTES ABORT TEST OPERATIONS AND RETURN TO STEP 11

**EVACUATE ALL PERSONNEL FROM T-CELL AND 116 BLAST ROOM BEFORE PROCEEDING**

14. WARN all non-test personnel in 110 and surrounding area of impending test
15. TURN OFF air-conditioning unit in 116 blast room
16. TURN ON overhead vent in 116 blast room to 100%
17. VERIFY test area is clear
18. PLACE chains on 116 blast room, t-cell, and outside t-cell control room
19. TURN ON outside and inside warning lights
20. VERIFY personnel are accounted for
21. VERIFY continuity in igniter with multimeter without leads being connected to power supply by flipping switch “Flip this one” in labview interface. Make sure the switch is set to OFF before continuing.
22. ATTACH leads to power supply
23. TURN ON power supply
24. RECORD data
25. SCAN area to verify all readings and states are as expected
26. SOUND klaxon alarm for five seconds
27. COUNT DOWN from five
28. RUN test (press control “Flip this one” in labview interface)

### **Shut Down, Data Collation, and Clean Up**

1. STOP acquire
2. TURN OFF power supply
3. DISCONNECT leads from power supply
4. VERIFY pressure and thrust data saved to TDMS file. Double click the TDMS file and save the excel document to the DARPA data folder on the desktop
5. SAVE all video data to flash drive
6. SHUT DOWN LabView system
7. WAIT for T-motor assembly to cool down and exhaust smoke to clear from test area
8. REMOVE chains from outside control room, 116 blast room, and test cell
9. TURN ON air-conditioning unit in 116 blast room
10. Turn OFF overhead vent in 116 blast room
11. TURN OFF warning lights
12. ENTER test cell
13. DETACH teflon waveguide from T-motor assembly
14. TURN OFF microwave interferometer
15. WAIT until the oscilloscope has recorded a full screen of data (5 minutes after single has been pushed)
16. SAVE screenshot and signal data from oscilloscope to flash drive
17. TURN OFF oscilloscope
18. REMOVE test warning signs from outside test cell
19. REMOVE oscilloscope, BNC cables, and microwave interferometry system from test cell
20. DETACH AI cable from pressure transducer
21. REMOVE T-motor assembly from unistrut, bring into control room
22. REMOVE unistrut extensions from stand B
23. CLOSE garage door

24. CLOSE DOWN test cell
25. DISASSEMBLE T-motor assembly
26. CLEAN each part of T-motor assembly thoroughly with acetone and wipes
27. PUT AWAY all T-motor components

### **Abort and Emergency Procedures**

#### **Hang Fire**

1. TURN OFF power supply
2. REMOVE igniter leads from power supply
3. TEST continuity of ignition system
4. If continuity fails WAIT five minutes before entering test cell
5. TEST continuity at all points in system
6. If continuity fails again DISASSEMBLE T-motor assembly and REPLACE igniter, resume procedures at step 29 in “T-Motor Assembly”
7. If continuity does not fail REPLACE leads in control room
8. If continuity is held RESUME procedures at step 13 in “Run Test Operation”

#### **Rapid Unscheduled Disassembly**

1. TURN OFF power supply
2. REMOVE igniter leads from power supply
3. LISTEN for NO<sub>2</sub> alarm
4. If NO<sub>2</sub> alarm sounds EVACUATE building immediately and CALL Dr. Pourpoint at (765) 463-1615
5. If alarm does not sound TURN ON personal NO<sub>2</sub> sensor and WAIT for smoke to clear in test cell
6. ENTER test cell
7. INSPECT other setups in room for damage
8. If other setups are damaged EVACUATE building immediately and CALL Dr. Pourpoint at (765) 463-1615
9. If setups are not damaged DISCONNECT and REMOVE microwave interferometry system from test cell
10. REMOVE T-motor assembly from test cell, bring into control room
11. SHUT DOWN LabView system
12. CLEAN and INSPECT T-motor assembly for damage
13. INFORM Dr. Son or Tim Manship of anomaly
14. SHUT DOWN test setup as per section five, “Shut Down, Data Collation, and Clean Up”

#### **Power Outage**

1. TURN OFF power supply
2. REMOVE igniter leads from power supply
3. WAIT for power to come back on
4. If power comes on in less than ten minutes RESUME test operations
5. If power does not come back on for more than ten minutes ENTER test cell

6. REMOVE igniter leads from T-motor assembly
7. REMOVE T-motor assembly from test cell, bring into control room

## Appendix F PSP High Altitude Team Members

### Project Managers

Nick Hoyer   Christina Lumpp

### Project Engineers

Harry Amadeo   Tommy Neidlein   Evan Rittner

### Leads

Josh Bailey	Elliot Basem	Elizabeth Bradshaw	Benjamin Davenport
Samantha Galicki	Om Gupta	Mahmoud Harraz	Steven Huang
Hannah Kadlec	Omkar Kerkar	Justin Kruse	Cary Leimer
Falak Mandali	Tim Osifchin	Jackson Swiader	Vincent Wang

### Members

Alexander Abbruzzi	Ben Abrams	Anish Agrawal	Corey Auerbach
Joey Bellofatto	Guilherme Camara	Mitchell Carey	Mitchell Carey
Luke Cranfill	Daniel Cyze	Joshua Daniel	Luigi David
Joseph Dunne	Ignacio Esteban	Jacob Fisher	Abigail Frank
Aditya Godbole	Siddharth Goel	Colton Gomoll	Sarah Govostis
Alexander Haynes	Kazim Jafri	Jeffrey Kaji	Jonathan Kim
Sardar Konurbayev	Joseph Ligresti	Isaac Lopez	Toe Lyan
Arturo García Martínez	Reilly Nash	Travis Reeves	William Ruiz
William Russell	Rob Sammelson	Petra Schwaab	Kevin Tracz
Taylor Vicente	Ryan Williams	Abby Woodbury	

## Bibliography

- [1] Active Stabilization Test Rocket (ASTRo). URL: <http://burpg.org/astro>.
- [2] Ben Brockert. *Numeric analysis of nose cone heating: first steps*. Dec. 22, 2013. URL: <https://sugarshotsolidworks.wordpress.com/2013/12/22/numeric-analysis-of-nose-cone-heating-first-steps/>.
- [3] *Buckling of Thin-Walled Circular Cylinders*. NASA/SP-8007-2020. Nov. 2020.
- [4] Howard D. Curtis. *Orbital Mechanics for Engineering Students*. 3rd ed., pp. 576–583. ISBN: 9780080977478.
- [5] Jack Davies et al. “Preliminary design and test of high altitude two-stage rockets in New Zealand”. In: *Aerospace Science and Technology* 128.107741 (Sept. 2022). DOI: <https://doi.org/10.1016/j.ast.2022.107741>.
- [6] Donald G. Eide and Chester A. Vaughn. *Equations of Motion and Design Criteria for the Despin of a Vehicle by the Radial Release of Weights and Cables of Finite Mass*. AD0270287. Defense Technical Information Center, Jan. 1, 1962.
- [7] Eugene L. Fleeman. *Tactical Missile Design*. American Institute of Aeronautics and Astronautics Inc. ISBN: 1563474948.
- [8] Charles W. Freeman. “Solid Rocket Motor Static Fire Test Stand Optimization: Load Cell Effects and other Uncertainties.” University of Alabama, 2018. URL: <https://louis.uah.edu/cgi/viewcontent.cgi?article=1262&context=uah-theses>.
- [9] George Gerard. “Optimum Structural Design Concepts for Aerospace Vehicles”. In: *Journal of Spacecraft and Rockets* (Jan. 1966). DOI: <https://doi.org/10.2514/3.28379>.
- [10] *Hazardous Waste Disposal Guidelines*. Mar. 12, 2022. URL: <https://www.purdue.edu/ehps/rem/> (visited on 11/13/2022).
- [11] Steven D. Heister et al. *Rocket Propulsion*. Cambridge University Press, 2019. ISBN: 9781108422277.
- [12] J. Hilbing and S. Heister. *Radial Slot Flows in Solid Rocket Motors*. AIAA-1993-2309. 1993.
- [13] Zachary Howard. *How to Calculate Fin Flutter Speed*. July 19, 2011. URL: <https://apogeerockets.com/education/downloads/Newsletter291.pdf>.
- [14] Magni Johannsson. “Optimization of Solid Rocket Grain Geometries”. Deutsches Zentrum für Luft- und Raumfahrt eV, 2012. URL: <http://www.diva-portal.org/smash/get/diva2:513657/fulltext01.pdf>.
- [15] Coleman Merchant. “Princeton SpaceShot: Design & Construction of a High Performance Two Stage Sounding Rocket”. Princeton University, May 6, 2019.
- [16] Richard Nakka. *Experimental Rocketry*. URL: <https://www.nakka-rocketry.net/rocket.html>.
- [17] F.P.J. Rimrott. *Introductory Attitude Dynamics*. Springer, 2011. ISBN: 9781461281290.
- [18] Nathan Robbins. “Performance of Nose Cone Geometries on Sounding Rockets”. In: 260774713 ()

- [19] Tijen Seyidoglu and Manfred A. Bohn. *Characterization of Aging Behavior of Butacene®Based Composite Propellants by Loss Factor Curves*. STO-MP-AVT-268.
- [20] Robert Stengel. *Space System Design*. MAE 342. Princeton University.
- [21] Wei Tian, Zhichun Yang, and Tian Zhao. “Nonlinear aeroelastic characteristics of an all-movable fin with freeplay and aerodynamic nonlinearities in hypersonic flow”. In: *International Journal of Non-Linear Mechanics* 116 (Nov. 2019). DOI: <https://doi.org/10.1016/j.ijnonlinmec.2019.06.004>.
- [22] B. Zeller. *Solid Propellant Grain Design*. Ed. by A. Davenas. Elsevier Ltd., 1993, pp. 35–84.